Transits

Transits

$$b R_* = a \cos i$$

flux = star + planet
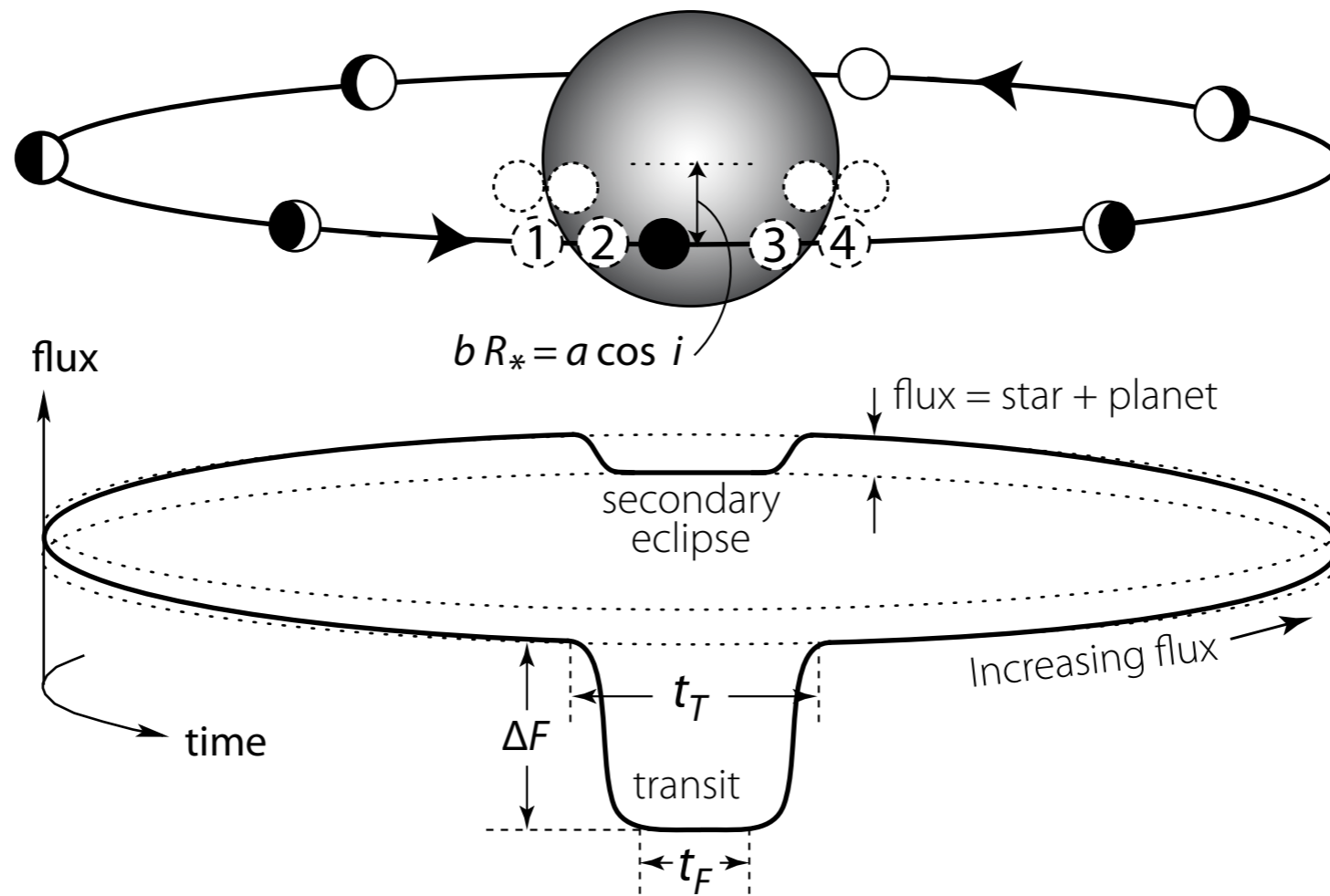
secondary eclipse
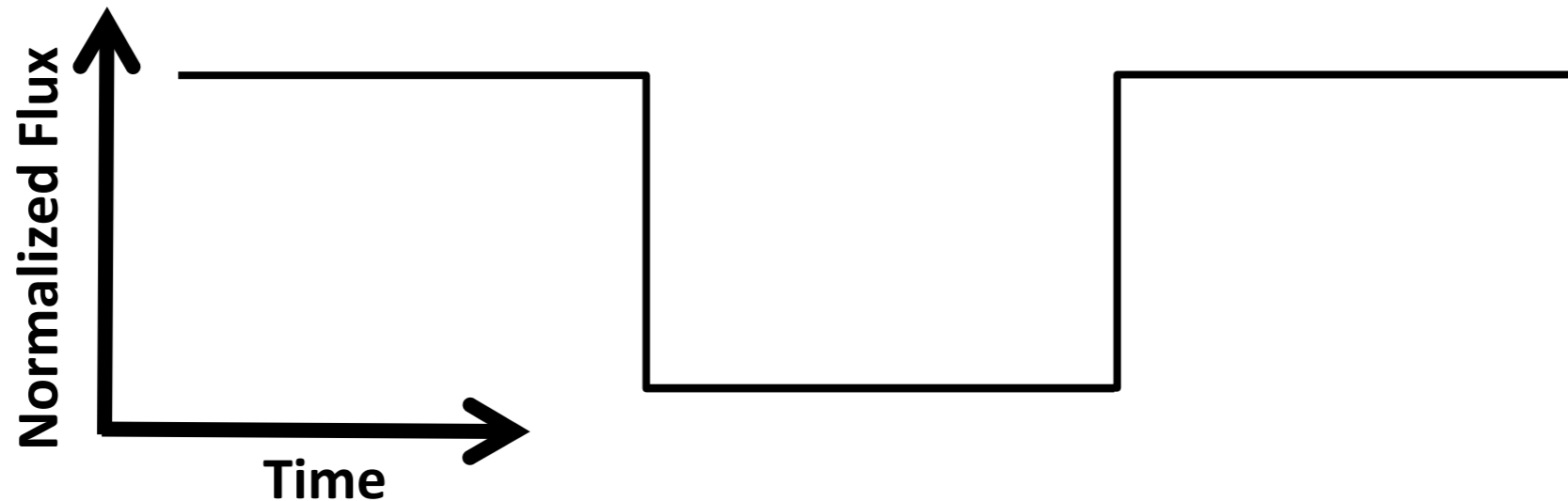
Increasing flux

flux

time

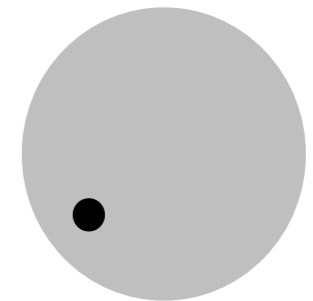ΔF

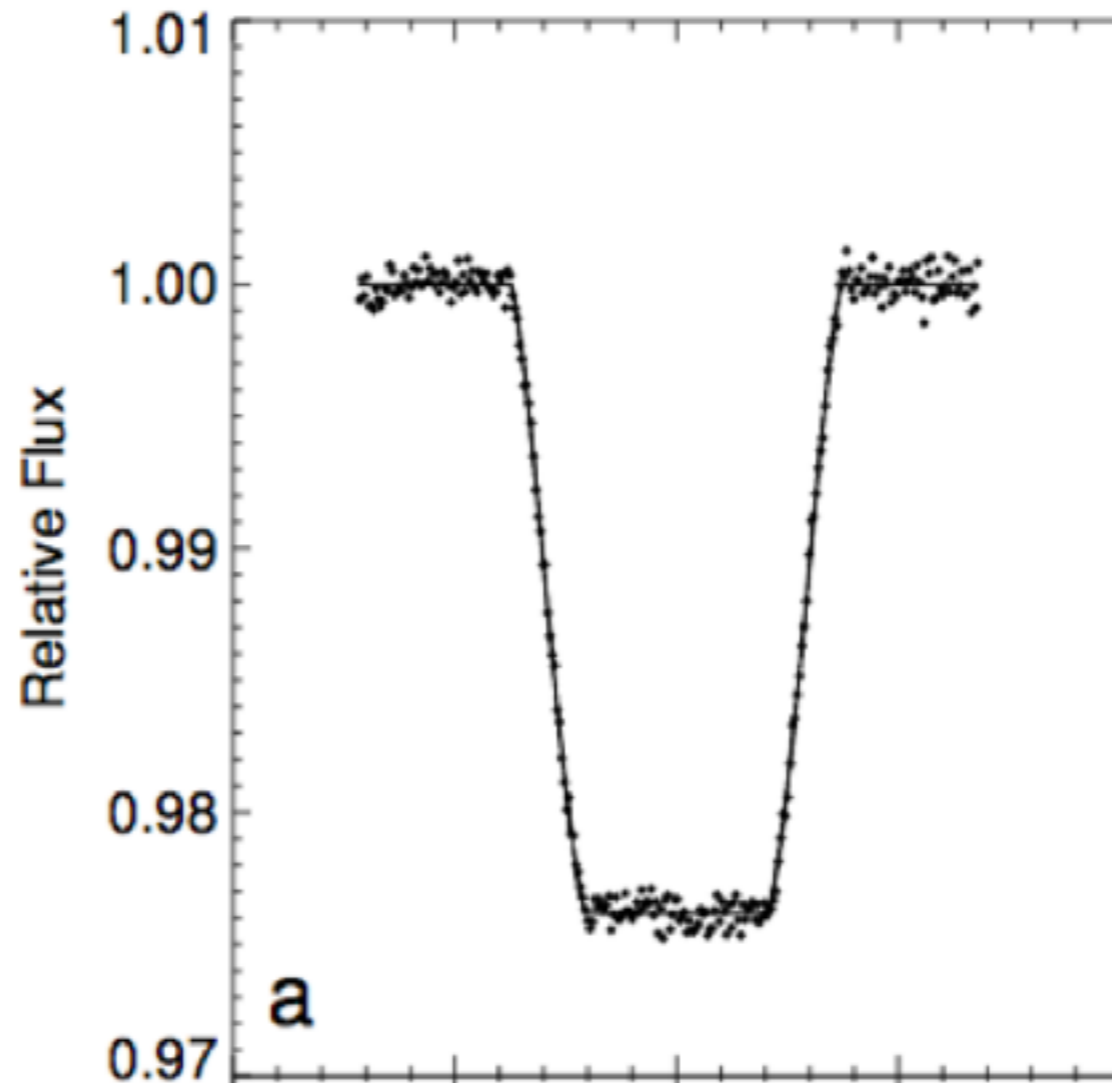t_T

transit

t_F

Transit Light-Curve

- Transit LC provides functions of time and flux

- The simple box-car transit model is used for transit search algorithms. Examples: Quasi-periodic Automatic Transit Search (QATS) and Box Least-Squares (BLS) algorithms (Carter & Agol 2012; Cameron et al. 2006)

Example: Mid-infrared transit
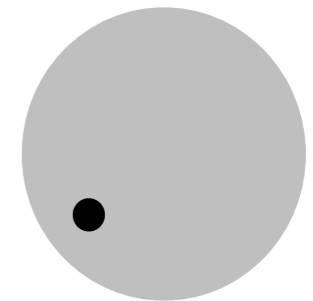
8 micron transit
of HD 189733
observed with
Spitzer

$$\frac{R_p}{R_*} = 0.1545 \pm 0.0002$$

Example: Mid-infrared transit

8 micron
transit of HD
189733
observed with
Spitzer

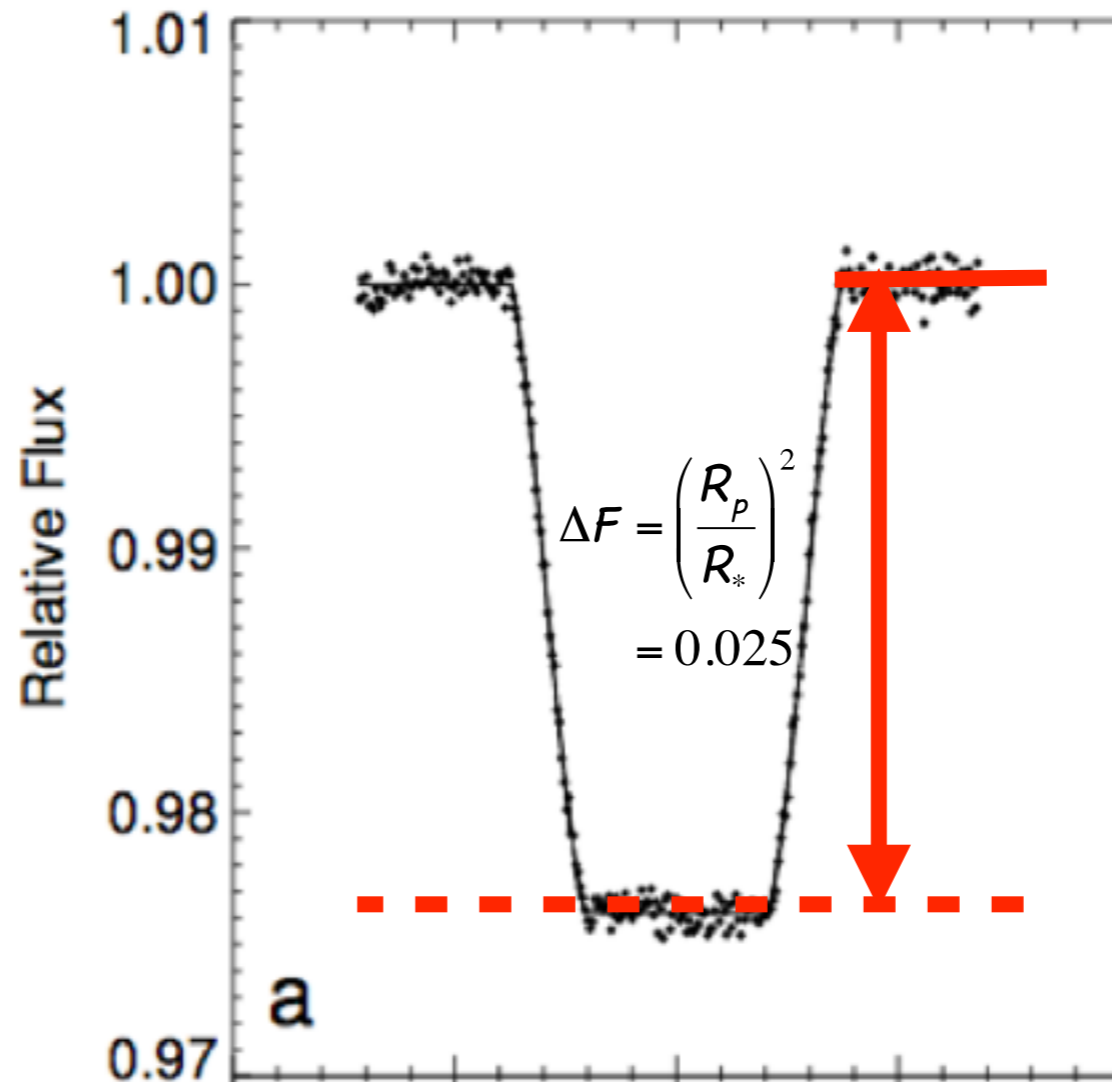$$\frac{R_p}{R_*} = 0.1545 \pm 0.0002$$

$$\Delta F = \left(\frac{R_p}{R_*}\right)^2 = 0.025$$
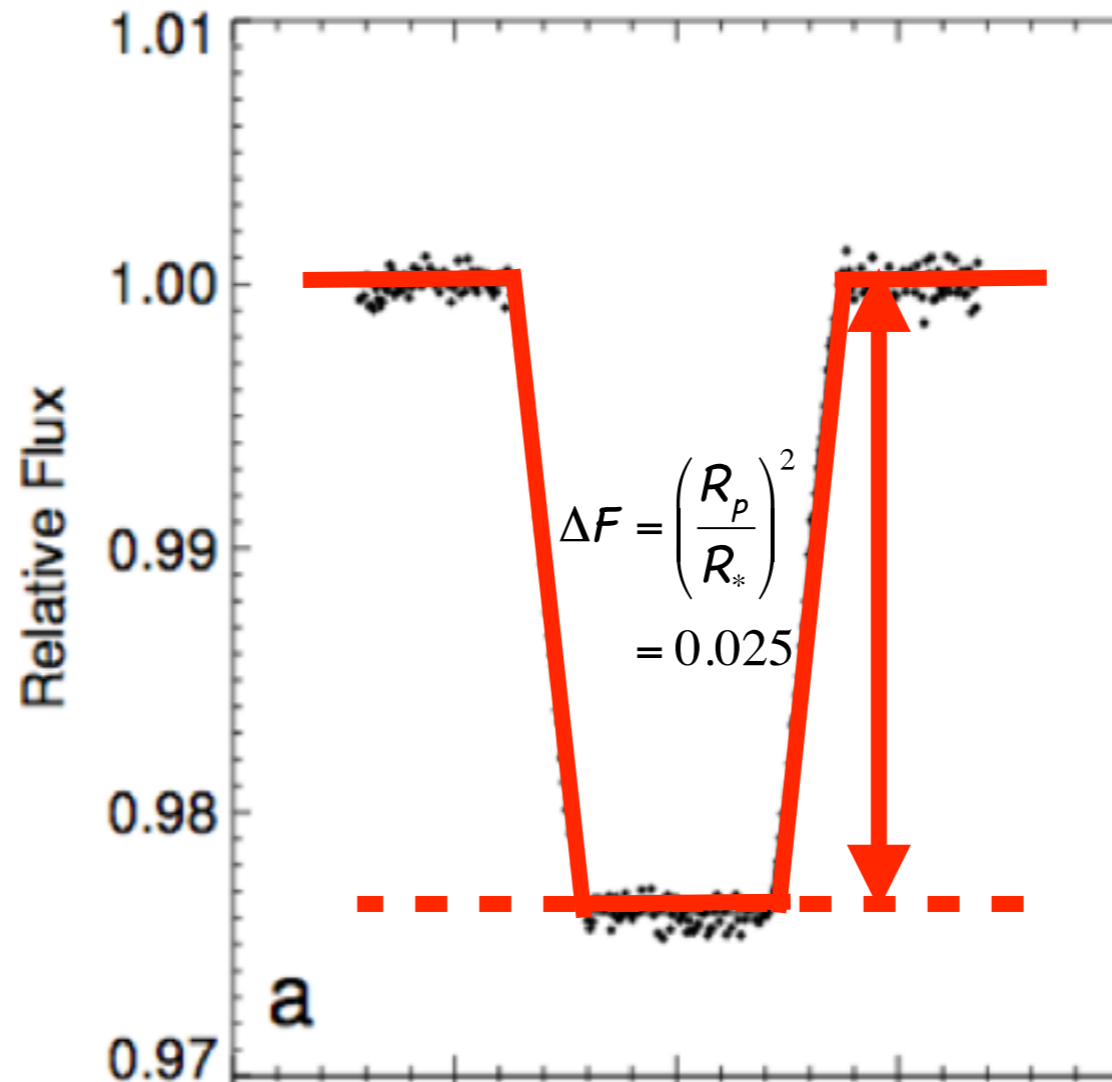
Example: Mid-infrared transit

8 micron transit of HD 189733 observed with Spitzer

$$\frac{R_p}{R_*} = 0.1545 \pm 0.0002$$

Inside plot:
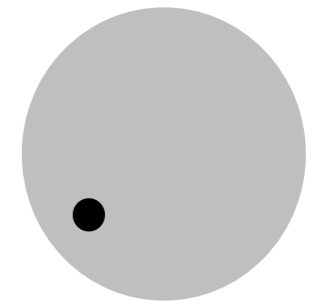$$\Delta F = \left(\frac{R_p}{R_*}\right)^2$$
$$= 0.025$$

a

Very simple shape

Trapezoidal Transit Light Curve:
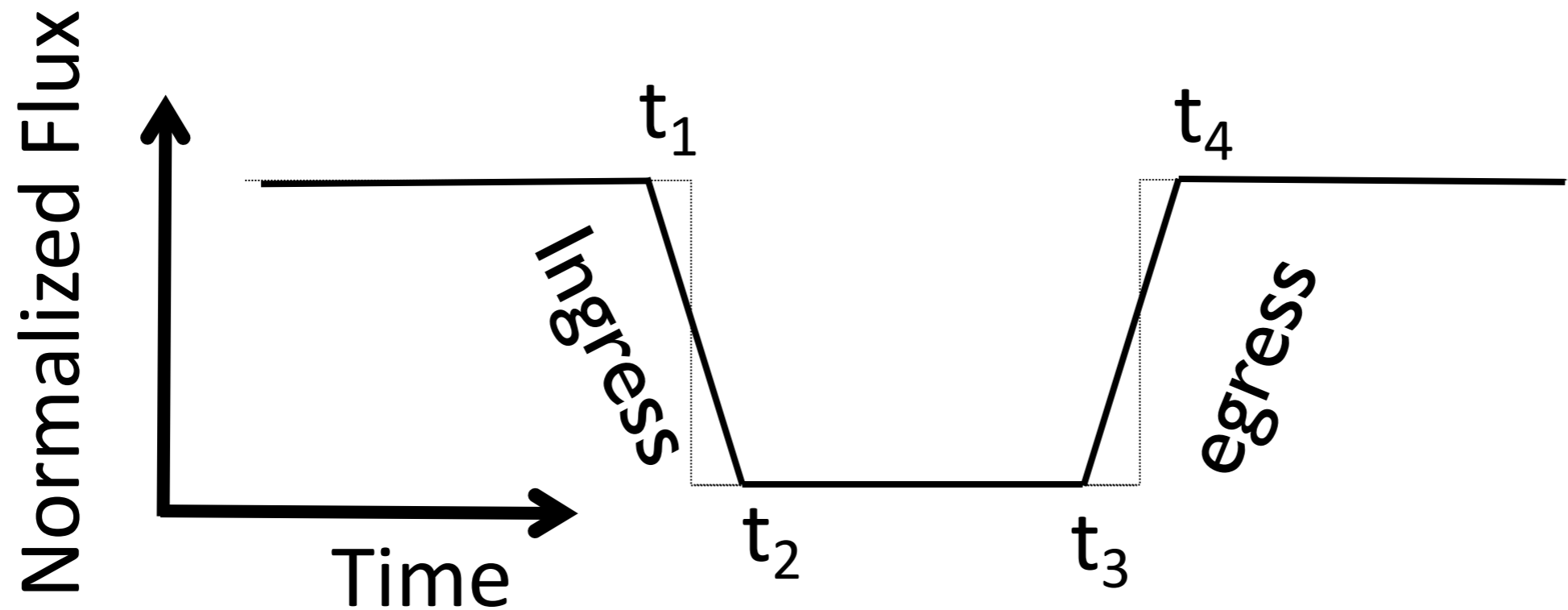
- Ingress duration $(t_2 - t_1)$
- Transit duration $(t_4 - t_1)$
- Transit time: $(t_2 - t_3)/2$
- Orbital period

Key Transit Ingredients (circular orbit)

$$\frac{a}{R_{\star}} = \frac{P}{2\pi}\frac{v}{R_{\star}}$$

Impact Parameter

b/R_*

v/R_*

Planet Velocity across stellar disk

Relative flux

$\left(\frac{R_p}{R_{\star}}\right)^2$

t_0

Time
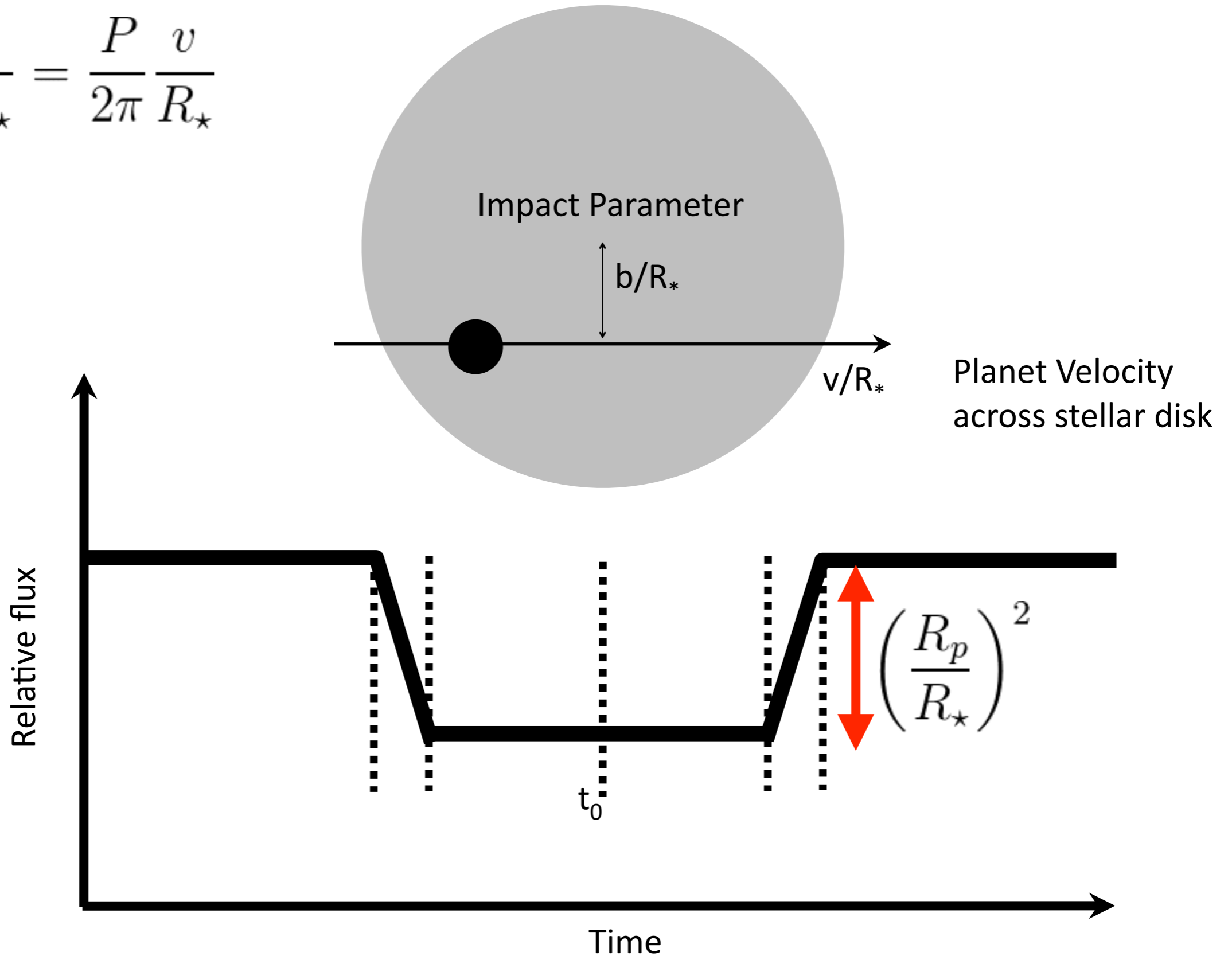
Key Transit Ingredients (circular orbit)

$$\frac{a}{R_\star} = \frac{P}{2\pi} \frac{v}{R_\star}$$

$$\frac{b}{R_\star} = \sqrt{1 + \Delta F - 2\Delta F^{1/2} \left(\frac{t_T^2 + t_F^2}{t_T^2 - t_F^2} \right)}$$

$$\frac{v}{R_\star} = 4 \left[\Delta F (t_T^2 - t_F^2) \right]^{-1/2}$$

Key Transit Ingredients (circular orbit)
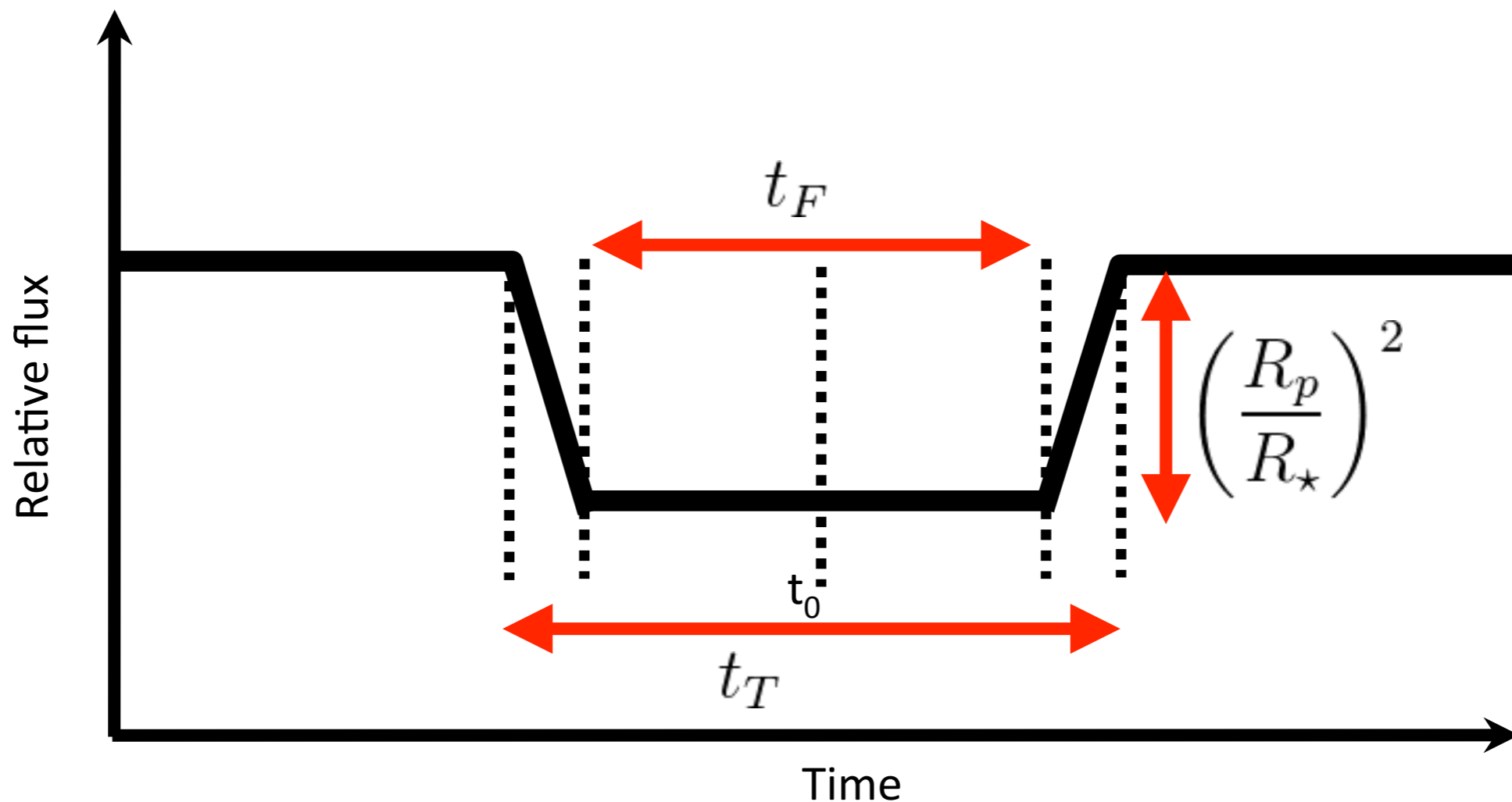
$$\frac{a}{R_\star} = \frac{P}{2\pi} \frac{v}{R_\star}$$

$$\frac{b}{R_\star} = \sqrt{1 + \Delta F - 2\Delta F^{1/2} \left(\frac{t_T^2 + t_F^2}{t_T^2 - t_F^2} \right)}$$

$$P \rightarrow \left(\frac{a}{R_\star} \right)$$

$$\frac{v}{R_\star} = 4 \left[\Delta F (t_T^2 - t_F^2) \right]^{-1/2}$$

$$\rho_\star = \frac{24}{\pi^2} \frac{P \Delta F^{3/4}}{G(t_T^2 - t_F^2)^{3/2}}$$

(stellar density)
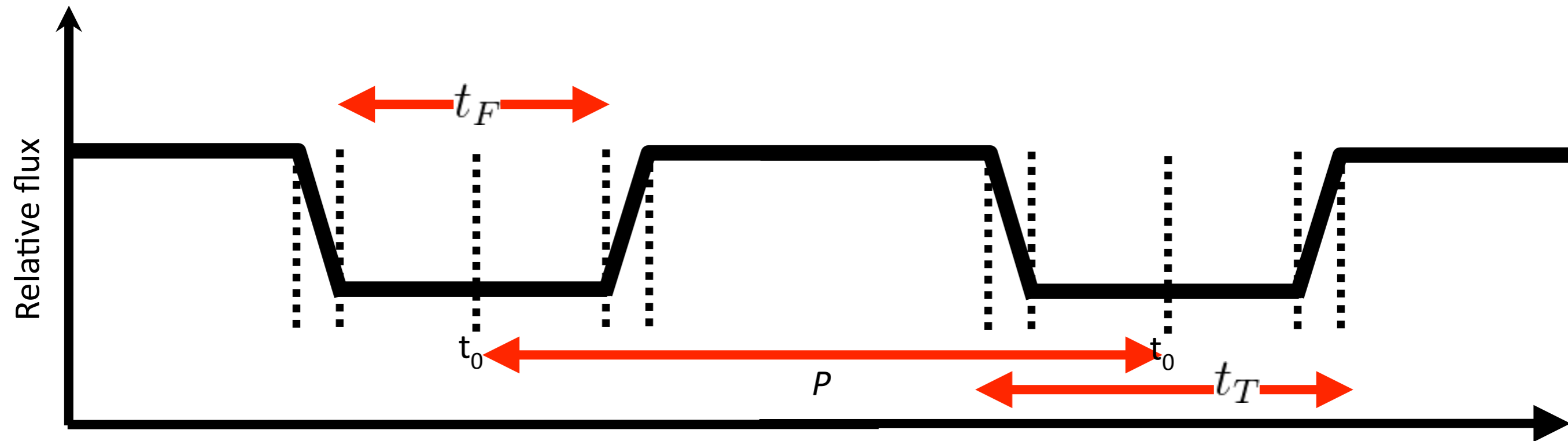
Mandel & Agol (2002); Seager &
Mallen-Ornelas (2003); Winn (2010)

Angular size

- Dimensionless angular sizes can be estimated from light curves (radians are dimensionless)

- For Kepler-36b,c know a_1/R_*, a_2/R_*, R_p/R_*, so $R_p/(a_2-a_1)$ gives angular size at conjunction: ≈2.7 x angular diameter of moon viewed from Earth

Kepler 36c seen from 36b

Credit: NASA; Frank Melchior, frankacaba.com; Eric Agol

from E. Agol

Estimating Transit Duration
for circular and edge-on orbit:

$$t_T \sim 13 \left(\frac{M_\star}{M_\odot} \right)^{-1/2} \left(\frac{a}{R_\odot} \right)^{1/2} \left(\frac{R_\star}{R_\odot} \right)$$

(from kepler.nasa.gov)

Transit Properties of Solar System Objects

Planet	Orbital Period P (years)	Semi-Major Axis a (A.U.)	Transit Duration (hours)	Transit Depth (%)
Mercury	0.241	0.39	8.1	0.0012
Venus	0.615	0.72	11.0	0.0076
Earth	1.000	1.00	13.0	0.0084
Mars	1.880	1.52	16.0	0.0024
Jupiter	11.86	5.20	29.6	1.01
Saturn	29.5	9.5	40.1	0.75
Uranus	84.0	19.2	57.0	0.135
Neptune	164.8	30.1	71.3	0.127
	$P^2 M^* = a^3$ M^* = star mass (Sun = 1)		13sqrt(a)	%=$(d_p/d^*)^2$

Area of overlap of two circles: ingress/egress

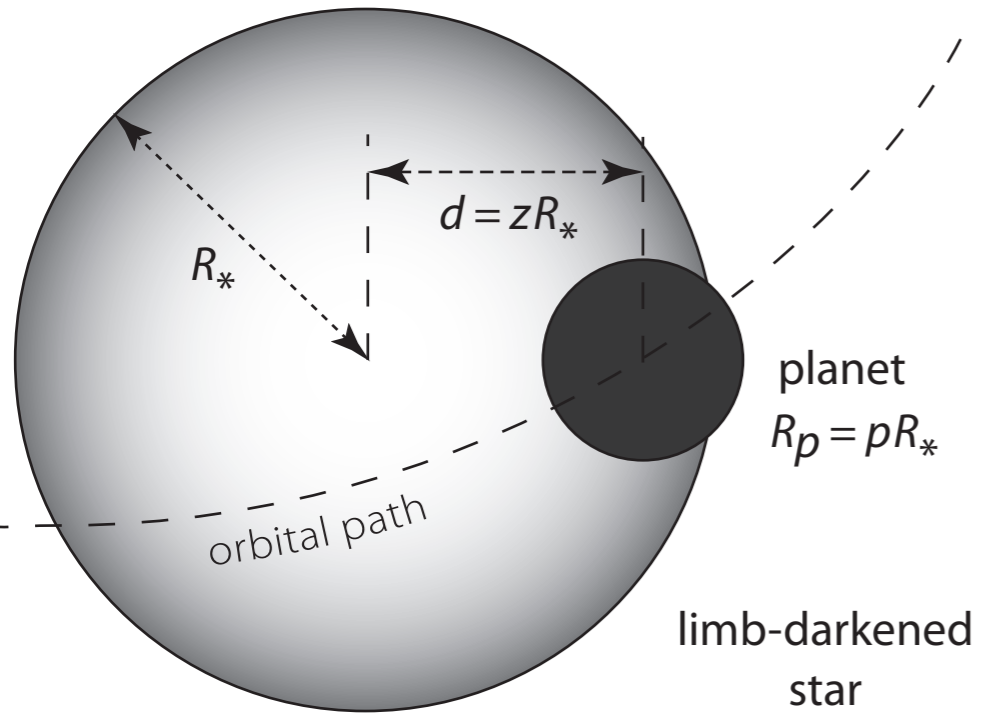$$\beta = 2\cos^{-1}\left(\frac{d^2 - r_1^2 + r_2^2}{2dr_2}\right) \qquad \alpha = 2\cos^{-1}\left(\frac{d^2 - r_2^2 + r_1^2}{2dr_1}\right)$$
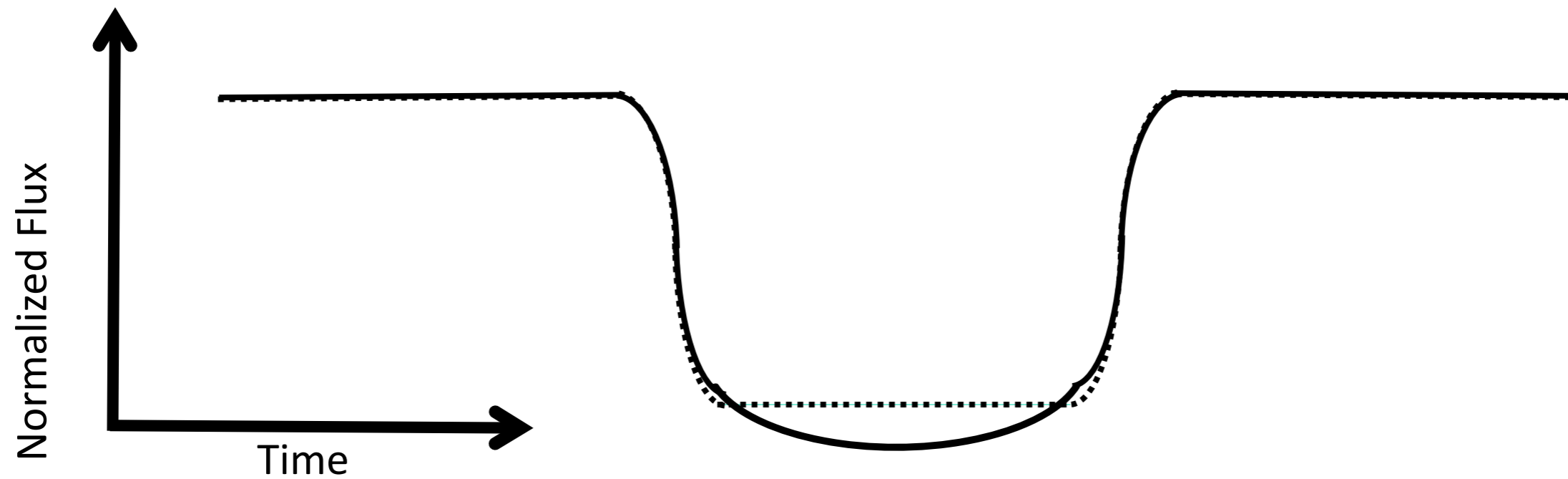
Getting more complicated …

$$\delta(r_1, r_2, d) = \frac{1}{2}\frac{r_1^2}{r_2^2}(\alpha - \sin\alpha) + \frac{1}{2}(\beta - \sin\beta)$$
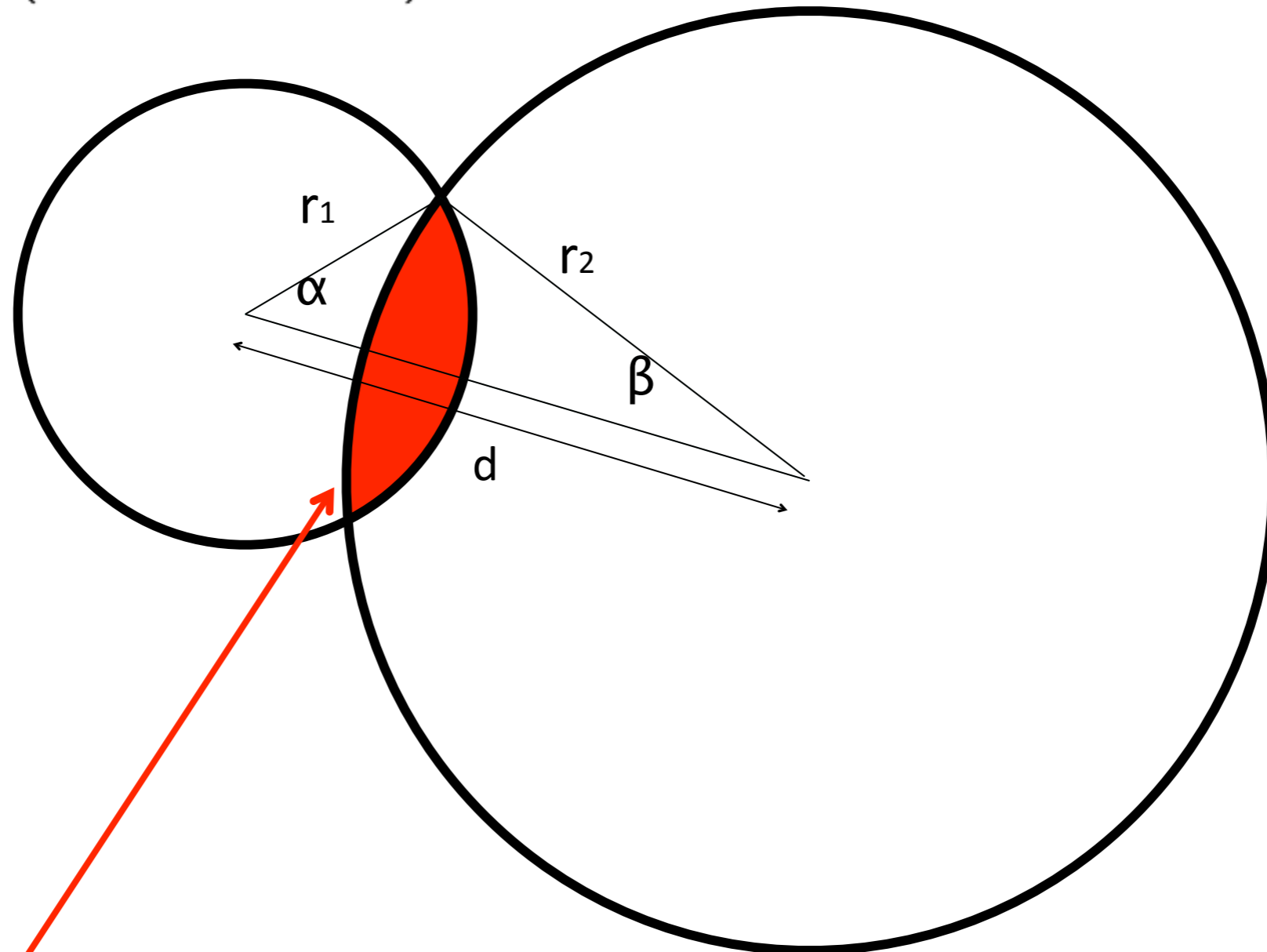
see Kopal (1975) , Mandel & Agol 2002

Limb-darkened Transit Light Curve:

$d = zR_*$

R_*

planet
$R_p = pR_*$

orbital path
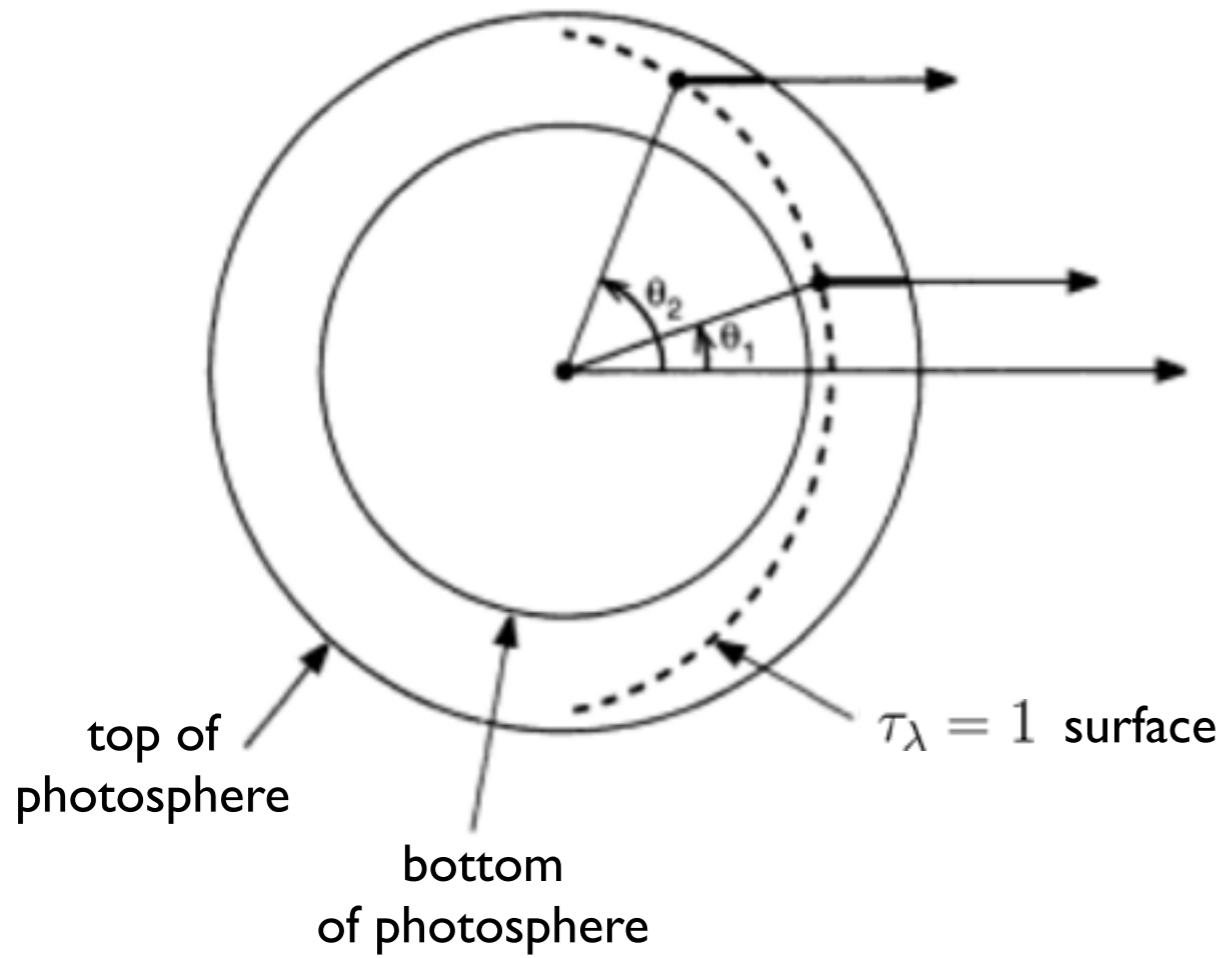
limb-darkened
star

Limb-darkening alters ingress / egress shapes and complicates determination of transit depth and time. Depending on data quality, can lead to degeneracies between b, Rp/Rs and stellar limb-darkening properties.

Normalized Flux
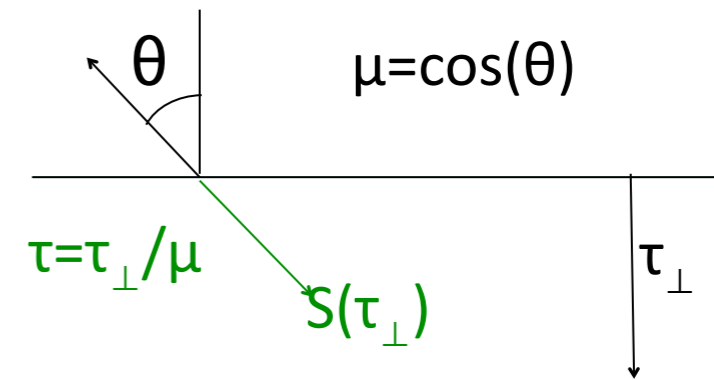
Time

Limb-darkening

$$\mu = \cos(\theta)$$

to observer $\qquad \mu = 1, \theta = 0$

top of
photosphere

bottom
of photosphere

$\tau_\lambda = 1$ surface

Limb-darkening

- approximate solution to plane-parallel radiative transfer yields linear source function

$$S_\nu = a + b\tau_\nu$$

- line-of-sight surface intensity becomes linear function of mu.

$$I_\nu(0) = \int_0^\infty S_\nu e^{-\tau_v \sec\theta} \sec\theta \, d\tau_\nu$$

$$I_\nu(0) = a + b\cos\theta$$

- At glancing angles, tau = 1 corresponds to greater height in the atmosphere.

Limb-darkening Law
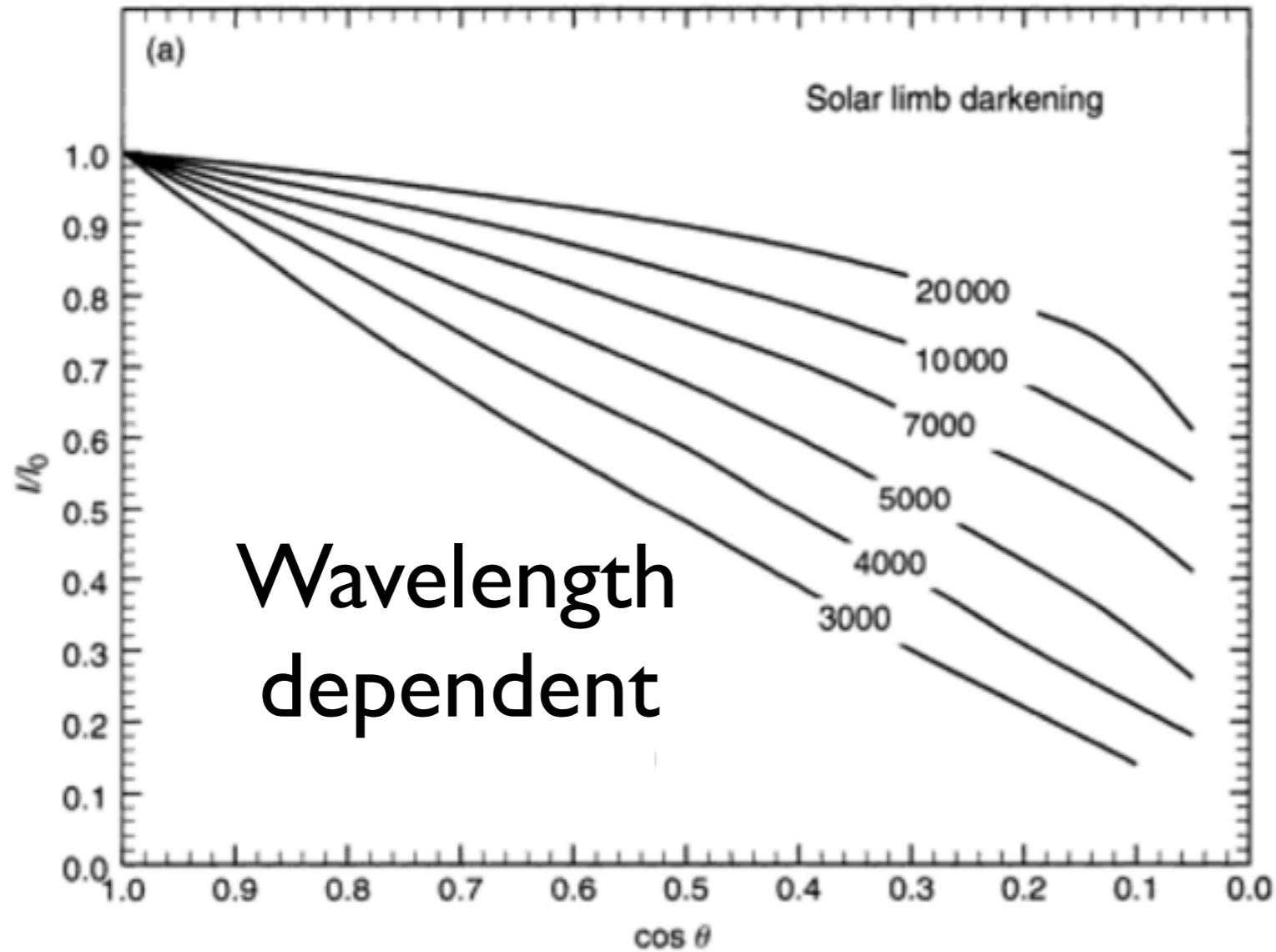

$$\mu = \cos(\theta)$$
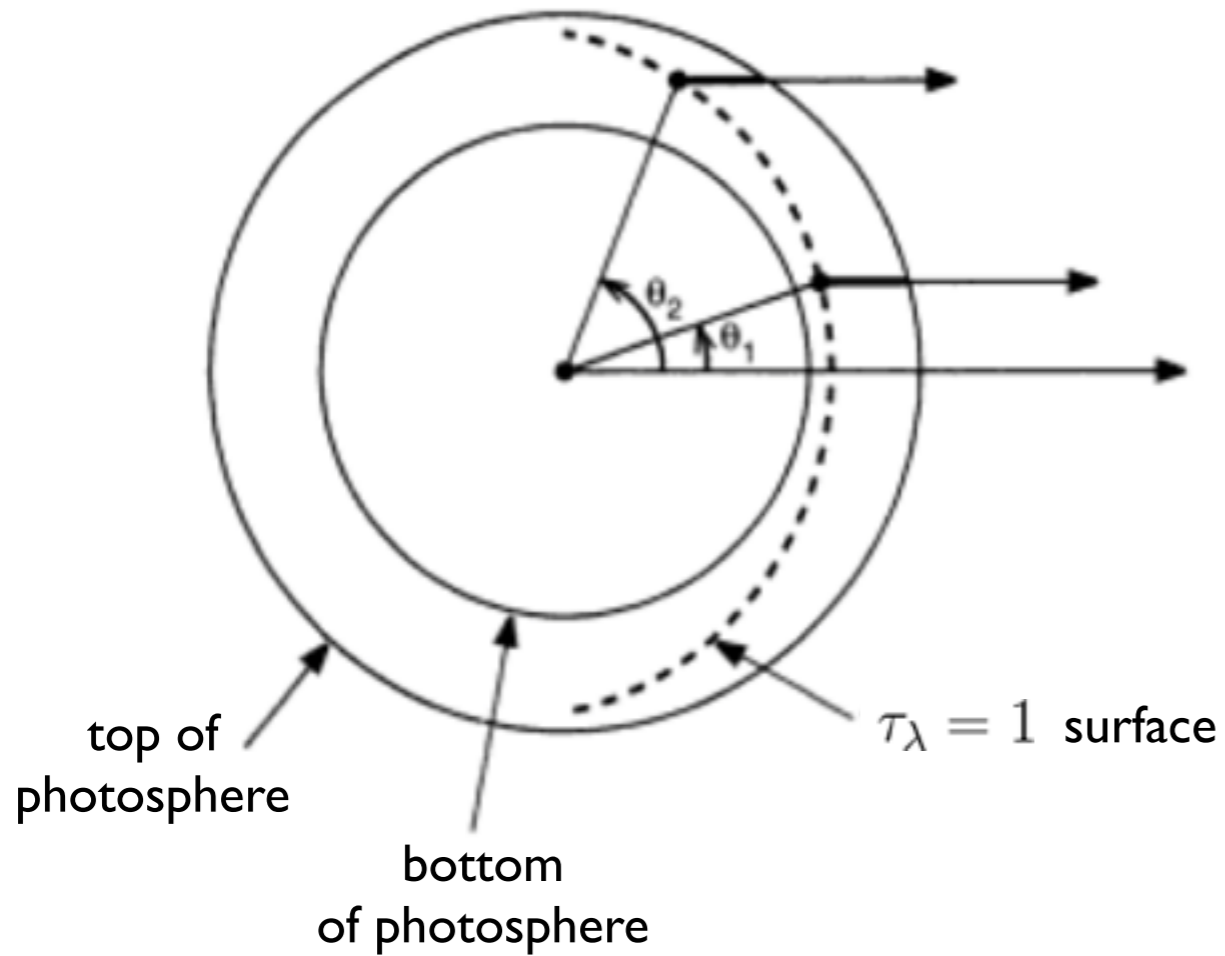
to observer

$$\mu = 1, \theta = 0$$

Going a step farther, Eddington approximation predicts that limb ~ 40% of central intensity

$$\frac{I(0,\mu)}{I(0,1)} = \frac{3}{5}\left(\mu + \frac{2}{3}\right)$$

Limb-darkening (the Sun)

fairly linear!

Limb-darkening (the Sun)
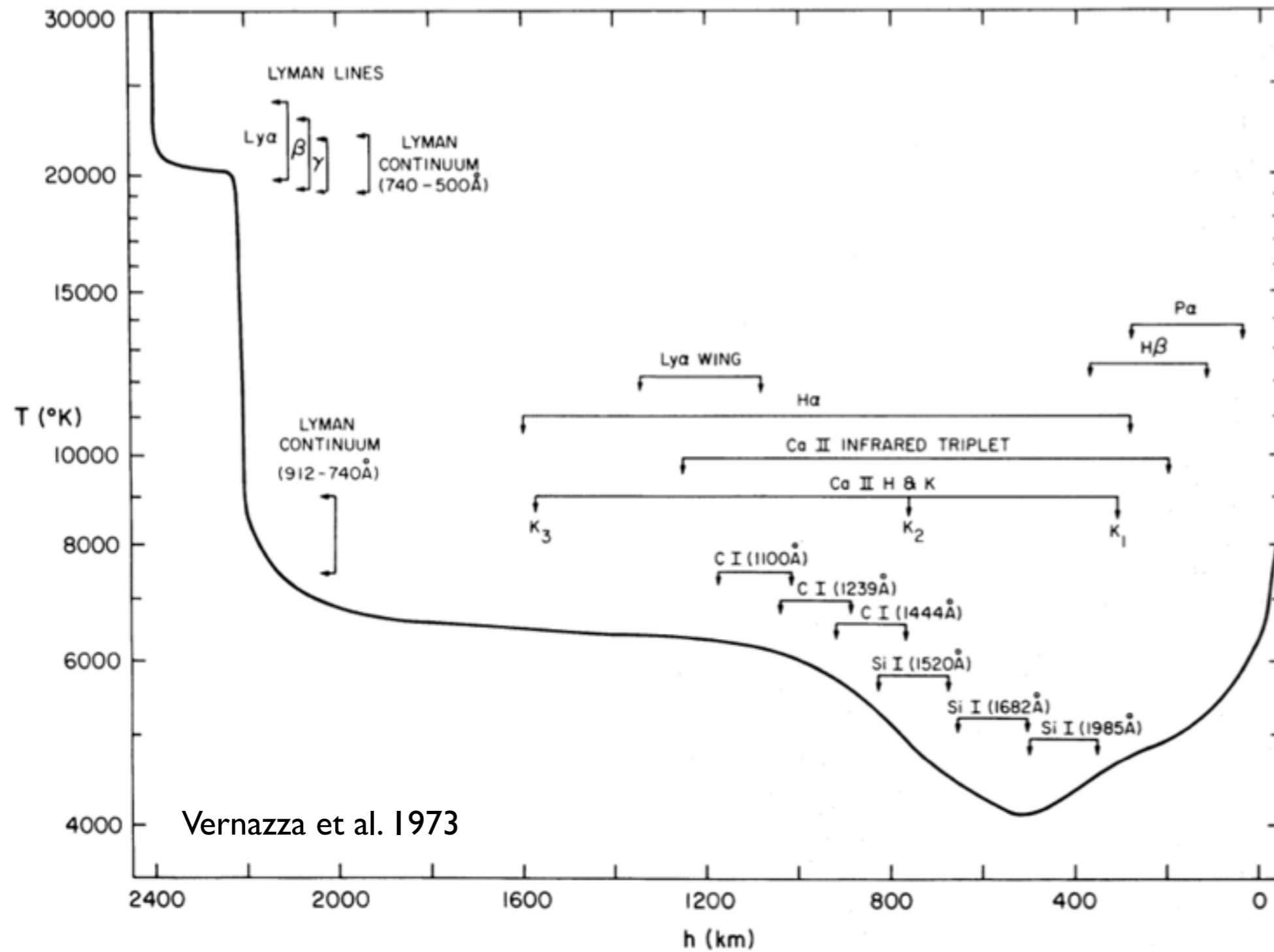## (can be used to infer structure of atmosphere)
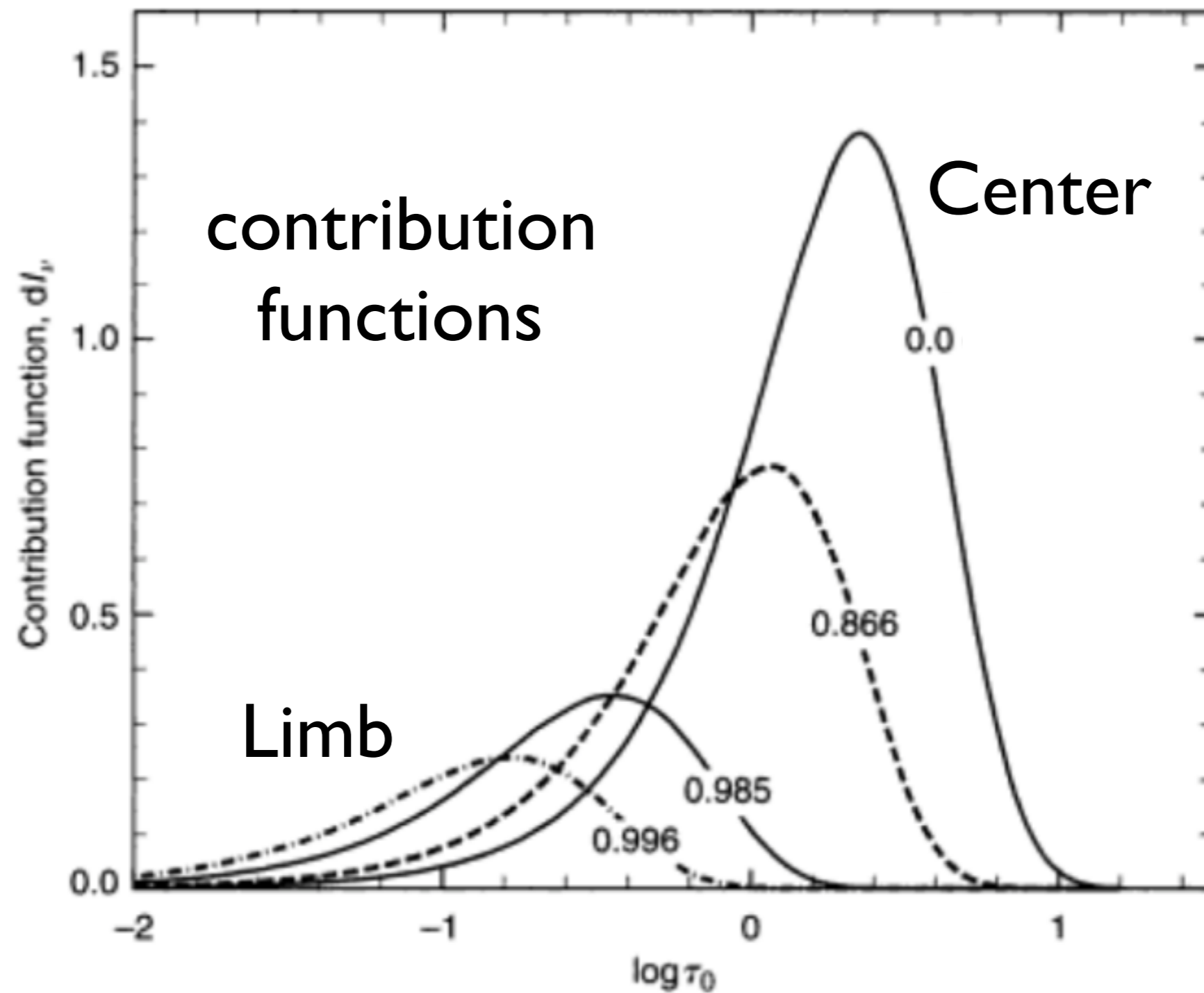
(model) temperature structure of the Sun

Vernazza et al. 1973
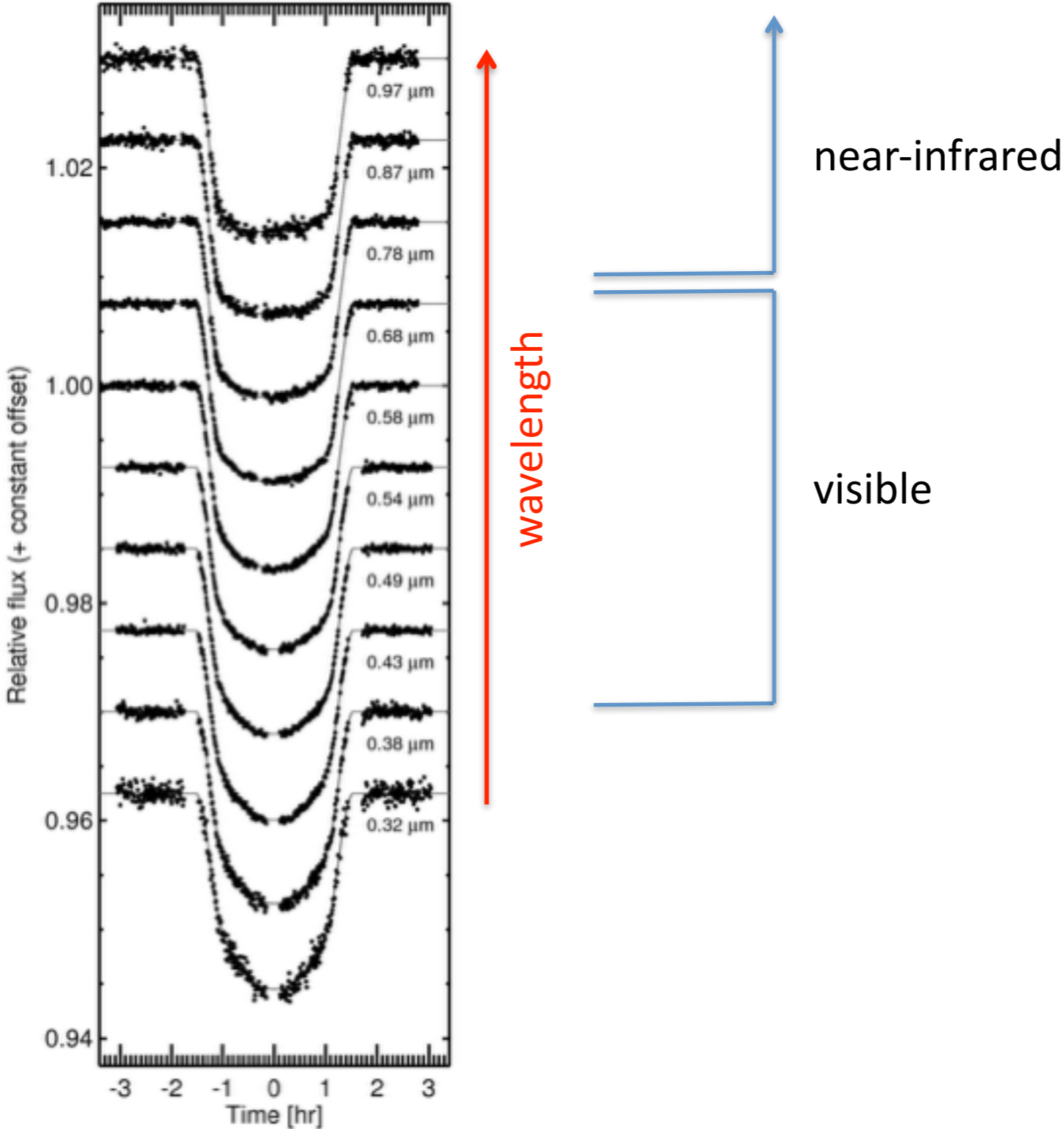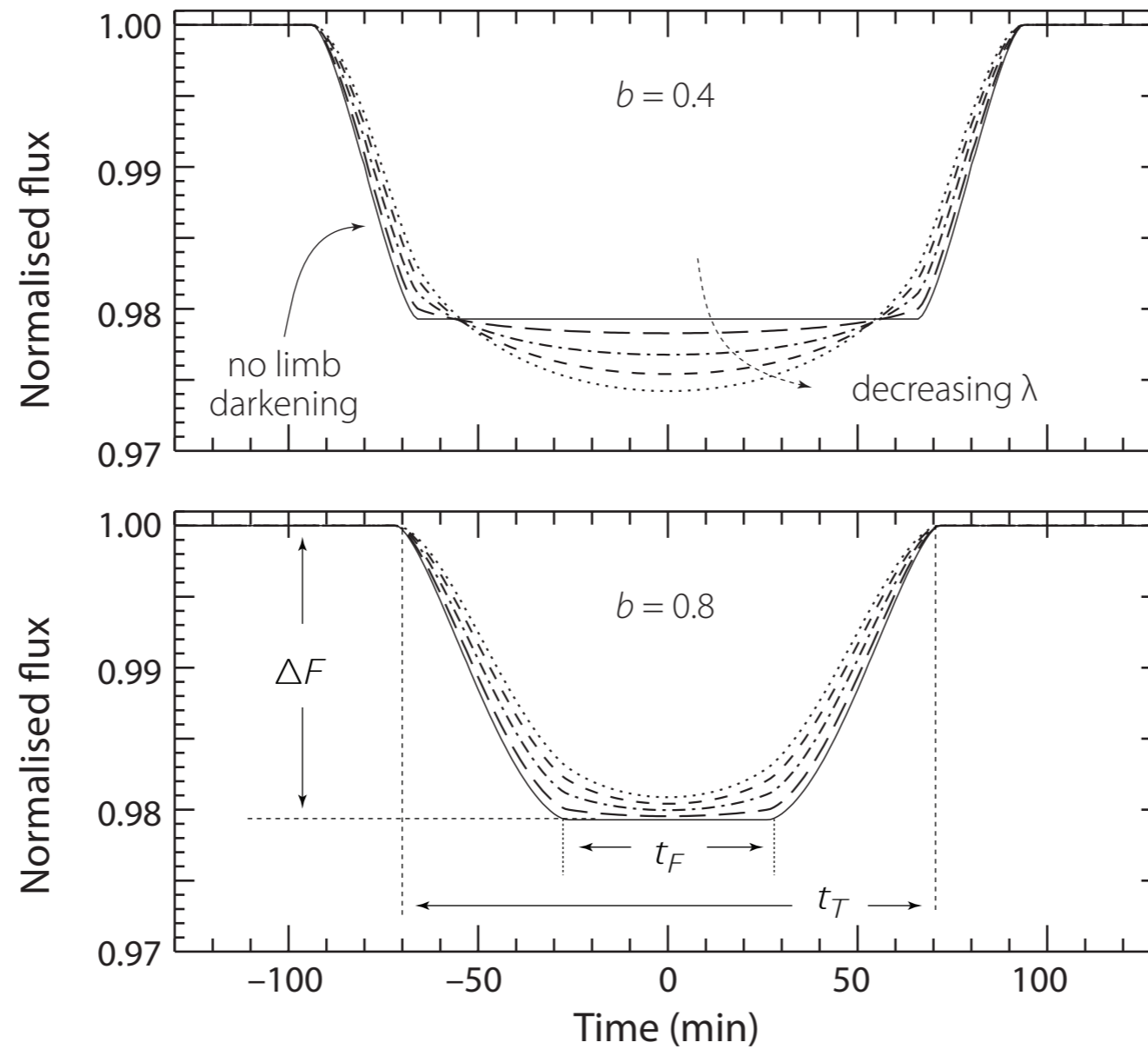
Limb Darkening

Model LCs at two different impact parameters and wavelength from 3 to 0.45 microns (Seager et al. 2003).

Limb-darkening (in practice)

HD189733 (8 microns)
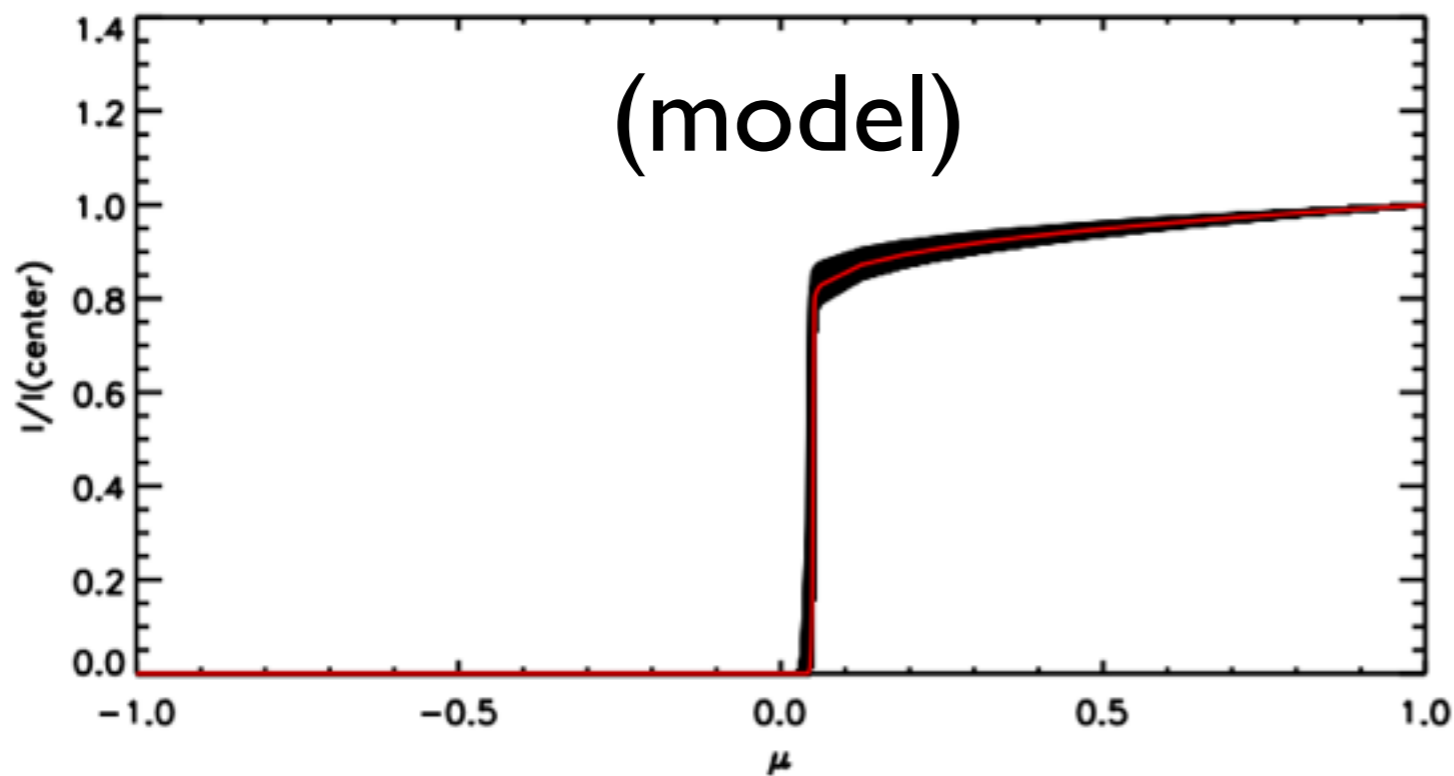
(model)

fits to models of various forms:

Linear

$$\frac{I(\mu)}{I(1)} = 1 - u(1 - \mu). \tag{1}$$

Quadratic

$$\frac{I(\mu)}{I(1)} = 1 - a(1 - \mu) - b(1 - \mu)^2. \tag{2}$$

Square root

$$\frac{I(\mu)}{I(1)} = 1 - c(1 - \mu) - d(1 - \sqrt{\mu}). \tag{3}$$

Logarithmic

$$\frac{I(\mu)}{I(1)} = 1 - e(1 - \mu) - f\mu \ln(\mu) \tag{4}$$

(Clarret et al. 2004)

Limb Darkening

GJ1214 (M4) at 1.5 μm

$$\frac{I(\mu)}{I(1)} = 1 - a(1-\mu) - b(1-\mu)^2$$

a = 0.10
b = 0.33
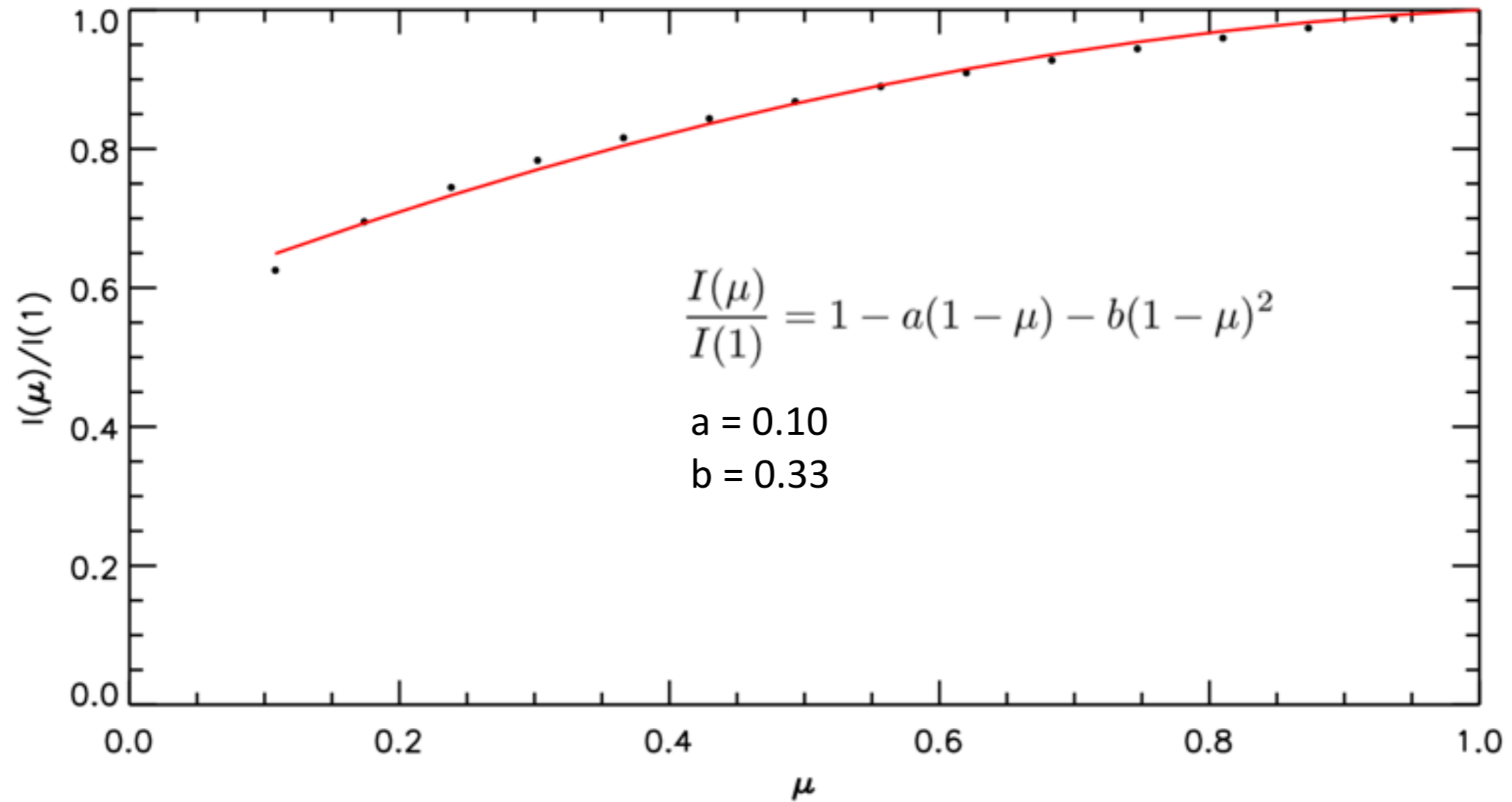
LC model requires Integration over limb darkening

$$F(r_1, r_2, d, I(r)) = \int_{visible\ area} r\, dr\, d\phi \times I(r)$$

$$= \frac{1}{2} \int_{visible\ area} dr^2\, d\phi \times \frac{dI(r)}{2dr}$$

$$= \pi \int_0^{r_2^2} dr^2\, \frac{dI(r)}{dr}(1 - \delta(r_1, r, d))$$

I(r)

r
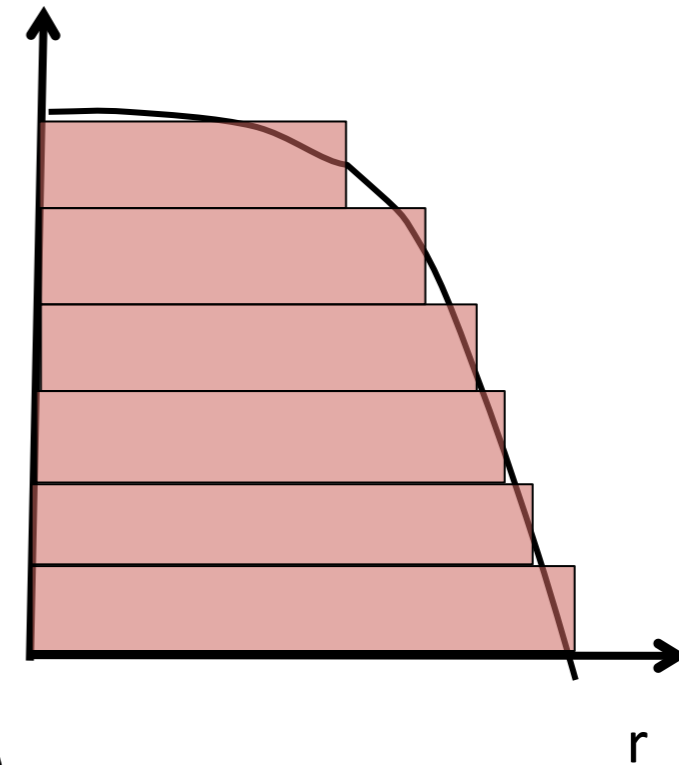
Analytic for quadratic & 'non-linear' limb-darkening models (Mandel & Agol 2002; Pal 2008)

14

If the LC data quality is high, then you can
fit for the limb-darkening coefficients
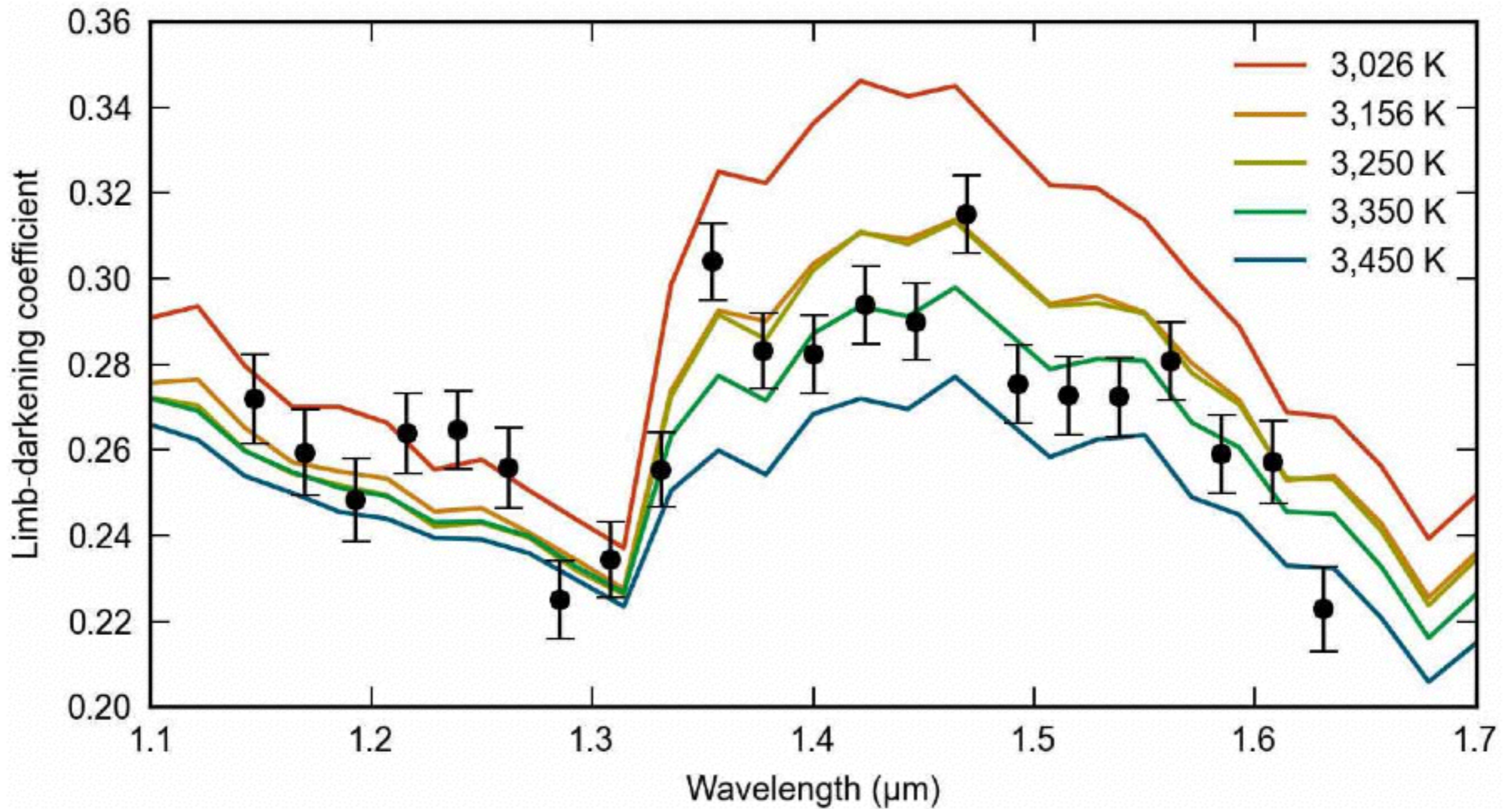
Kreidberg et al. (2014)

Beyond 'basic' light curves

- Planet asymmetry: rotational & thermal oblateness (Carter & Winn 2010; Dobbs-Dixon et al. 2012)

- Wavelength dependence (Knutson, Bean)

- Moons, rings (Kipping, Barnes)

- Secondary eclipse mapping (Majeau et al. 2012)

- Refraction (longer periods; Sidis & Sari 2011), gravitational lensing (irrelevant)

- Star spots, granulation, flares, gravity darkening (Sanchis-Ojeda, Winn)

- Light travel time, Doppler effects, relativistic effects (Avi Shporer)

- Reflected light, polarization, mutual events

- Duration variations (Miralda-Escude 2002)

Recap:

The things that you can directly measure:
- Transit duration
- Ingress/egress time
- Transit depth
- Mid-transit time
- Time between successive transits

Things that you can derive from these observables:
- Orbital period
- Orbital ephemeris
- Ratio of the size of the planet to the size of the host star (R_p/R_s)
- Impact parameter, $b = a \cos i / R_s$ for $e = 0$

Things that you can use these values to determine with K and e from RV, and estimate of M_s:
- Ratio of the size of the semi-major axis to the size of the host star (a/R_s)
- Orbital inclination
- Planet mass
- a for the orbit using Newton's version of Kepler's third law
- Radius of the star
- Radius of the planet
- Density of the star
- Surface gravity of the planet
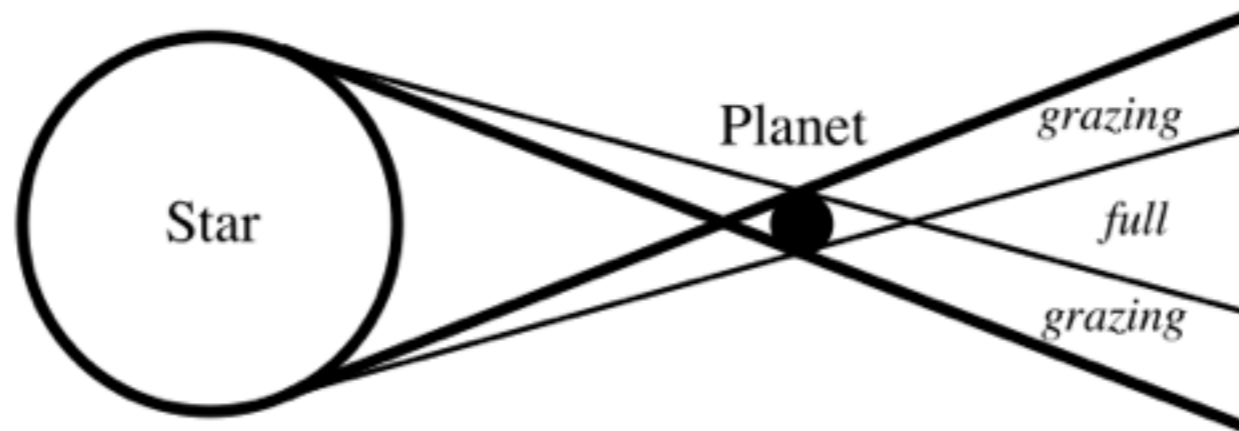
Transit Searches

- Initial transit searches focused on planets already known via RV method

- Later, large surveys (HAT, WASP, CoRoT, Kepler)

$$A_{total} = 4\pi dist^2$$

$$a_{shadow} = 4\pi dist^2(\sin\theta)$$

$$P = \frac{a_{shadow}}{A_{total}} = \frac{4\pi dist^2 \times \sin\theta}{4\pi dist^2} = \sin\theta$$

$$\sin\theta = \frac{R\star}{a_1}; \sin\theta = \frac{R_p}{a_2}$$

Celestial sphere

Star

Planet

Orbit

Θ

Shadow band

Planet

Star

grazing

full

grazing

Close-up
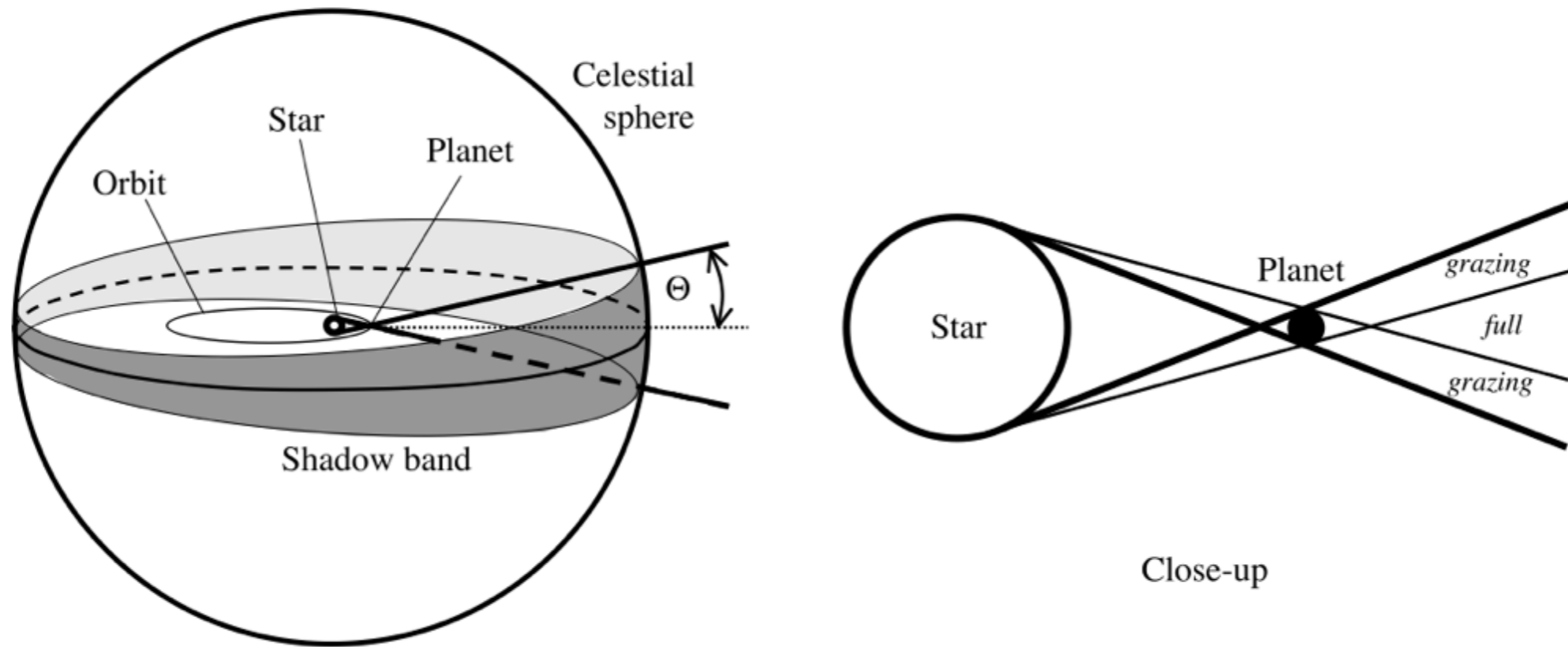
$$p_{\mathrm{tra}} = p_{\mathrm{occ}} = \frac{R_\star}{a} \approx 0.005 \left(\frac{R_\star}{R_\odot}\right)\left(\frac{a}{1\,\mathrm{AU}}\right)^{-1}$$

Winn (2011)

Transits with *eccentric* orbits:

- probability of transit changes with e

- transit time - eclipse time is strong function of e.

- transit symmetry is a function of e
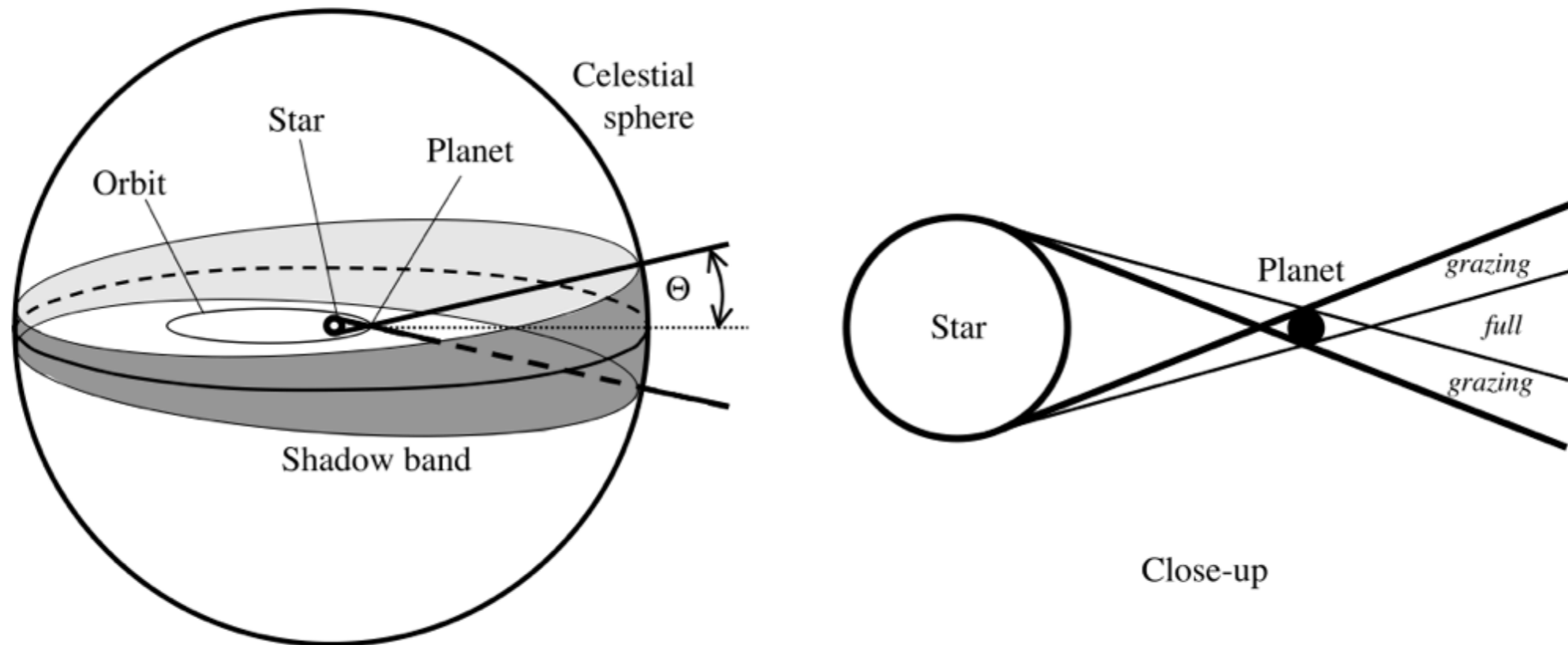
$$p_{\text{tra}} = \left(\frac{R_\star \pm R_p}{a} \right) \left(\frac{1 + e \sin \omega}{1 - e^2} \right)$$

What does this mean for transit surveys?

Celestial sphere

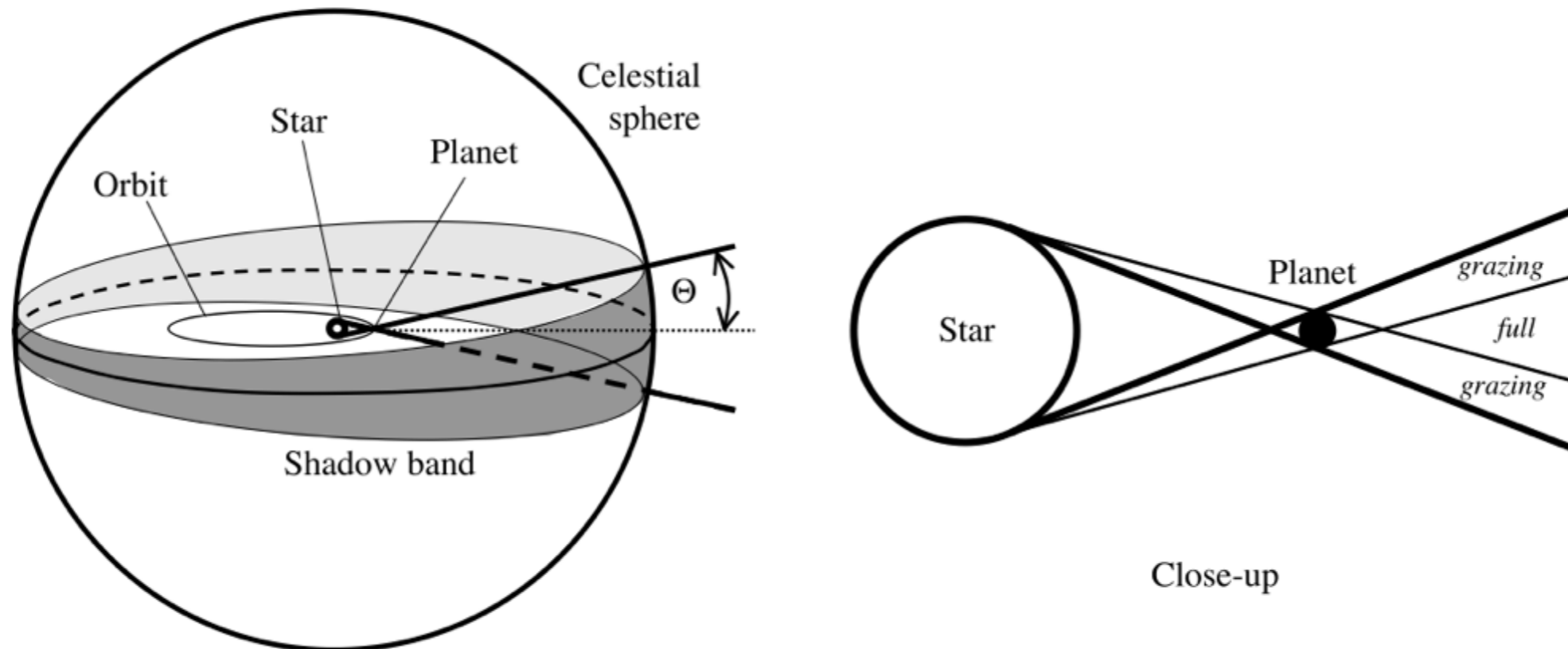Star

Planet

Orbit

Shadow band

Θ

Close-up

Star

Planet

grazing

full

grazing

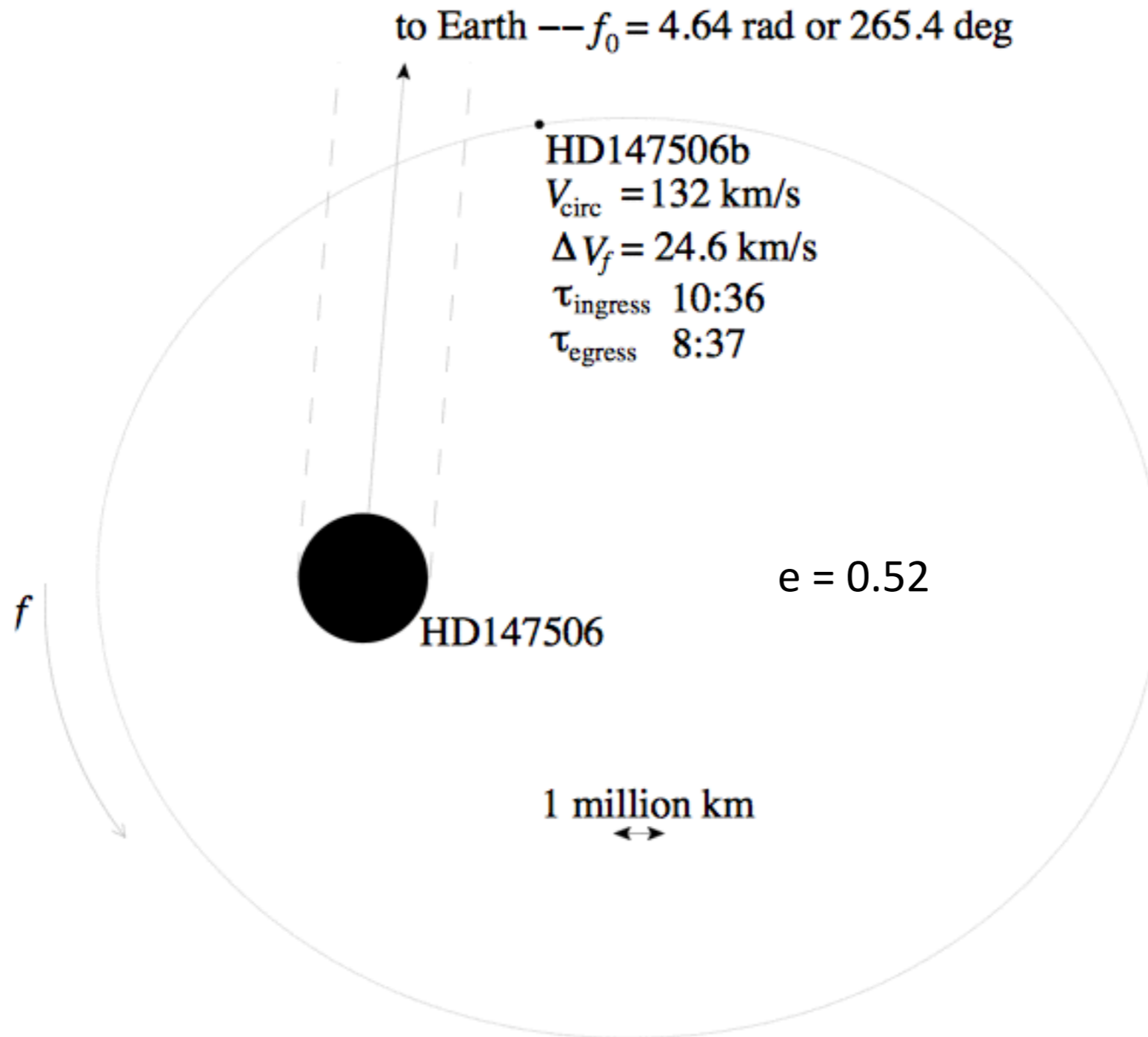$$p_{\mathrm{tra}} = \left(\frac{R_\star \pm R_p}{a} \right) \left(\frac{1 + e \sin \omega}{1 - e^2} \right)$$

For planets with same semi-major axis, Ptra increases for e > 0. Example: HD80606b has e ~ 0.93 and a ~ 0.5 au. Ptra goes from ~ 1% to ~ 8%. ... this planet transits.

Transit surveys biased toward finding ecc. planets.
Easy to correct .... if you know e.

Could have occultation or transit, not always both.

HD147506b: A Super-Massive Planet in an Eccentric Orbit Transiting a Bright Star

to Earth $-- f_0 = 4.64$ rad or 265.4 deg

HD147506b
$V_{circ} = 132$ km/s
$\Delta V_f = 24.6$ km/s
$\tau_{ingress}$ 10:36
τ_{egress} 8:37

Ingress and egress durations can differ by several minutes

f

HD147506

e = 0.52

1 million km

Barnes (2007)

Change in Velocity between ingress and egress

e=0.9
e=0.8
e=0.6
e=0.2

ΔV

True Anomaly f_0

(at mid-transit)

Barnes (2007)

Barnes (2007)
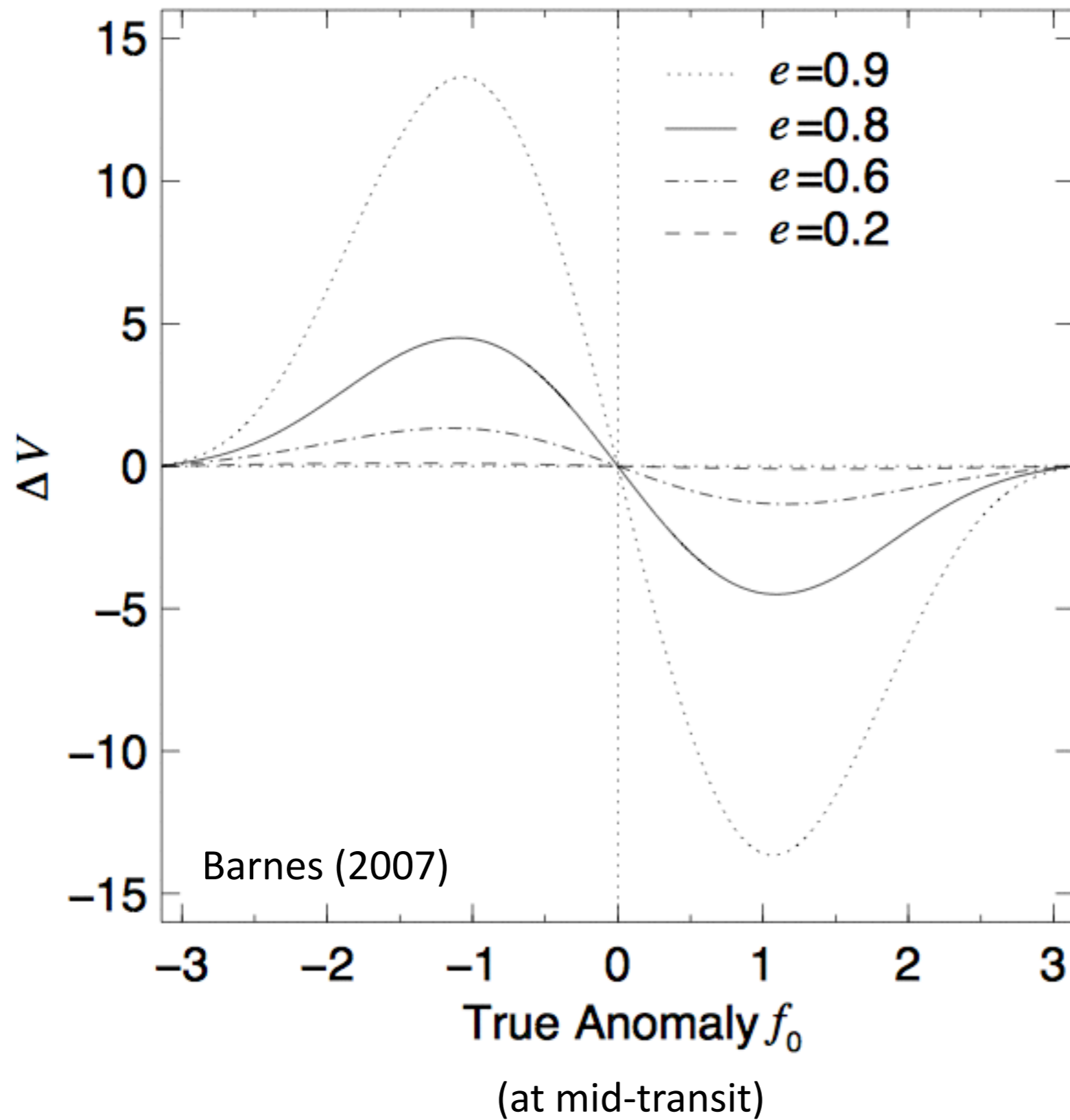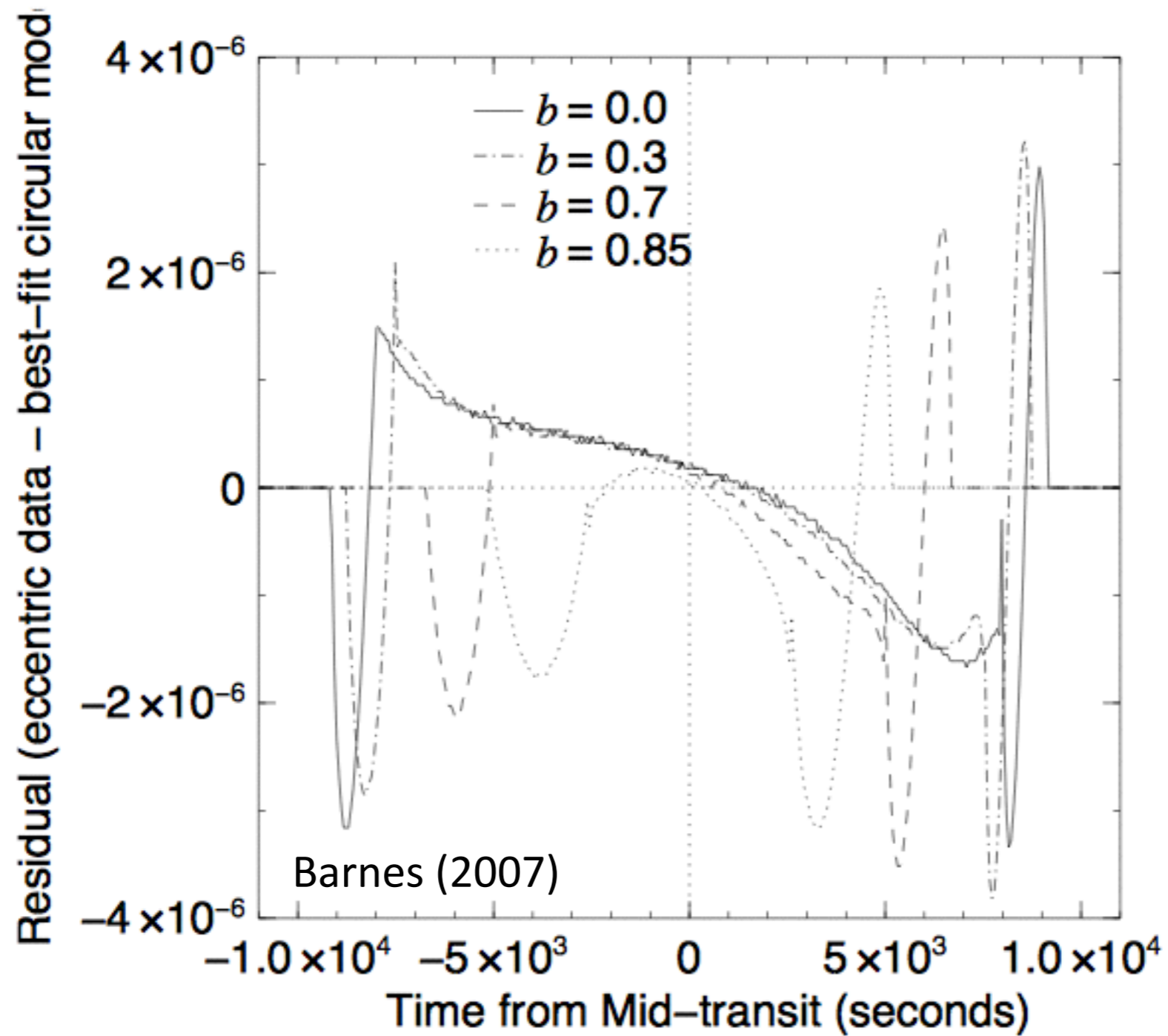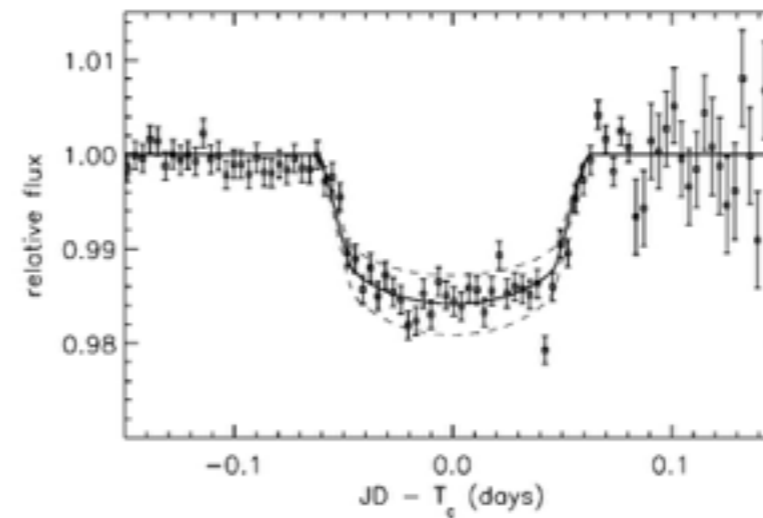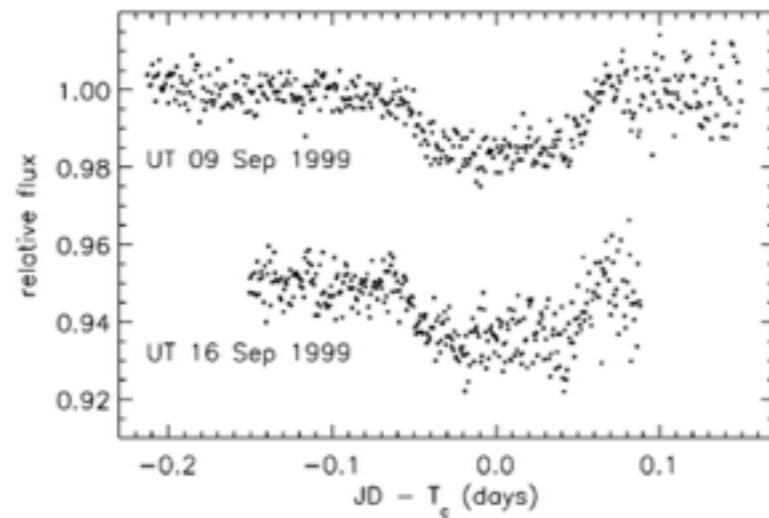
too small to measure for small planets

For Hot-Jupiters, P ~ 10% .... you only need 10 to find 1 (not exactly, but ...)

HD 209458b

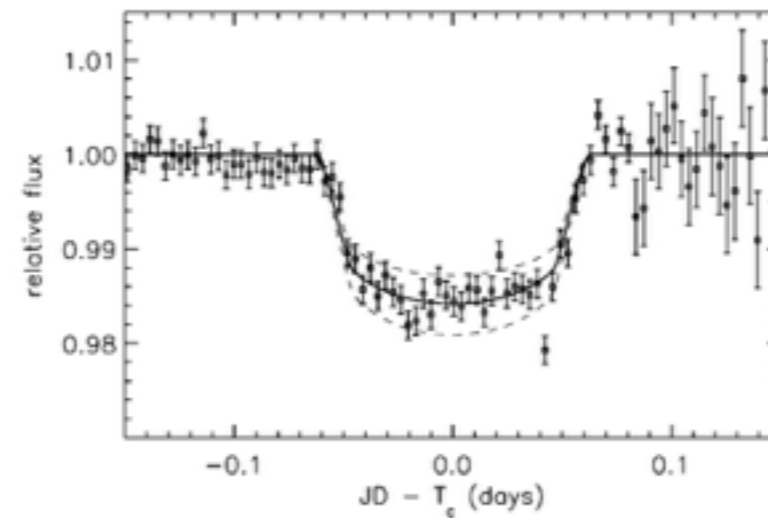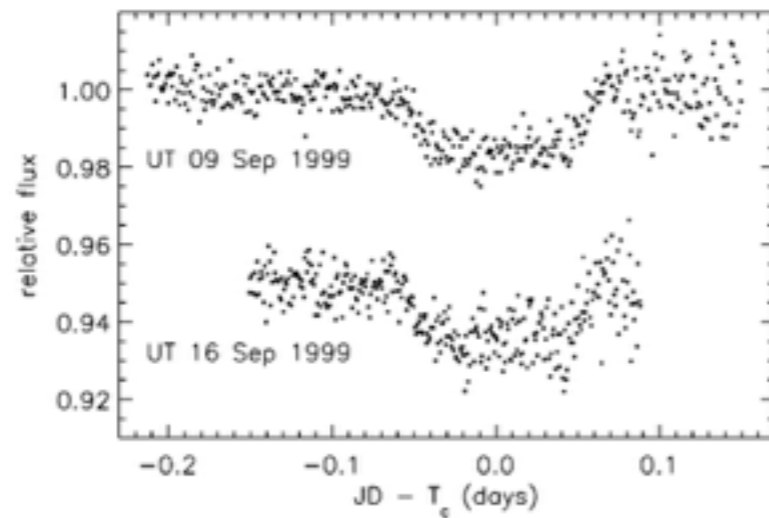Discovered when there were 11 Hot Jupiters known from RV

(from kepler.nasa.gov)

Transit Properties of Solar System Objects

Planet	Orbital Period P (years)	Semi-Major Axis a (A.U.)	Transit Duration (hours)	Transit Depth (%)	Geometric Probability (%)
Mercury	0.241	0.39	8.1	0.0012	1.19
Venus	0.615	0.72	11.0	0.0076	0.65
Earth	1.000	1.00	13.0	0.0084	0.47
Mars	1.880	1.52	16.0	0.0024	0.31
Jupiter	11.86	5.20	29.6	1.01	0.089
Saturn	29.5	9.5	40.1	0.75	0.049
Uranus	84.0	19.2	57.0	0.135	0.024
Neptune	164.8	30.1	71.3	0.127	0.015
	$P^2 M* = a^3$ $M*$ = star mass (Sun = 1)		$13 sqrt(a)$	$\% = (d_p/d*)^2$	$d*/2a$ $d*$ = dia. of star

For Hot-Jupiters, P ~ 10% .... you only need 10 to find 1
(not exactly, but ...)

For Hot-Jupiters, P ~ 10% .... you only need 10 to find 1 (not exactly, but ...)

HD 209458b

Transit discovered when there were 11 Hot Jupiters known from RV
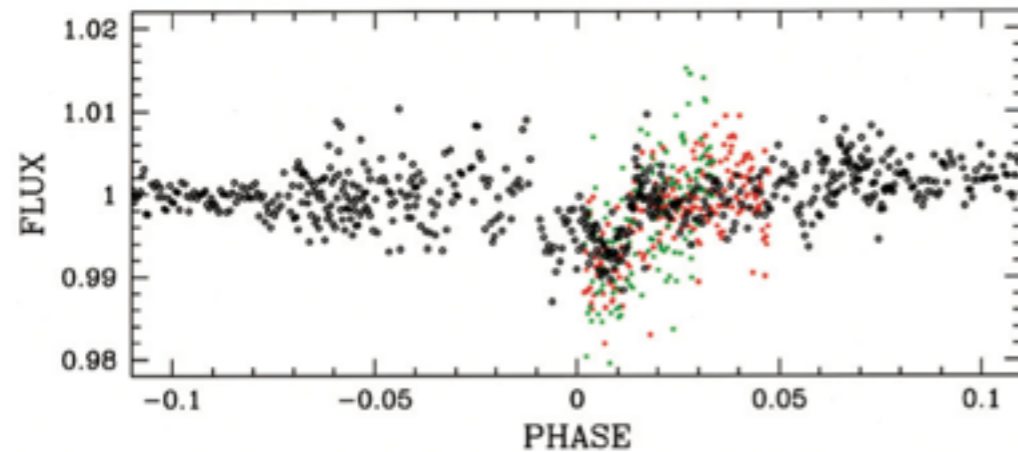
GJ 436b: the first Neptune

Fig. 1. OFXB (*black*) and Wise (*red*: 1 m, *green*: 46 cm) photometry phase-folded using the ephemerids and period presented in Maness et al. (2007).
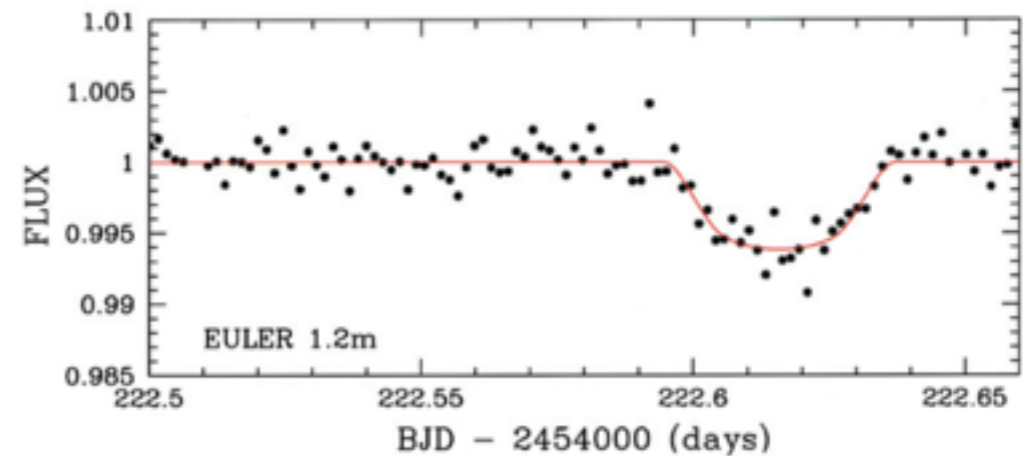

Fig. 2. Euler V-band transit photometry. The best-fit transit curve is superimposed in red.

Only a handful of known Neptune-mass planets from RV, but this one had been known for several years, prior to transit detection.

Gillon et al. 2007, ApJ, 472, L13

Star	
Stellar mass $[M_\odot]$	0.44 ($\pm$ 0.04)*
Stellar radius $[R_\odot]$	0.44 ($\pm$ 0.04)
Planet	
Period [days]	2.64385 $\pm$ 0.00009*
Eccentricity	0.16 $\pm$ 0.02*
Orbital inclination [°]	86.5 $\pm$ 0.2
Radius ratio	0.082 $\pm$ 0.005
Planet mass $[M_\oplus]$	22.6 $\pm$ 1.9
Planet radius $[R_\oplus]$	$3.95^{+0.41}_{-0.28}$
[km]	$25\,200^{+2600}_{-1800}$
T_{tr} [BJD]	$2\,454\,222.616 \pm 0.001$

Neptune: $10 < M_p < 20\ M_{Earth}$

This was a super exciting discovery!!!!!

Search for transits of known planets

55 Cnc e: a hot super-Earth

After subtracting out–of–transit variation
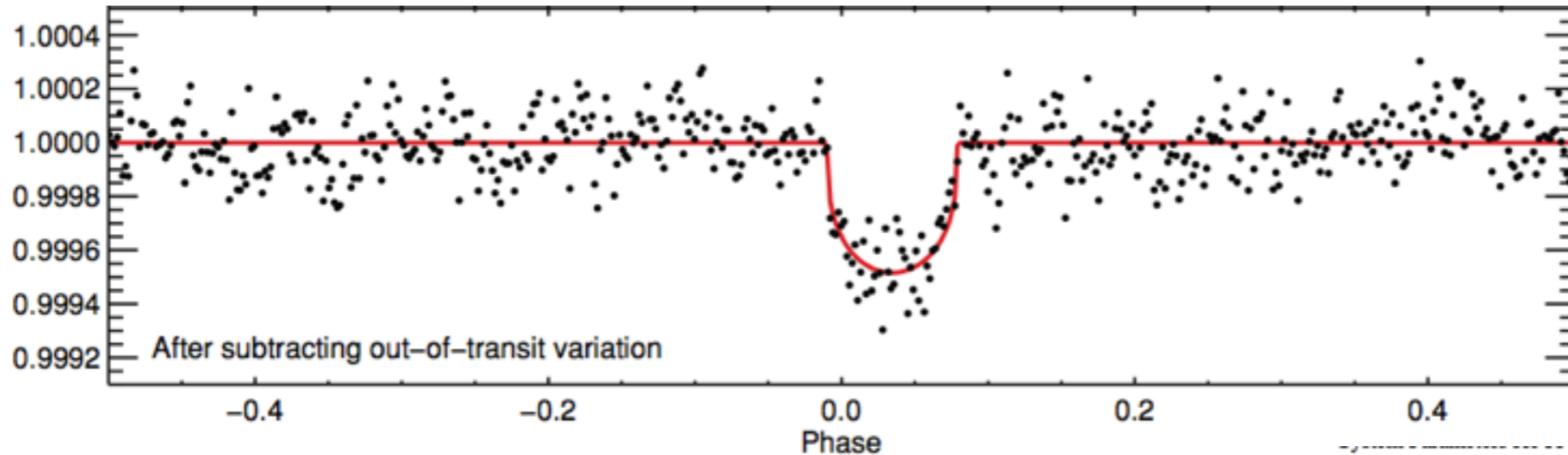
Only a handful of known super-Earths from RV, but this one had also been known since 2004!

The only transiting planet around a star that is visible with the naked eye.

Dawson & Fabrycky, 2010, ApJ, 722, 937
Winn et al. 2011, ApJ, 737, L18
Demory et al. 2011, A&A, 533, 114

| Parameter	Value
Transit epoch [HJD]	$2{,}455{,}607.05562 \pm 0.00087$
Transit depth, $(R_p/R_*)^2$ (ppm)	380 ± 52
Transit duration, first to fourth contact (days)	0.0658 ± 0.0013
Transit ingress or egress duration (days)	0.00134 ± 0.00011
Planet-to-star radius ratio, R_p/R_*	0.0195 ± 0.0013
Transit impact parameter	0.00 ± 0.24
Orbital inclination, i (deg)	90.0 ± 3.8
Fractional stellar radius, R_*/a	0.2769 ± 0.0043
Fractional planetary radius, R_p/a	0.00539 ± 0.00038
Orbital distance, a (AU)	0.01583 ± 0.00020
Amplitude of orbital phase modulation, ϵ_{pha} (ppm)	168 ± 70
Occultation depth, ϵ_{occ} (ppm)	48 ± 52
Planetary mass ($M_\oplus$)	8.63 ± 0.35
Planetary radius ($R_\oplus$)	2.00 ± 0.14
Planetary mean density (g cm^{-3})	$5.9 \pm {}^{1.5}_{1.1}$
Planetary surface gravity (m s^{-2})	$21.1 \pm {}^{3.5}_{2.7}$

super-Earth: $2 < M_p < 10\ M_{Earth}$

Geometric Probability is only part of the problem ... Suppose you know nothing about planets, but want to find them using the transit method. How many stars must you observe before finding just one?

N(stars) ~ 1/(f x P_{tra}) ... where f = freq. of planets.

If 1 / 100 stars have giant planets at 0.05AU, then observing > 1000 stars might yield one.

Turn it around, observe 100, 000s and you can determine f .... this is the main idea behind missions like Kepler and CoRoT.

Transit Searches: equipment
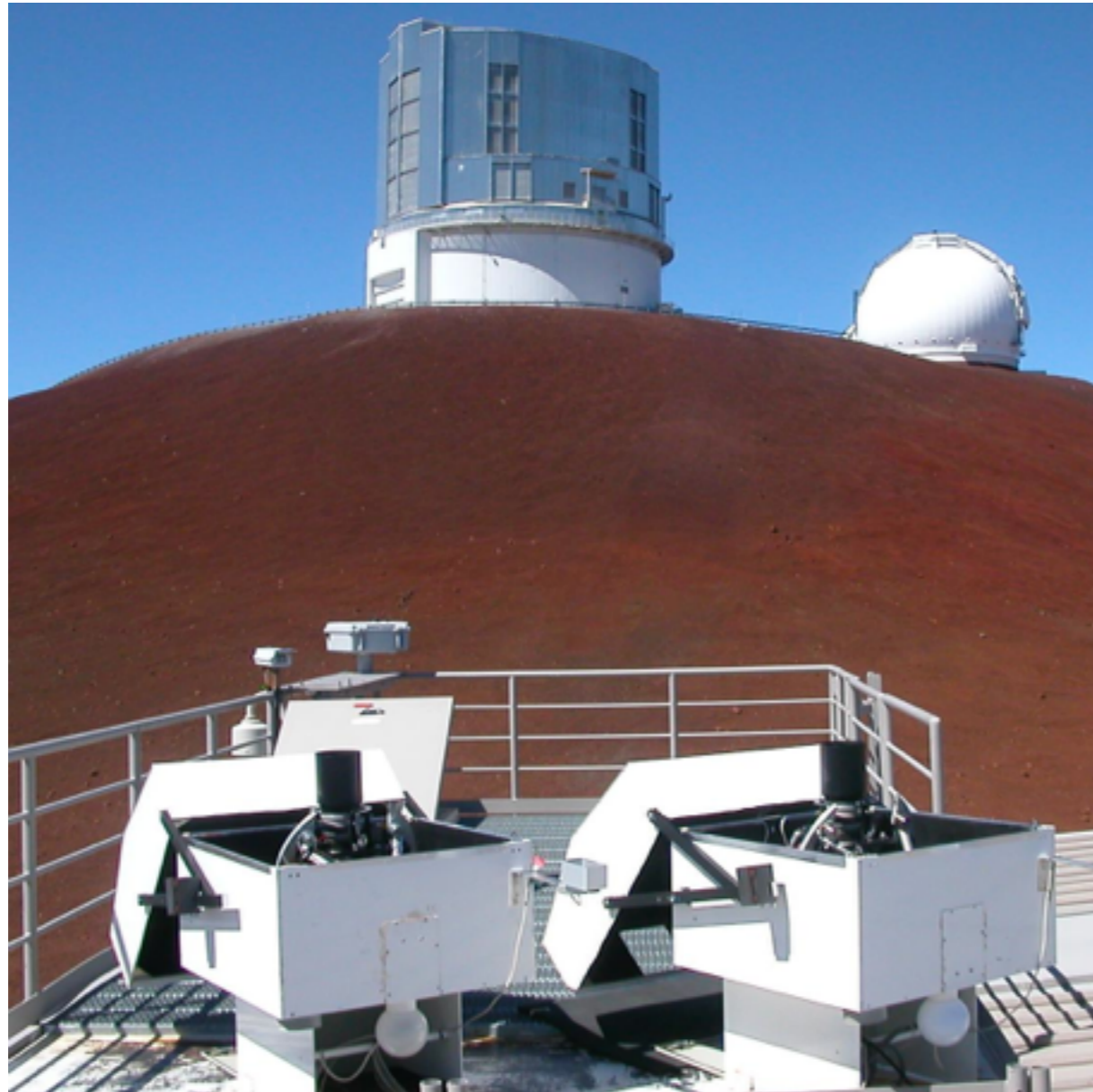
HATNet

Off-the-shelf Canon 200mm f/1.8 lenses with CCD detectors

Distributed network: 4 telescopes in AZ, 2 in HI

~40 transiting planets found to date, mostly Jupiters, but a few Neptunes

Transit Searches: equipment

SuperWASP

Off-the-shelf Canon 200mm f/1.8 lenses with CCD detectors

Two stations, one in the Canary Islands, and one in South Africa

Each station has eight cameras

~100 transiting planets found to date, all Jupiters

Transit Searches: equipment

SuperWASP

Off-the-shelf Canon 200mm f/1.8 lenses with CCD detectors

Two stations, one in the Canary Islands, and one in South Africa

Each station has eight cameras

80 transiting planets found to date, all Jupiters

NASA EXOPLANET ARCHIVE
NASA EXOPLANET SCIENCE INSTITUTE

Home   About the Archive   Data   Tools   User Guides & Helpdesk

☐ SuperWASP Survey Information

Data from the first WASP public data release were acquired from 2004 to 2008 and are made available via the Exoplanet Archive by the SuperWASP consortium.
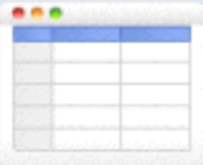
SuperWASP Survey

SuperWASP is the UK's leading extra-solar planet detection program comprised of a consortium of eight academic institutions. SuperWASP consists of two robotic observatories that operate continuously throughout the year, allowing coverage of both hemispheres of the sky. The first, SuperWASP-North, is located on the island of La Palma among the Isaac Newton Group(ING) of telescopes. The second, SuperWASP-South, is located at the site of the South African Astronomical Observatory (SAAO), just outside Sutherland, South Africa. The observatories each consist of eight wide-angle cameras that simultaneously monitor the sky for planetary transit events. The eight cameras allow the monitoring of millions of stars simultaneously, enabling the detection of rare transit events.

Exoplanet Archive SuperWASP resources

The Exoplanet Archive include nearly 18 million WASP time series. See the links below to search or download these data.

NOTE: Not all confirmed WASP planet light curves are available in the first public WASP data release, but may be included in future releases. To retrieve the currently available public WASP light curves for confirmed WASP planets, please see the Bulk Download page.

	Interactive Tables (Also see: How to use interactive tables)	API Query Documentation
SuperWASP Time Series Search Interface		

- SuperWASP Use Cases and FAQ
- SuperWASP Processing Performed at NExScI
- SuperWASP Bulk Download
- Distributions of WASP Targets

# Transiting Planets with LSST I: Potential for LSST Exoplanet Detection

Michael B. Lund, Joshua Pepper, Keivan G. Stassun

The Large Synoptic Survey Telescope (LSST) has been designed in order to satisfy several different scientific objectives that can be addressed by a ten-year synoptic sky survey. However, LSST will also provide a large amount of data that can then be exploited for additional science beyond its primary goals. We demonstrate the potential of using LSST data to search for transiting exoplanets, and in particular to find planets orbiting host stars that are members of stellar populations that have been less thoroughly probed by current exoplanet surveys. We find that existing algorithms can detect in simulated LSST light curves the transits of Hot Jupiters around solar-type stars, Hot Neptunes around K dwarfs, and planets orbiting stars in the Large Magellanic Cloud. We also show that LSST would have the sensitivity to potentially detect Super-Earths orbiting red dwarfs, including those in habitable zone orbits, if they are present in some fields that LSST will observe. From these results, we make the case that LSST has the ability to provide a valuable contribution to exoplanet science.

Transit Searches: timeline

exoplanets.org | 4/20/2013

HD 209458b

Distribution

First Publication Date
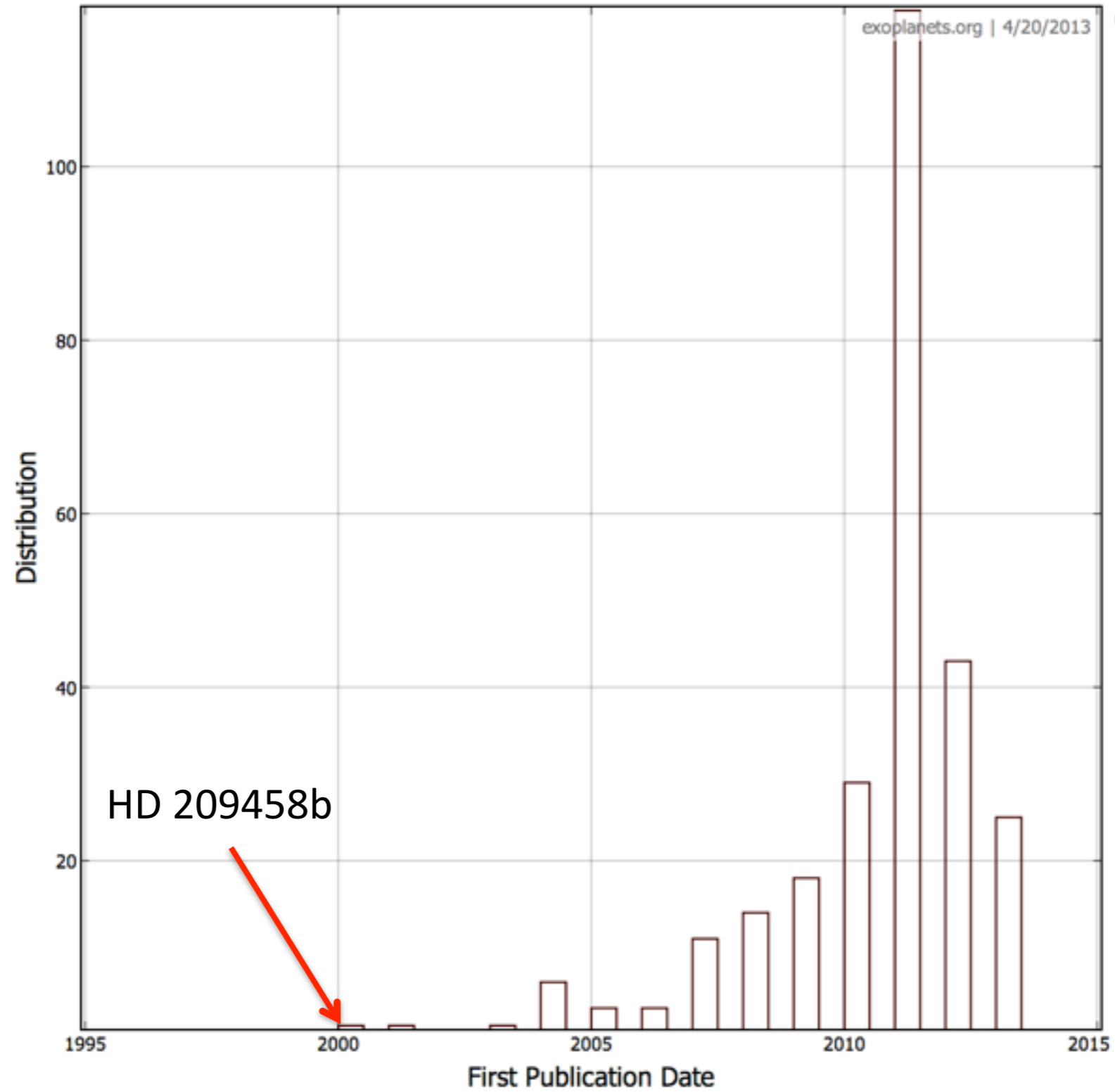
Transit Searches: why the drought?

1. More noise than expected from the Earth's atmosphere

Scintillation:

$$\sigma_{\rm scin} = \sigma_0 \frac{({\rm Airmass})^{7/4}}{D^{2/3}(\Delta t)^{1/2}} \exp\left(-\frac{h}{8000 \ {\rm m}}\right)$$

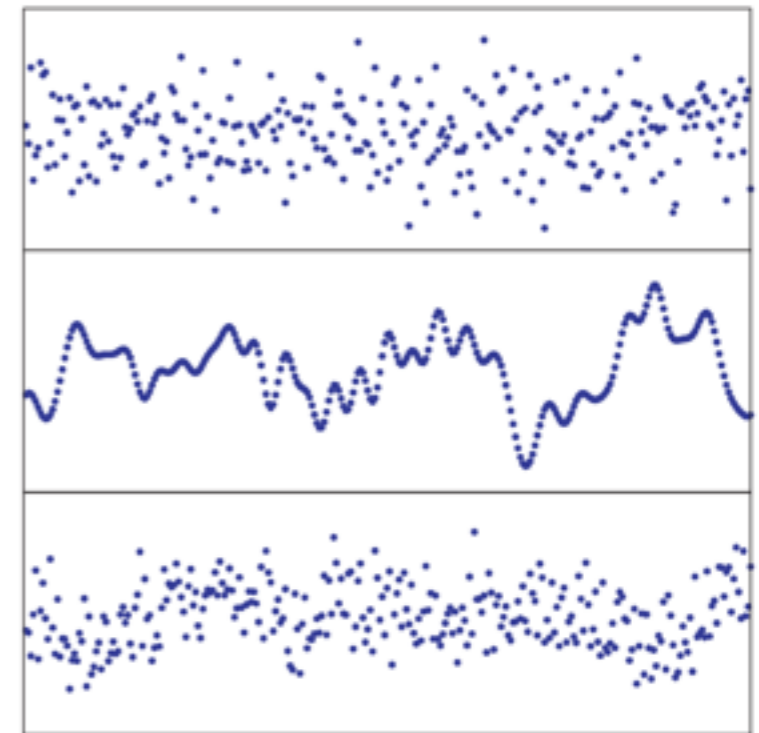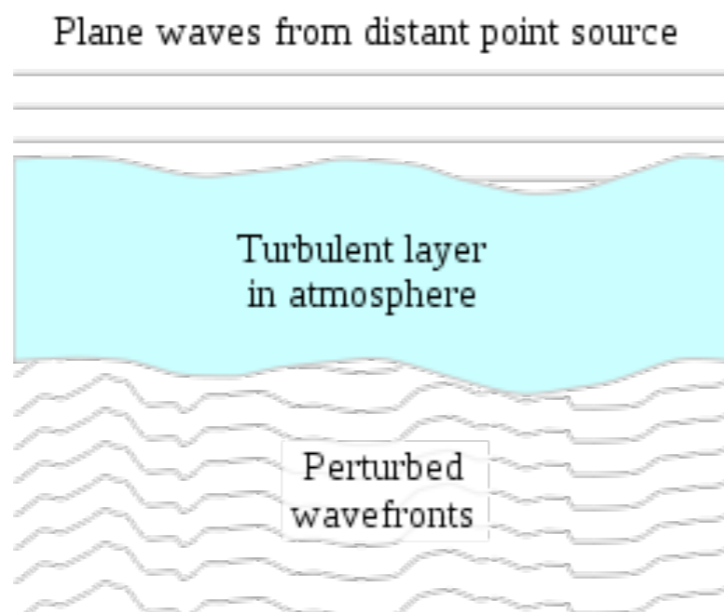The variations in intensity component of atmospheric 'seeing'.

Plane waves from distant point source

Turbulent layer in atmosphere

Perturbed wavefronts

Figure 2. Light curves with white noise only (top panel), red noise only (middle panel) and white and red noise (bottom panel). Typical light curves from a high-precision rapid time-series photometry for bright targets in transit surveys resemble portions of the bottom-panel curve.

Also "systematics" often have time variations of the same order as close-in planet transit durations.

Transit Searches: why the drought?

2. A high rate of astrophysical false positives
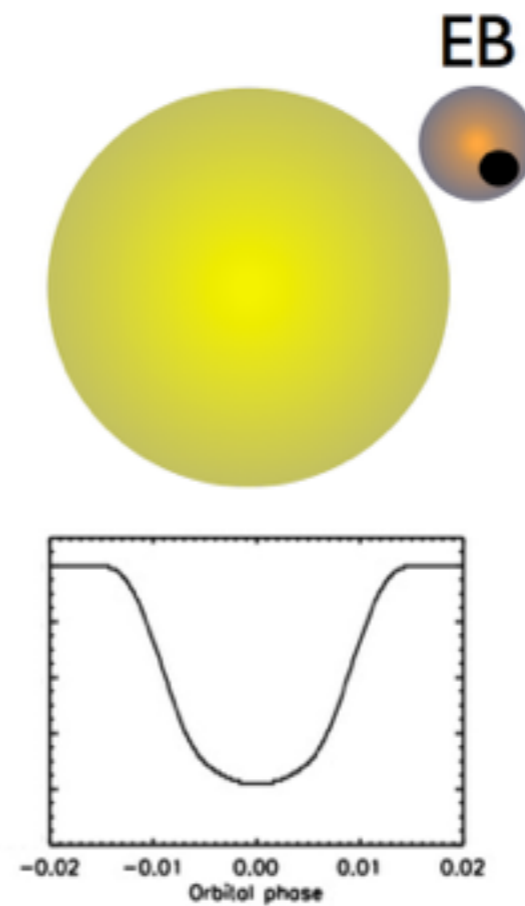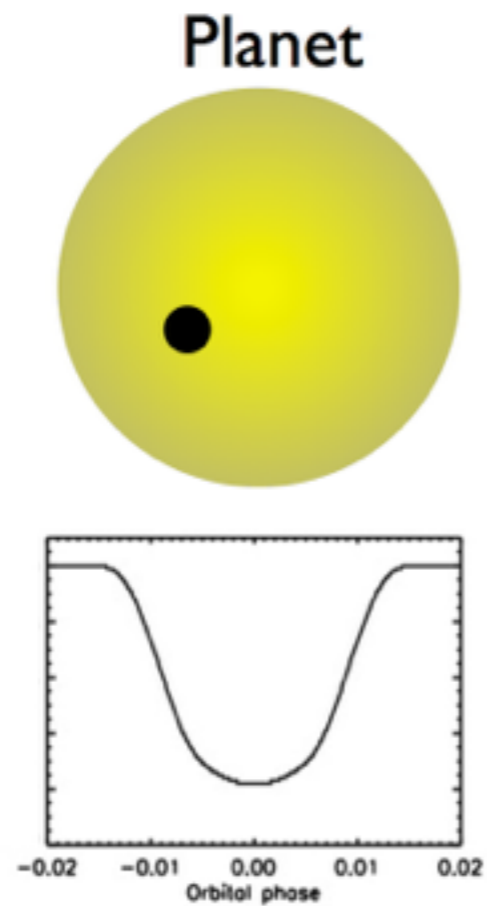
Transit Searches: why the drought?

3. Hot Jupiters are not very common

Frequency is a little less than 1%

Transits From Space:
2007+

Transit Searches: equipment

COROT (CNES+ESA)

A 27cm diameter space telescope dedicated to finding transiting planets

Cost: $170M

Launched in 2007

Observing strategy is to stare at fields for 150 days

~ 30 transiting planets found, plagued by false-positives, mostly Jupiters

First transiting super-Earth: COROT-7b

Spacecraft failure in late 2012

COROT-7b

The first transiting super-Earth, but difficult to follow-up

Parameters	Solutions using filtering algorithm		Adopted solution
	with the Pre-whitening	with the rotation harmonics	
	CoRoT-7b		
Period [days]	$0.85353 \pm 2 \times 10^{-5}$	0.8536 (fixed)	$0.853585 \pm 2.4 \times 10^{-5}$ (‡)
T_{tr} [JD]	2 454 446.7311 (fixed)	$2\,454\,446.721 \pm 0.028$	$2\,454\,446.731 \pm 0.003$ (‡)
T_0 [JD]		$2\,454\,446.508 \pm 0.029$	
K [m s^{-1}]	$(4.16 \pm 0.27)^\dagger\ 3.33 \pm 0.27\ (\pm1)^*$	$(1.9 \pm 0.4)^\dagger\ 3.8 \pm 0.8$	3.5 ± 0.6
e	0.07 ± 0.067	0 (fixed)	0
ω [deg]	91.55 ± 49.27	180 (fixed)	180
m [$M_\oplus$]	4.5 ± 1	5.2 ± 1	4.8 ± 0.8
a [AU]			0.017

Parameter	Value	Uncertainty
Period (day)	0.853585	$\pm 2.4\ 10^{-5}$
a (AU)	0.0172	$\pm 2.9 \times 10^{-4}$
$a/R_\star$	4.27	± 0.20
T_{14} (h)	1.125	± 0.05
impact parameter z	0.61	± 0.06
$k = R_{pl}/R_\star$	0.0187	$\pm 3 \times 10^{-4}$
R_{pl}/R_{Earth}	1.68	± 0.09
M_{pl}/M_{Earth}	<21	
i (deg)	80.1	± 0.3

Leger et al. 2009, A&A, 506, 287
Queloz et al. 2009, A&A, 506, 303

Transit Searches: equipment

Kepler (NASA)
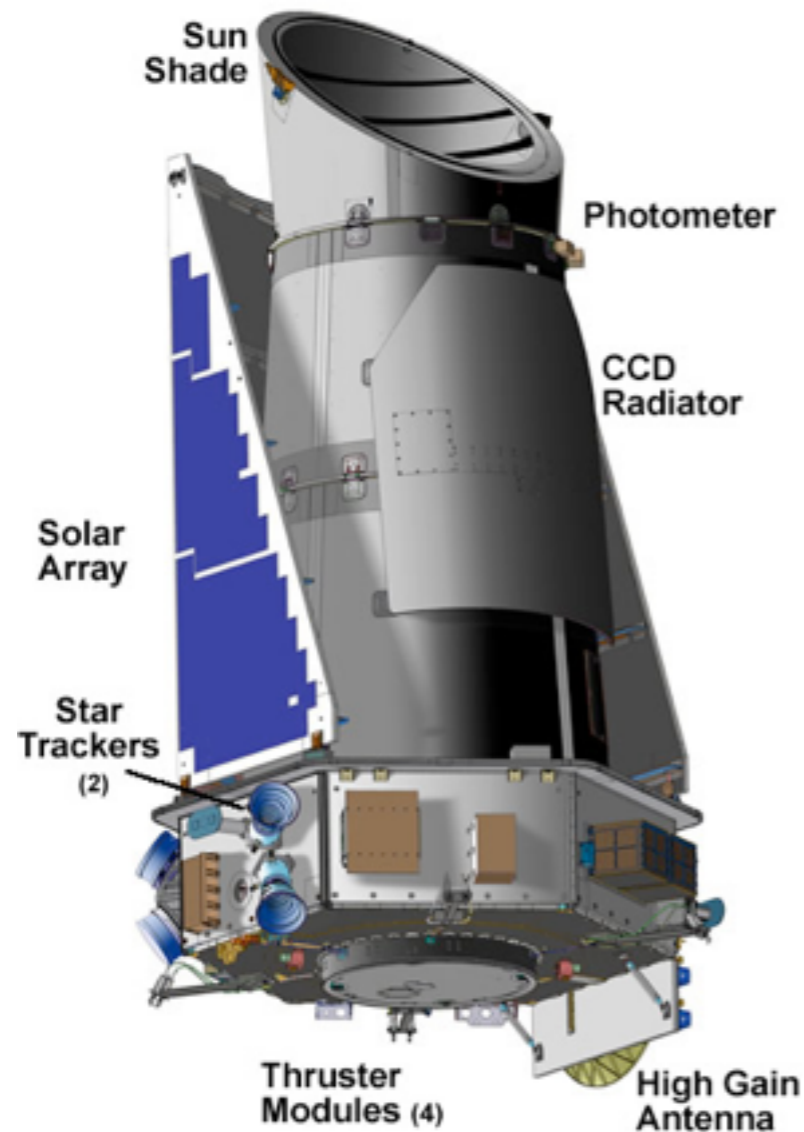
A custom-built, 0.95m diameter space telescope dedicated to finding transiting planets

Cost: $600M

Launched in 2009

Observing strategy is to stare at the same field for 3+ years

134 transiting planets found to date

Spacecraft failure in May 2013 —> K2 mission

TESS: Transiting Exoplanet Survey Satellite
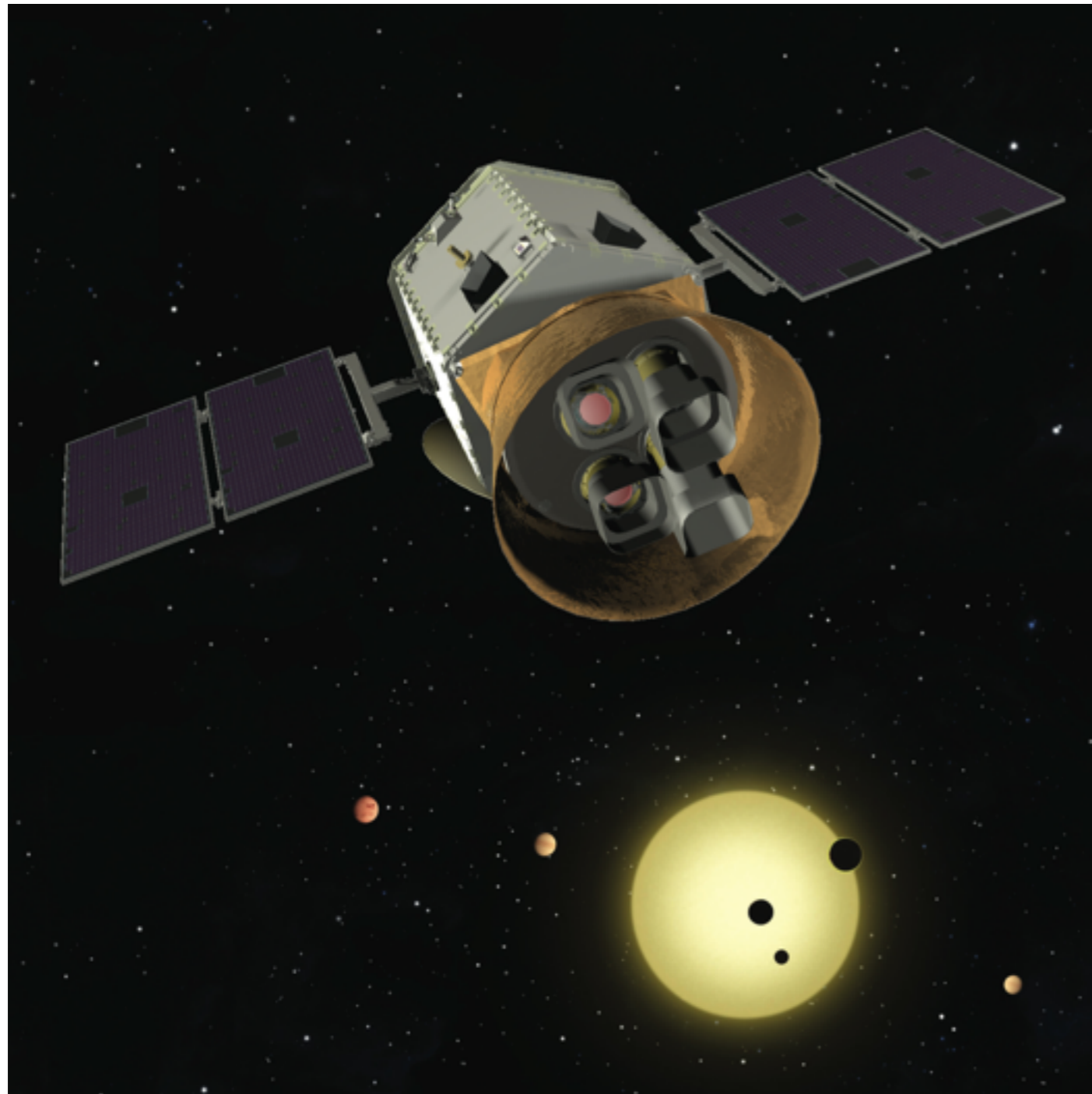
A new space telescope to find small transiting planets around bright stars – these are the planets that we could study in more detail.

NASA mission

$200M cost

4 x 10cm lenses

Mostly planets in short-period orbits, but may find habitable-zone planets around small stars

PLATO	
PLAnetary Transits and Oscillations of stars	
Theme	What are the conditions for planet formation and the emergence of life?
Primary Goal	Detection and characterisation of terrestrial exoplanets around bright solar-type stars, with emphasis on planets orbiting in the habitable zone.
Measurements	▪ Photometric monitoring of a large number of bright stars for the detection of planetary transits and the determination of the planetary radii (around 2% accuracy) ▪ Ground-based radial velocity follow-up observations for the determination of the planetary masses (around 10% accuracy) ▪ Asteroseismology for the determination of stellar masses, radii, and ages (up to 10% of the main sequence lifetime) ▪ Identification of bright targets for spectroscopic follow-up observations of planetary atmospheres with other ground and space facilities
Wavelength	Optical
Telescope	A number of small, optically fast, wide-field telescopes
Orbit	Large amplitude libration orbit around Sun-Earth Lagrangian point, L2
Lifetime	at least 6 years
Type	M-class Mission

covers about 50% of sky

proposed in 2007 …. 2024? launch
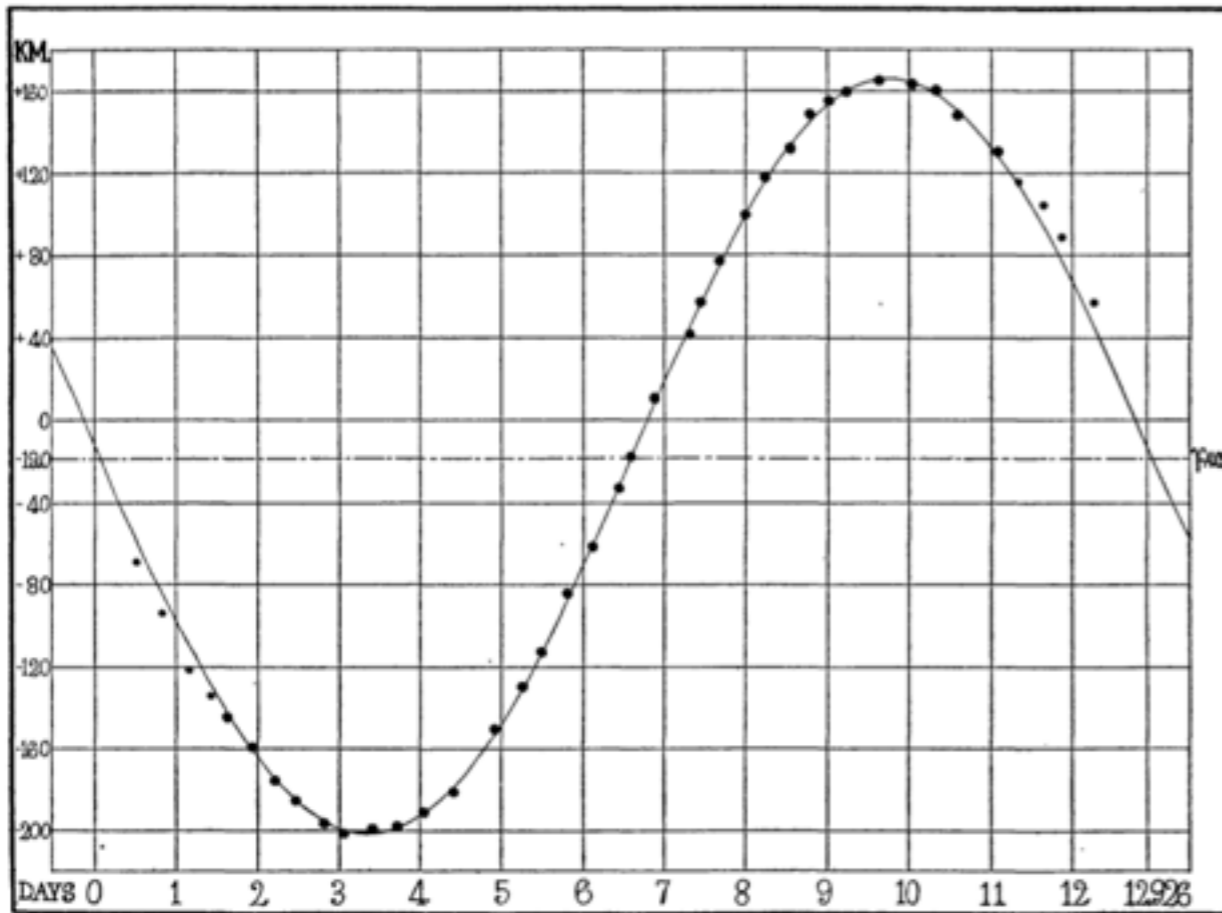
FIG. 1

The large dots are the normal places given by observation. Each place is determined by grouping from six to fifteen spectrograms. An unusually good agreement between observed motion and computed elliptical motion exists, and secondary oscillations are absent. The abnormal residuals given by the small dots will be explained in the paragraphs immediately following as a newly measured quantity here called the *rotational effect*.
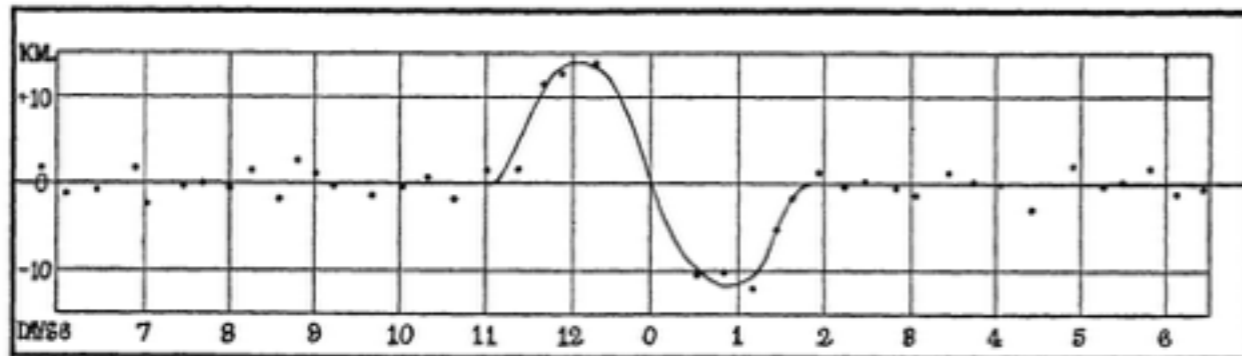
FIG. 2

"Rotational Effect"

predicted in 1890's (Holt)
... observed in 1920s

sleepers ...

Citations/Publication Year for 1924ApJ....60...15R

Rossiter (1924)
(1886 -- 1977)

Citations/Publication Year for 1924ApJ....60...22M
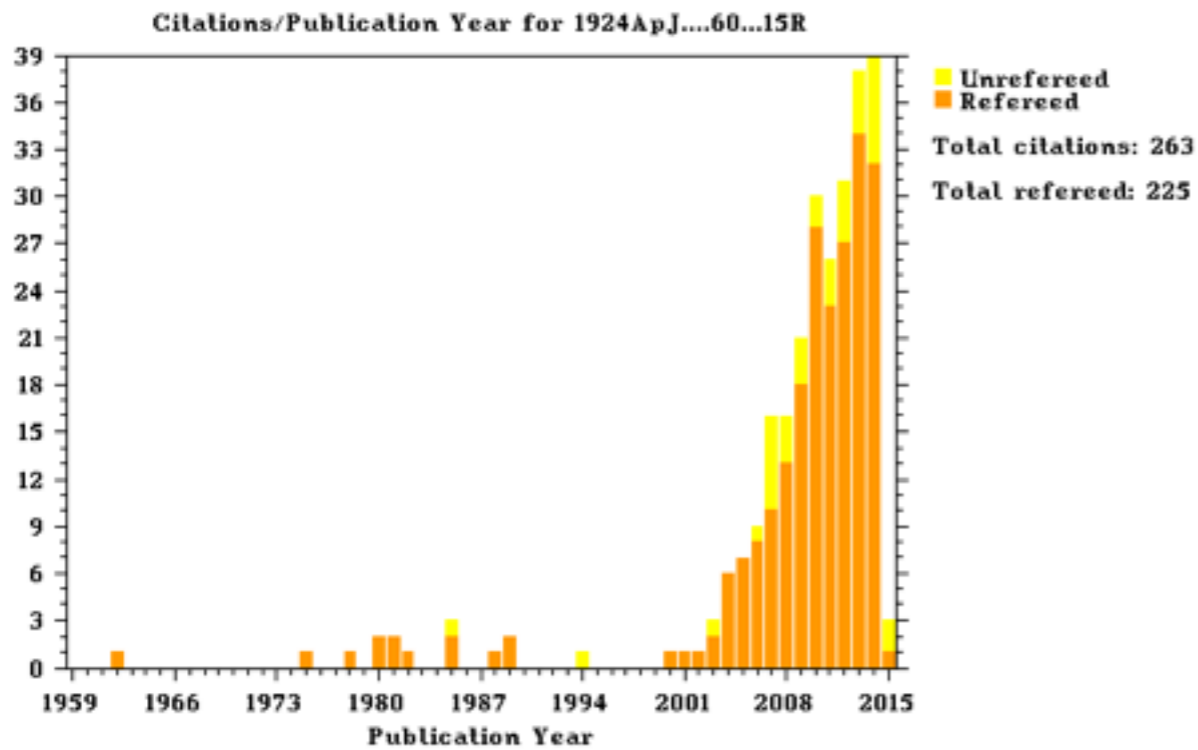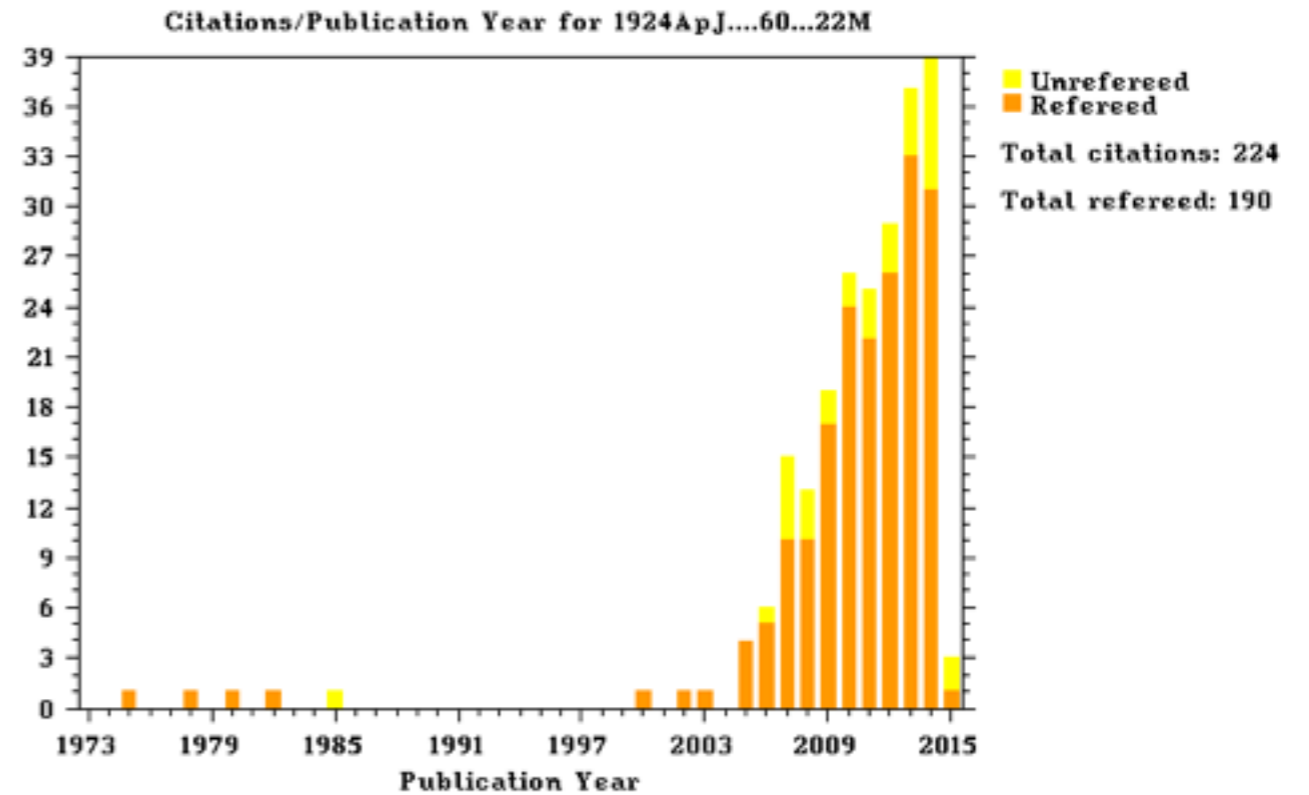
McLaughlin (1924)
(1901 -- 1965)

Rotational Broadening:

$$\mathbf{v} = \mathbf{\Omega} \times \mathbf{R}$$
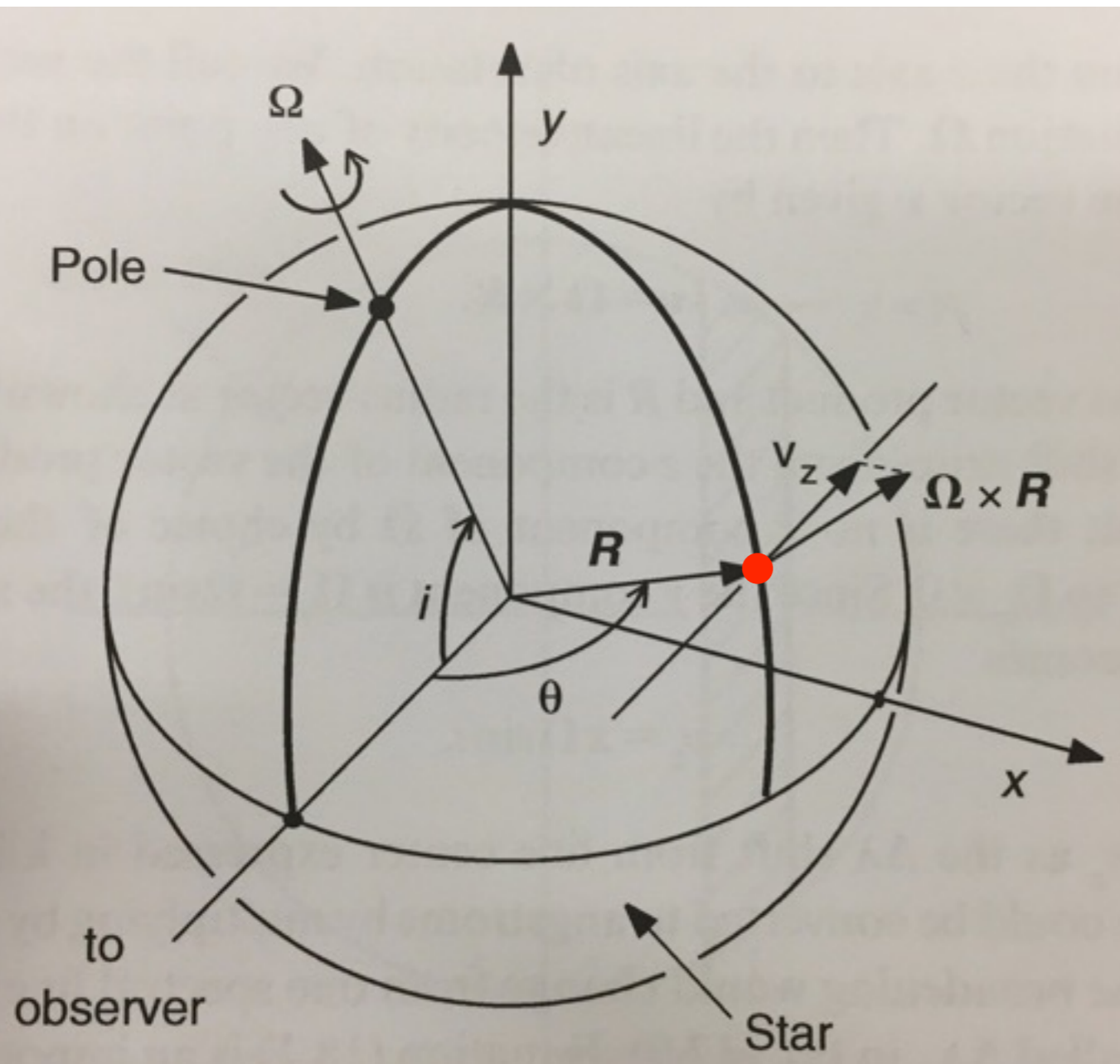
Orient coordinate system so
that rotation axis is in y-z plane

Rotational Broadening:

$$\mathbf{v} = \mathbf{\Omega} \times \mathbf{R}$$
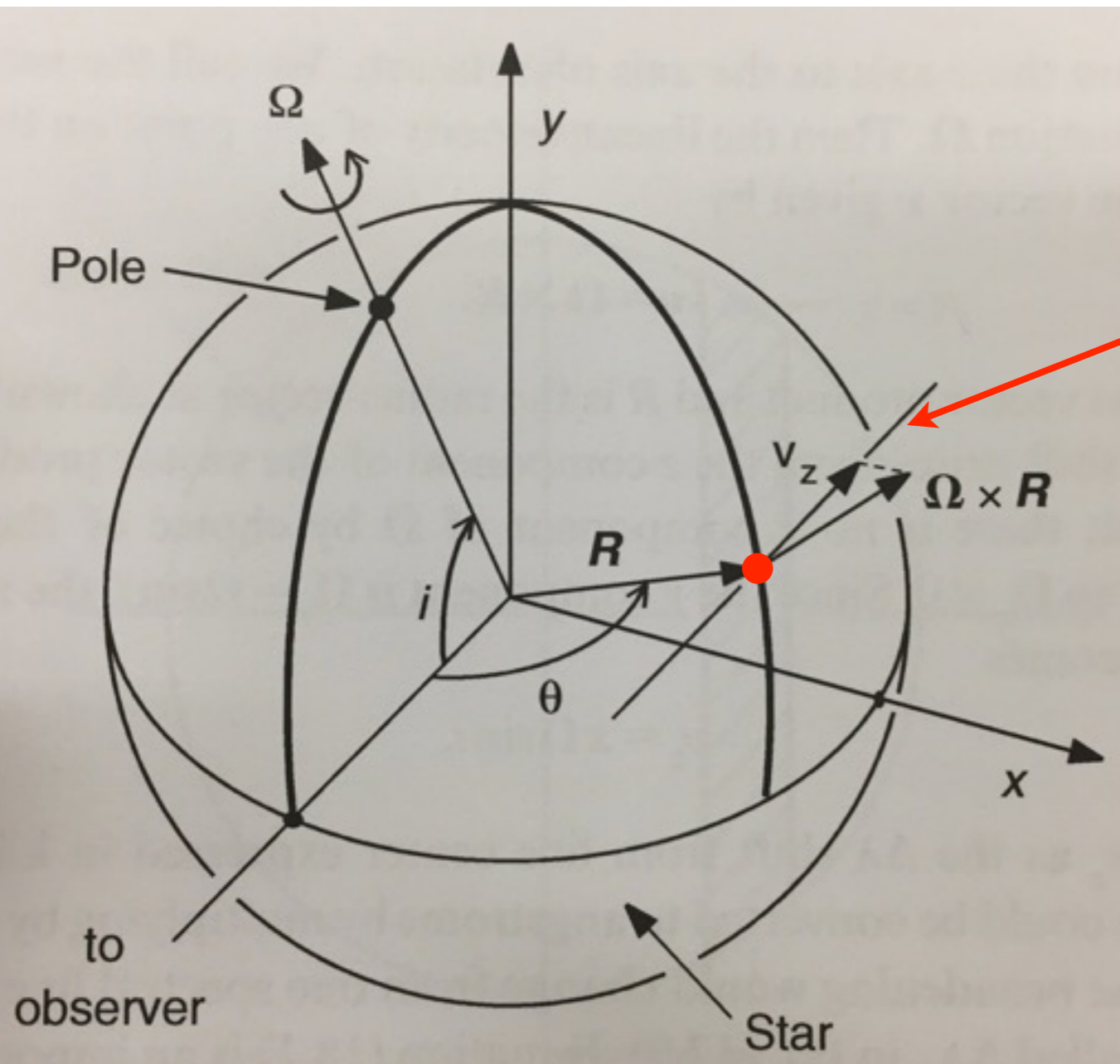
z-component
(line-of-sight)

$$v_z = y\Omega_x - x\Omega_y$$

Orient coordinate system so
that rotation axis is in y-z plane

Rotational Broadening:

Orient coordinate system so
that rotation axis is in y-z plane

$$\mathbf{v} = \boldsymbol{\Omega} \times \mathbf{R}$$
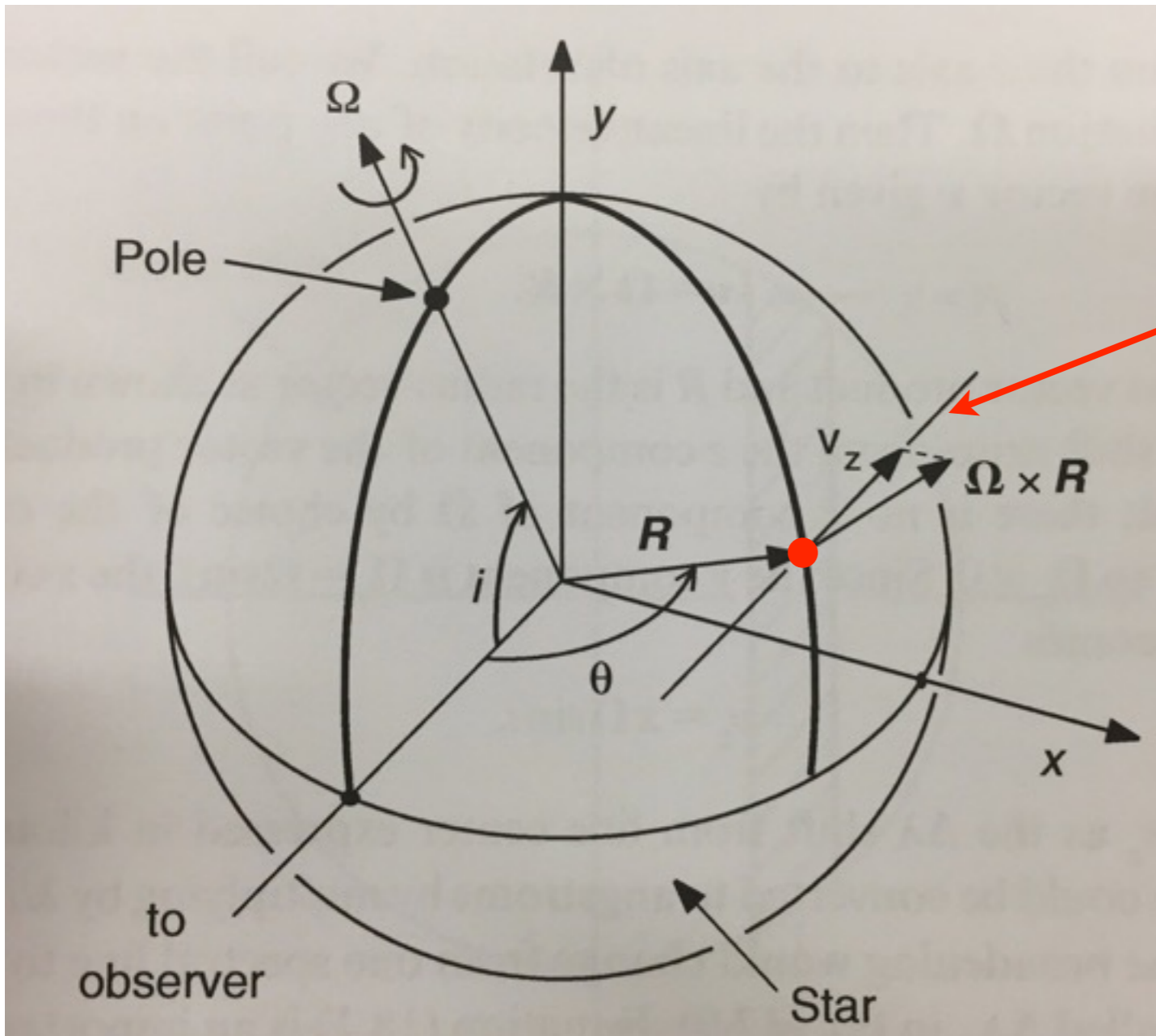
z-component
(line-of-sight)

$$v_z = y\Omega_x - x\Omega_y$$

$$\Omega_x = 0$$
$$\Omega_y = \Omega \sin(i)$$

$$v_z = x\Omega \sin(i)$$

lines of constant x,
parallel to y =>
lines of constant
Doppler shift

Rotational Broadening:
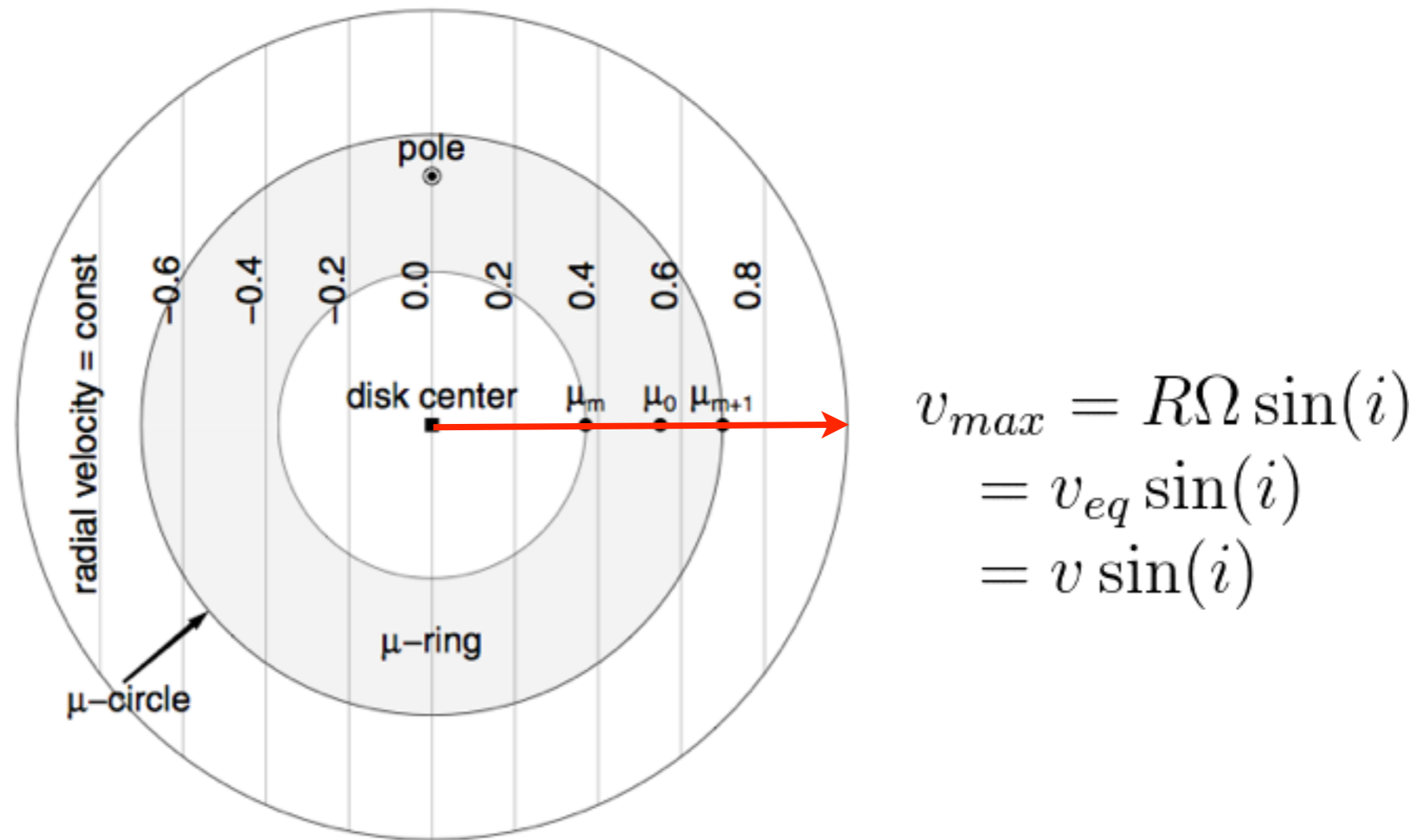
Fig. 1. Illustration of the apparent radial velocity distribution on a stellar disk for solid body rotation: vertical lines of constant radial velocity are labeled by their velocity in units of $V \sin(i)$. They lie parallel to rotational pole – disk center direction. For further explanations see text.

Rotational Broadening:
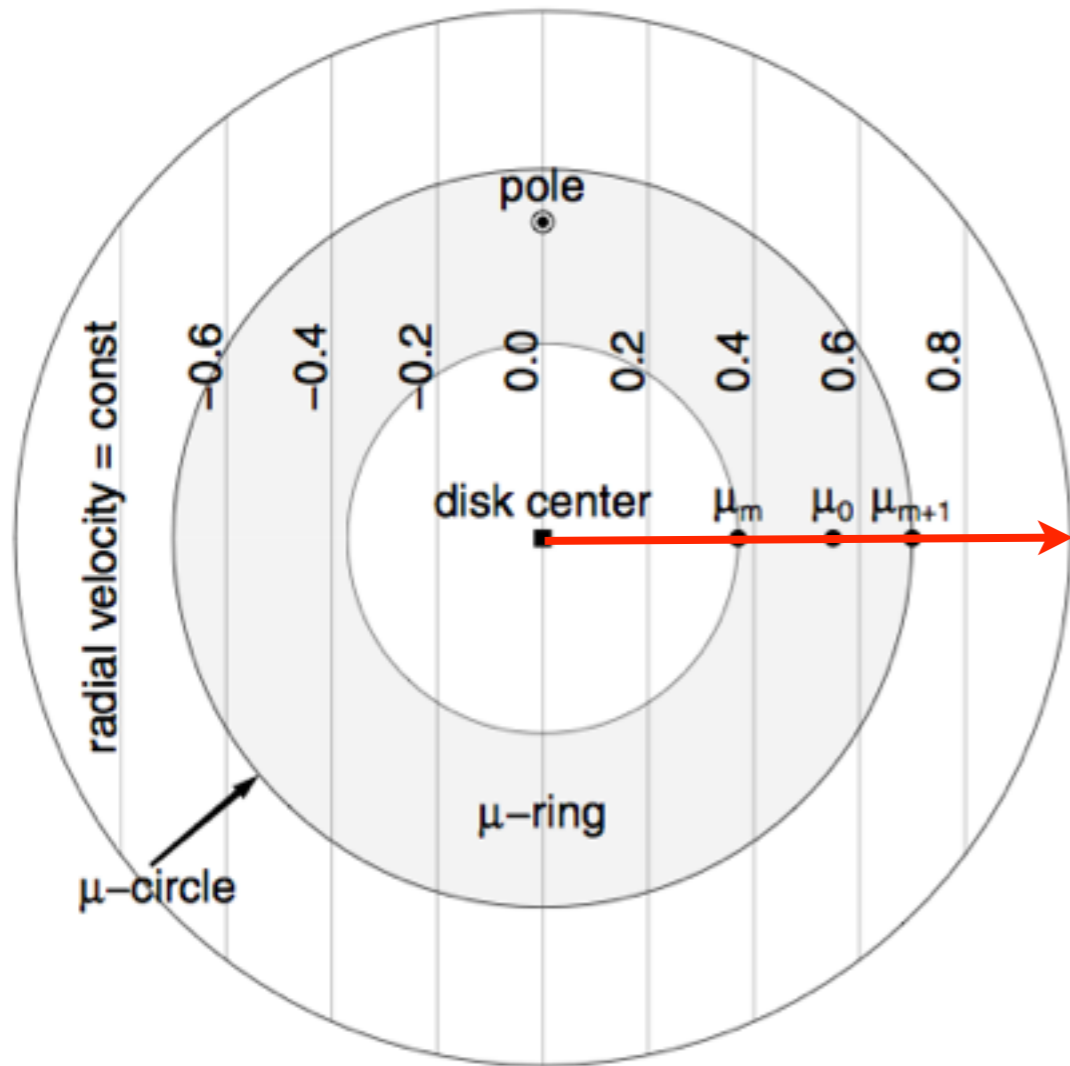
- assume line shape *H* uniform across disk

- observed line profile
$$= H(\Delta\lambda) * G(\Delta\lambda)$$

- G = rotational broadening kernel; essentially an intensity weighted integral of the projected doppler shift.

- all *intensity variations* factor in!

See: Ludwig (2007) and Gray (2005)

G (with linear limb-darkening)

Alternative

I(mu,lam)
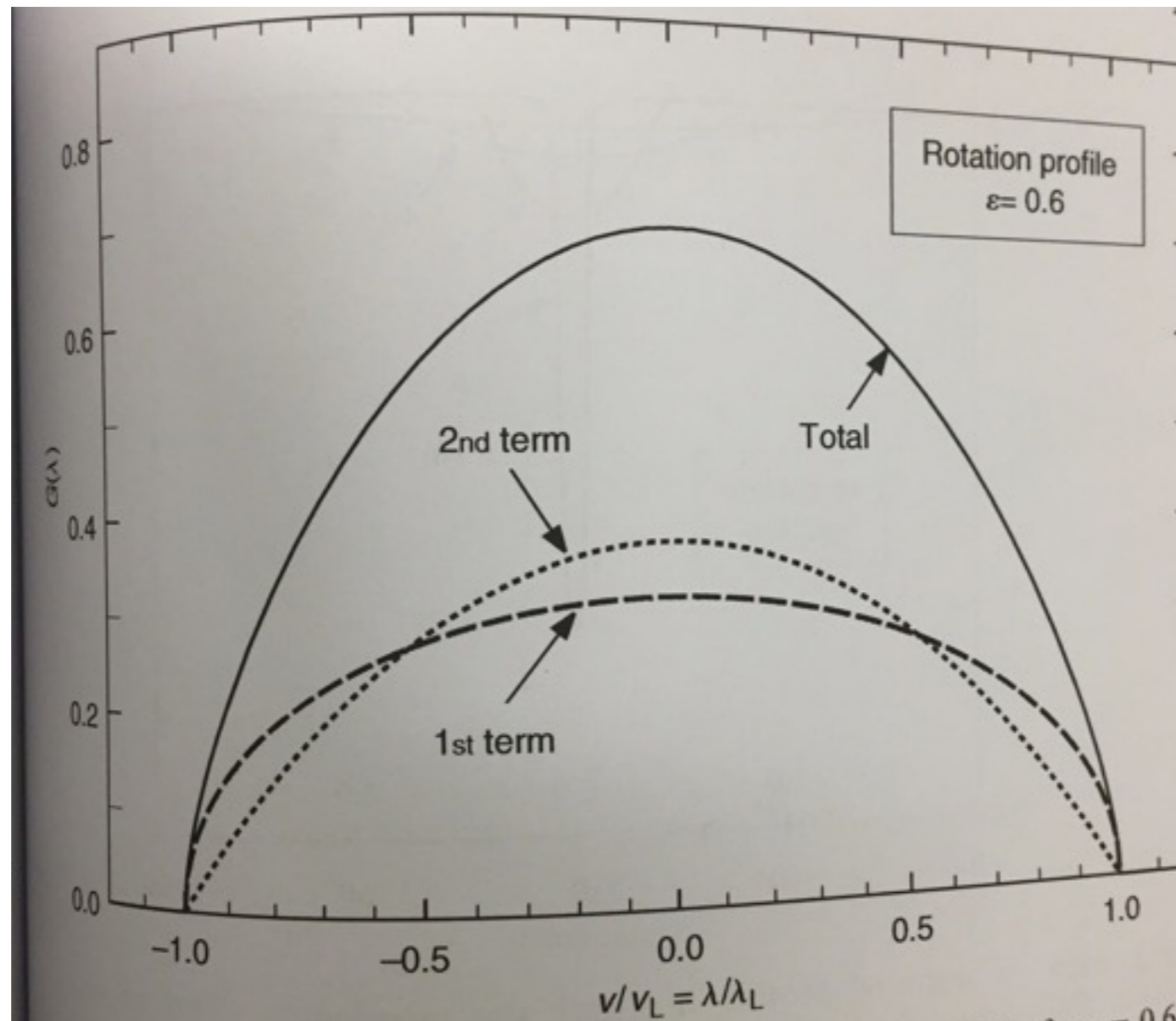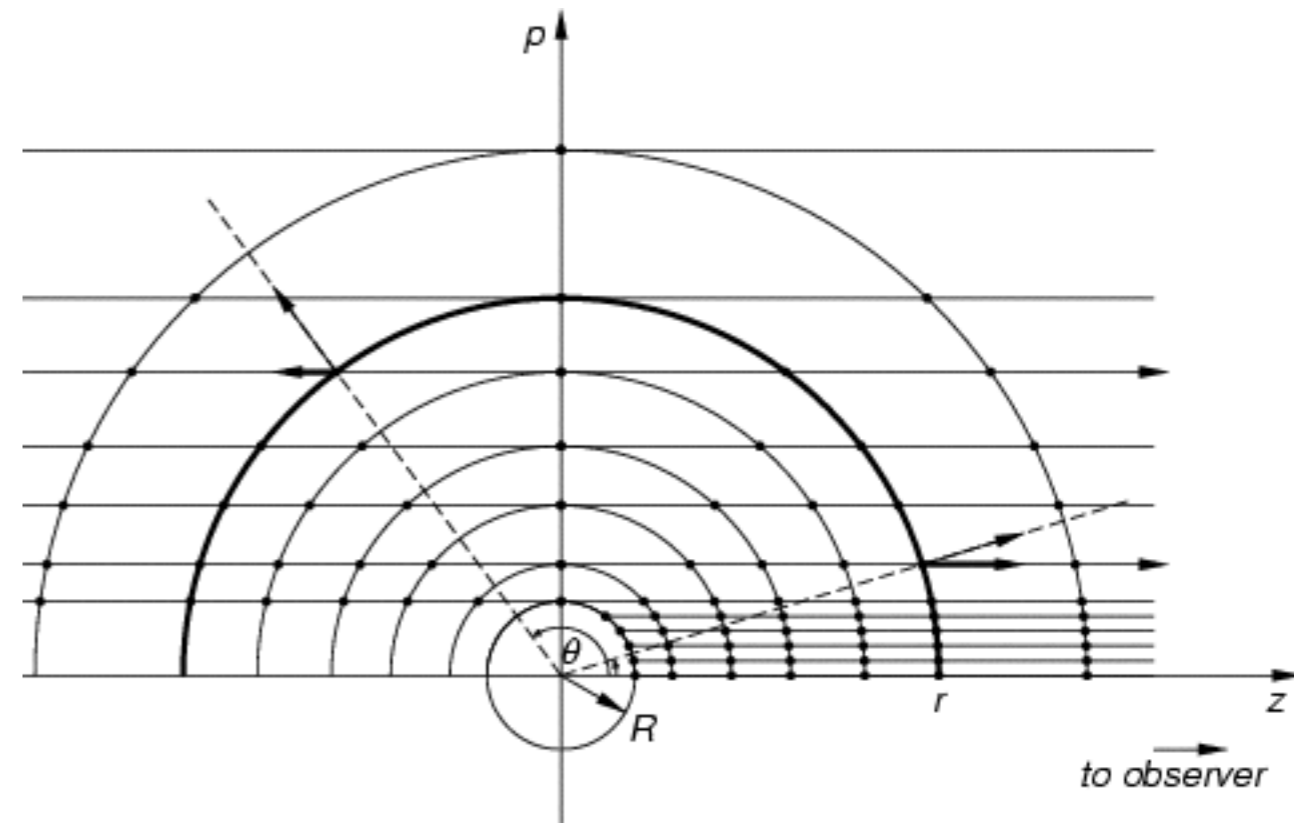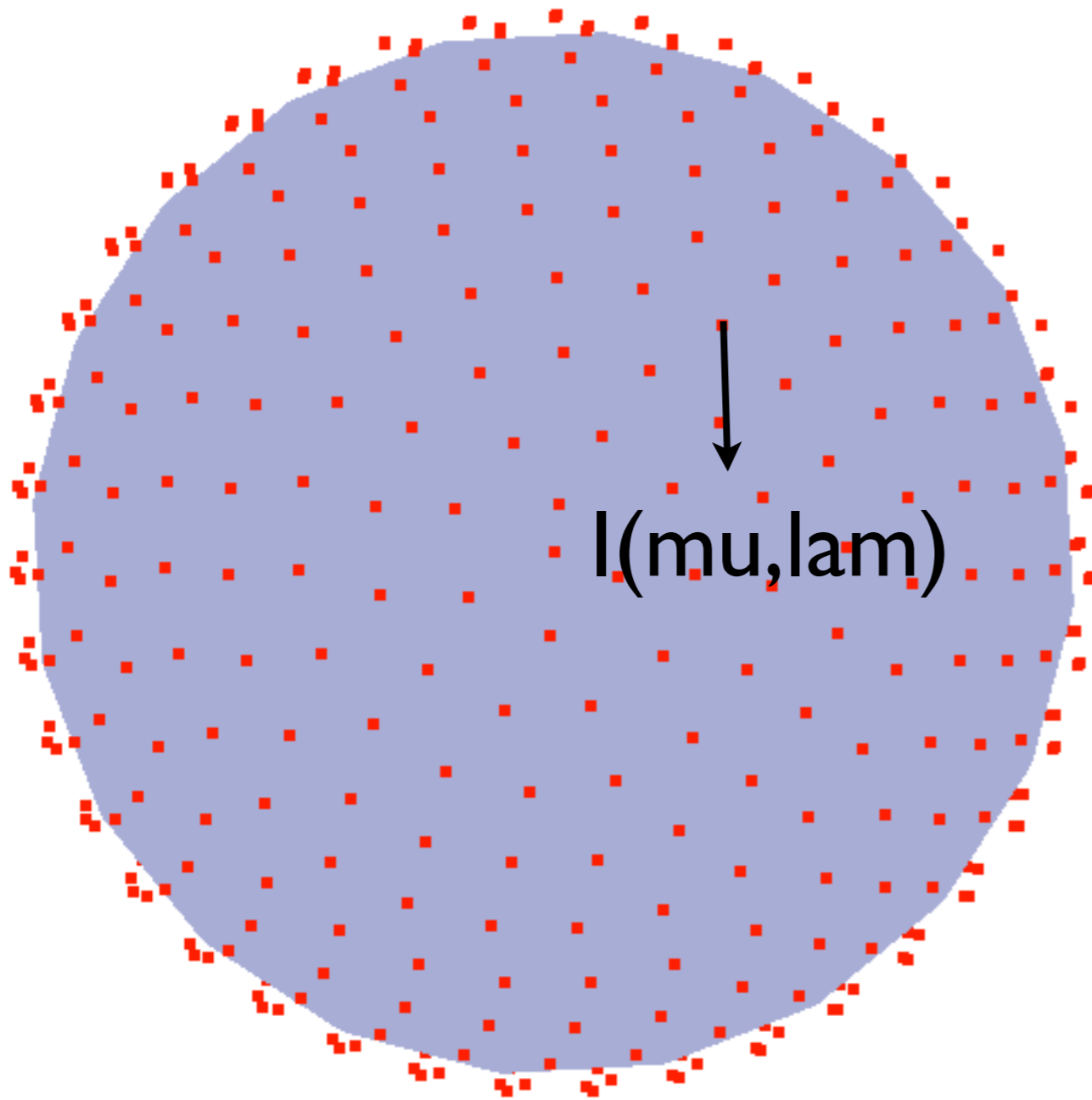
numerically integrate over surface
(int. weights important)

broadening example:

Three phases of a transit

Spin and orbit aligned

Spin and orbit misaligned by 60°
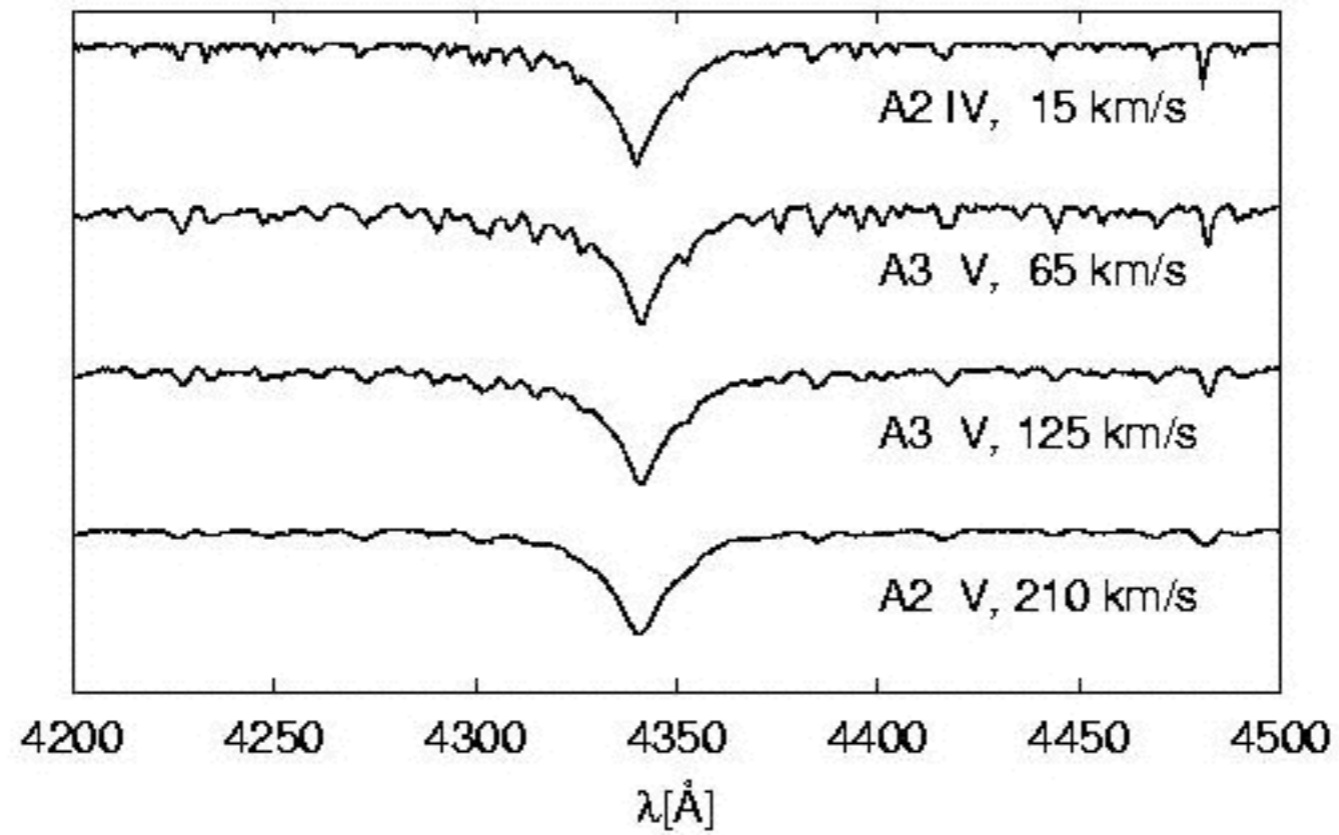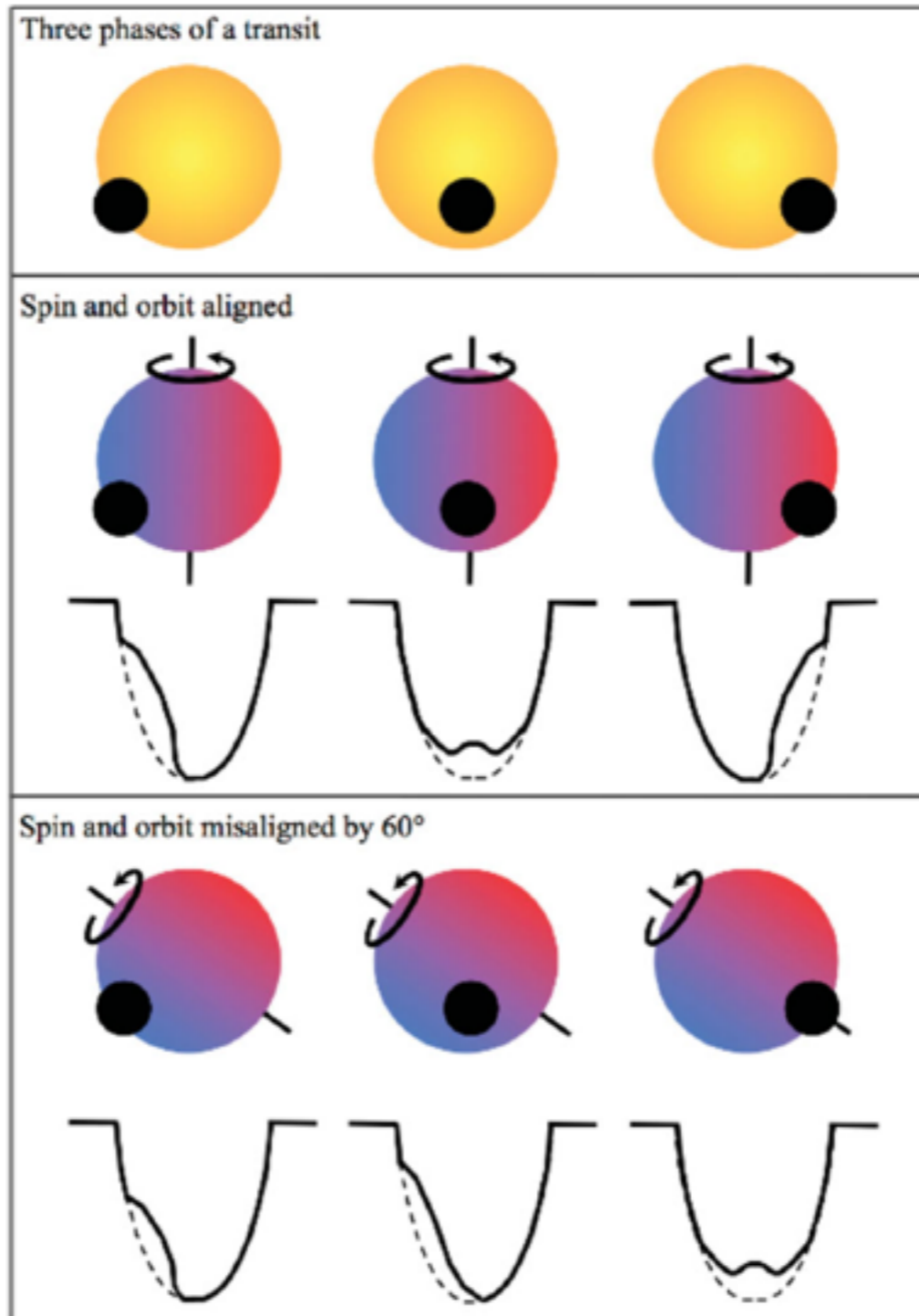
similar to star-spot induced bisector changes
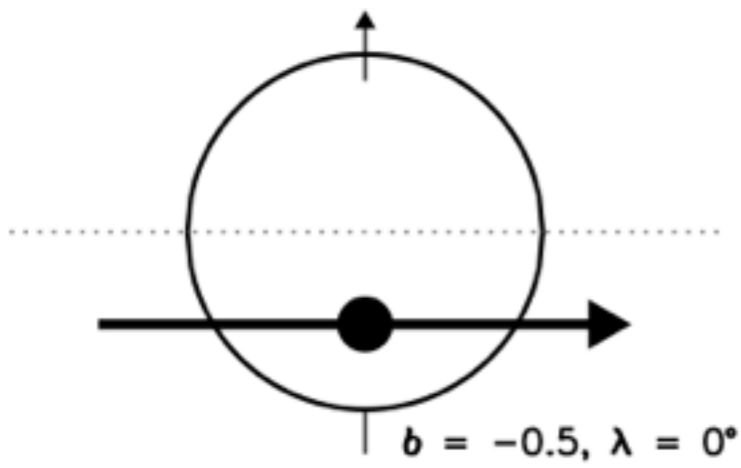also related to doppler-imaging of stars.
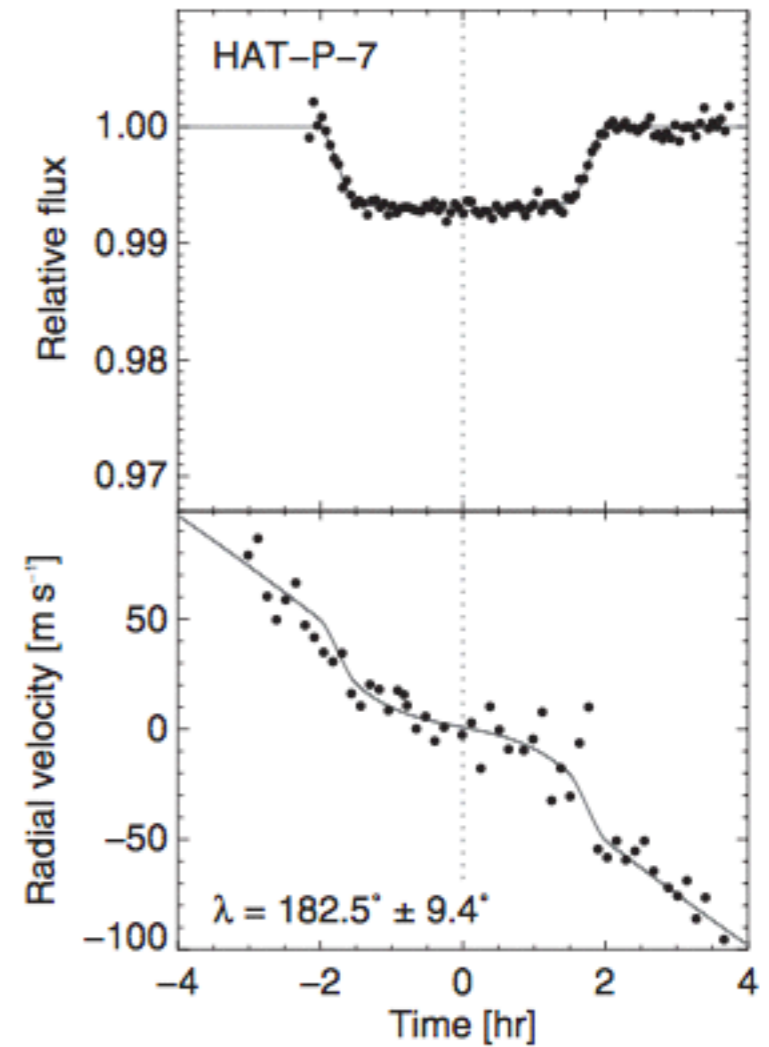
The Rossiter-McLaughlin Effect
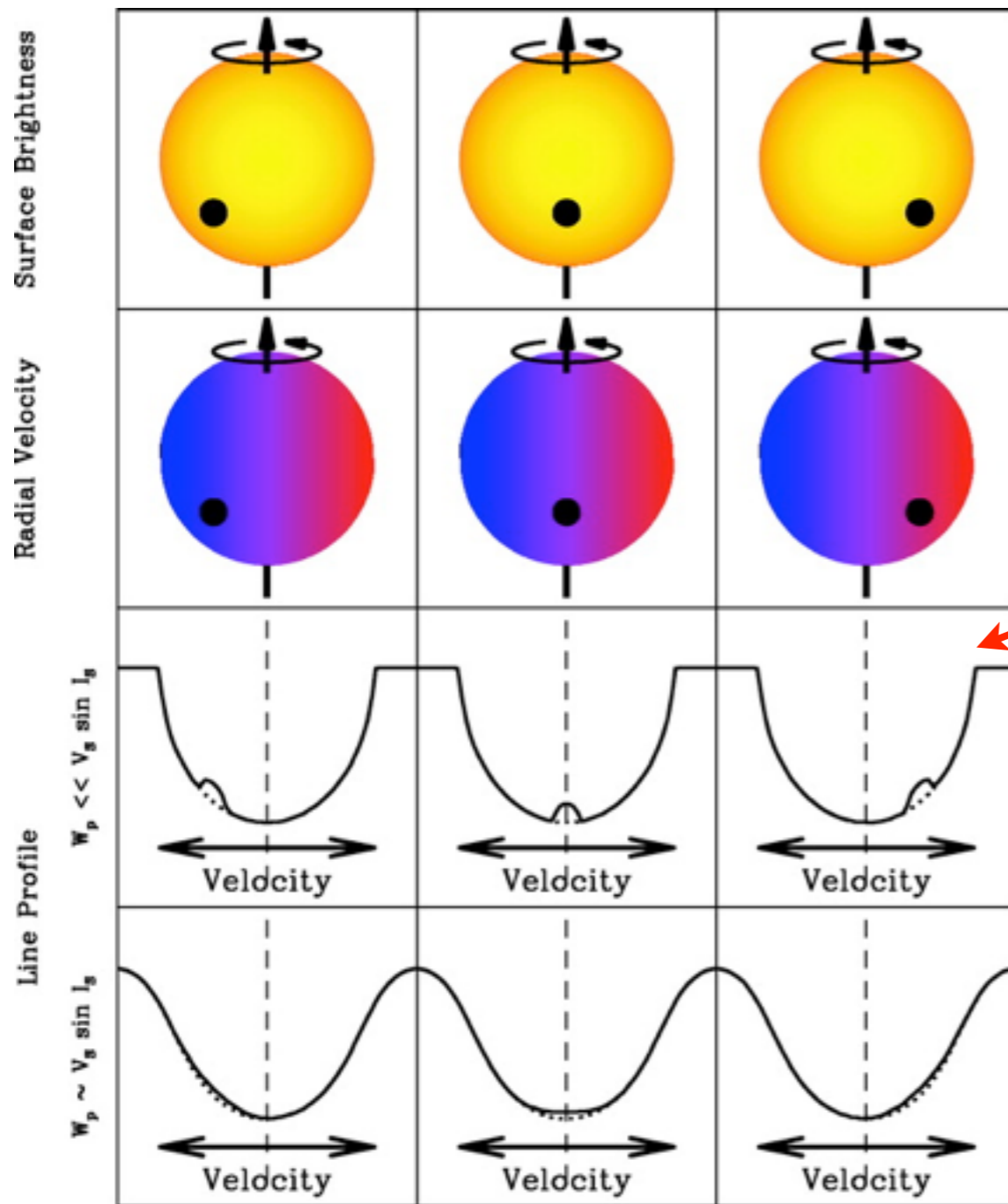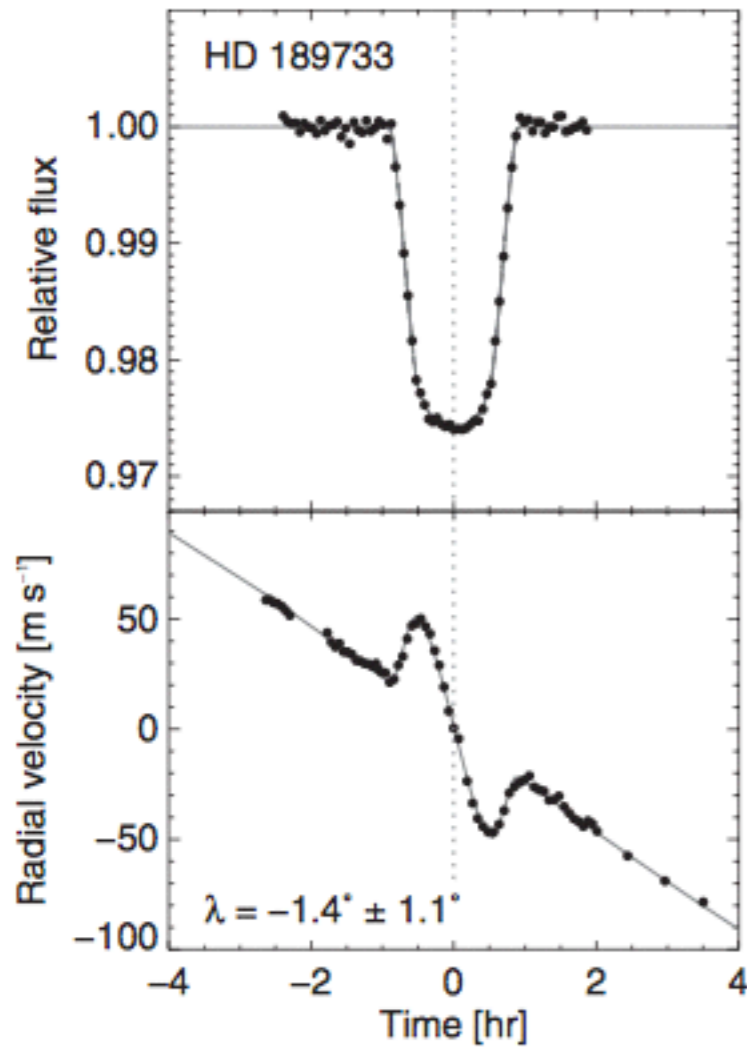

sharp edge unphysical...

rotation only

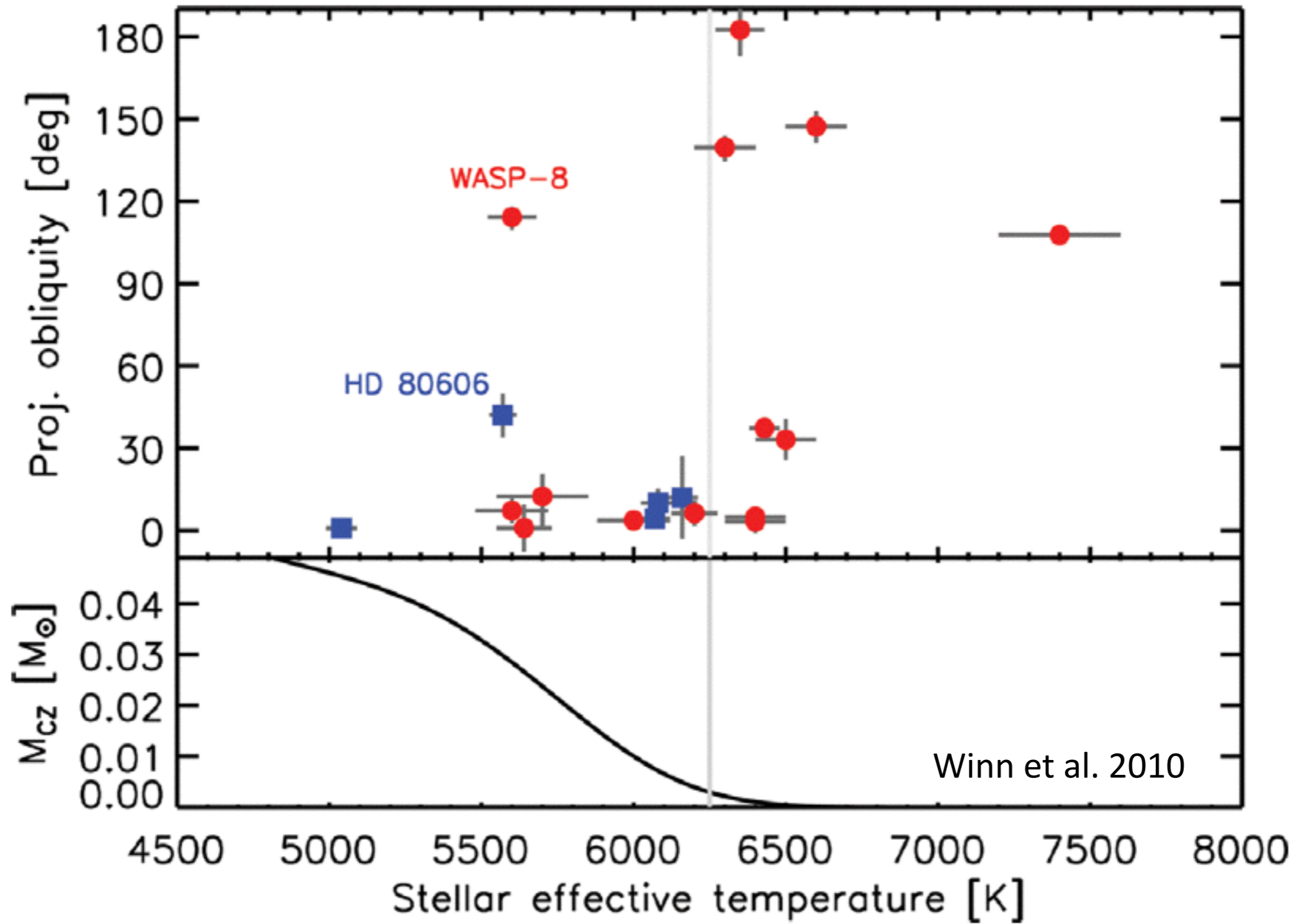rotation + other broadening

The Rossiter-McLaughlin Effect
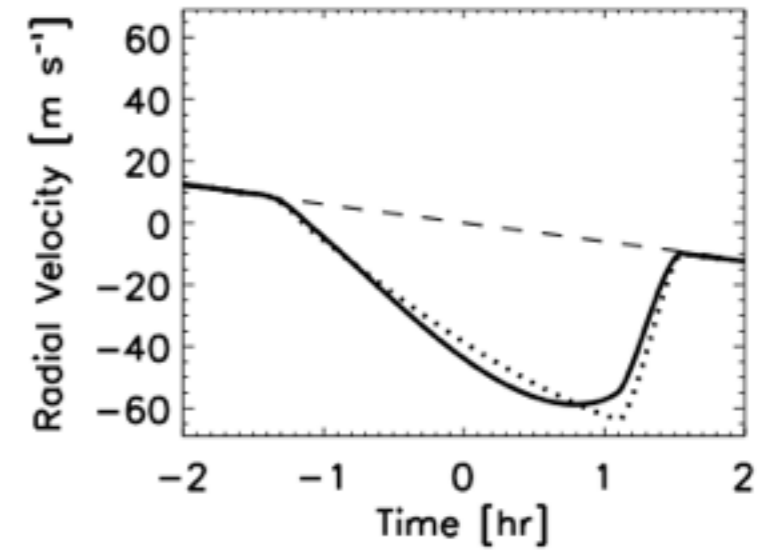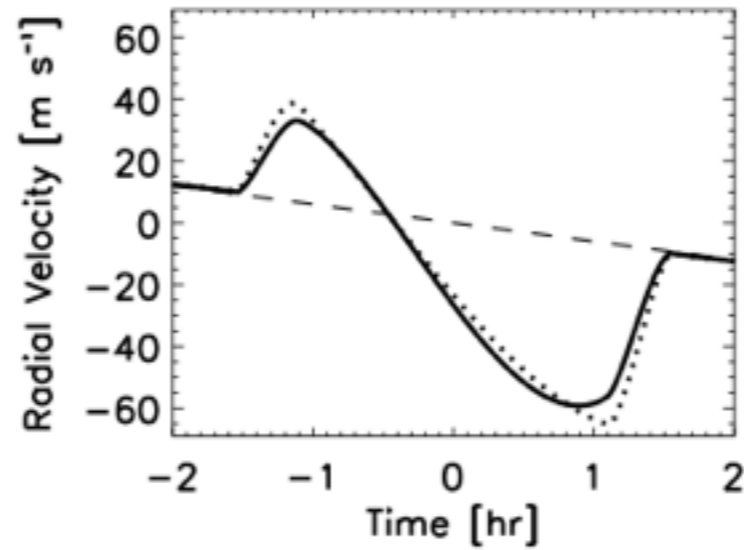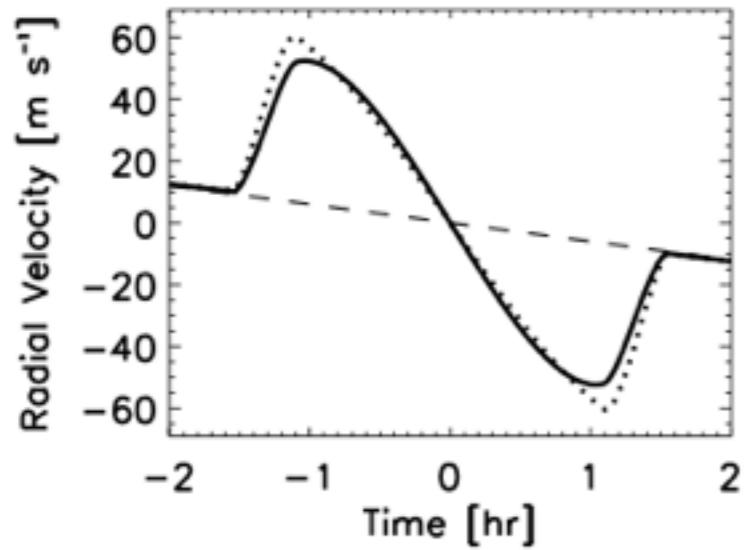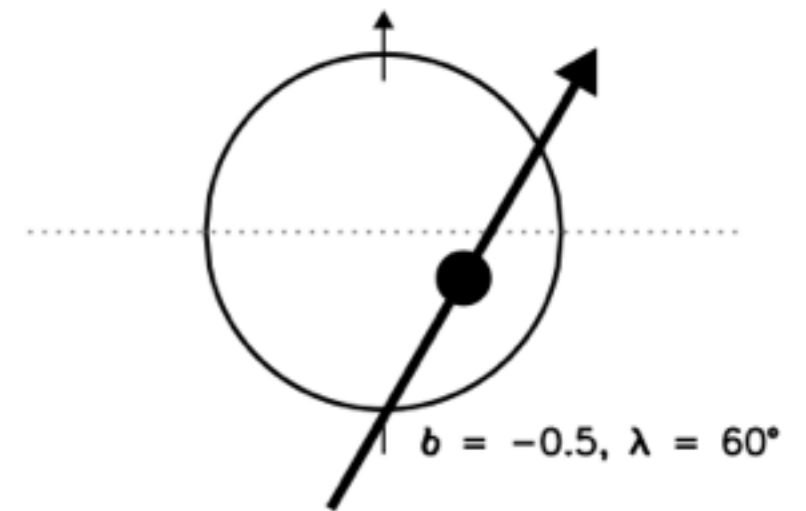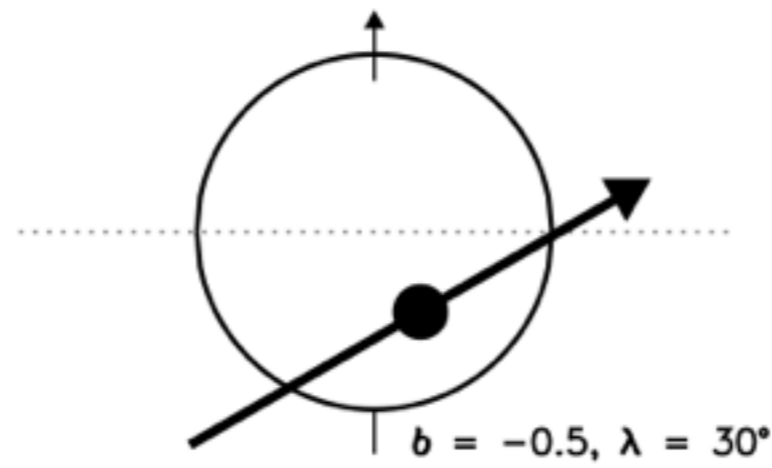
Real examples ...
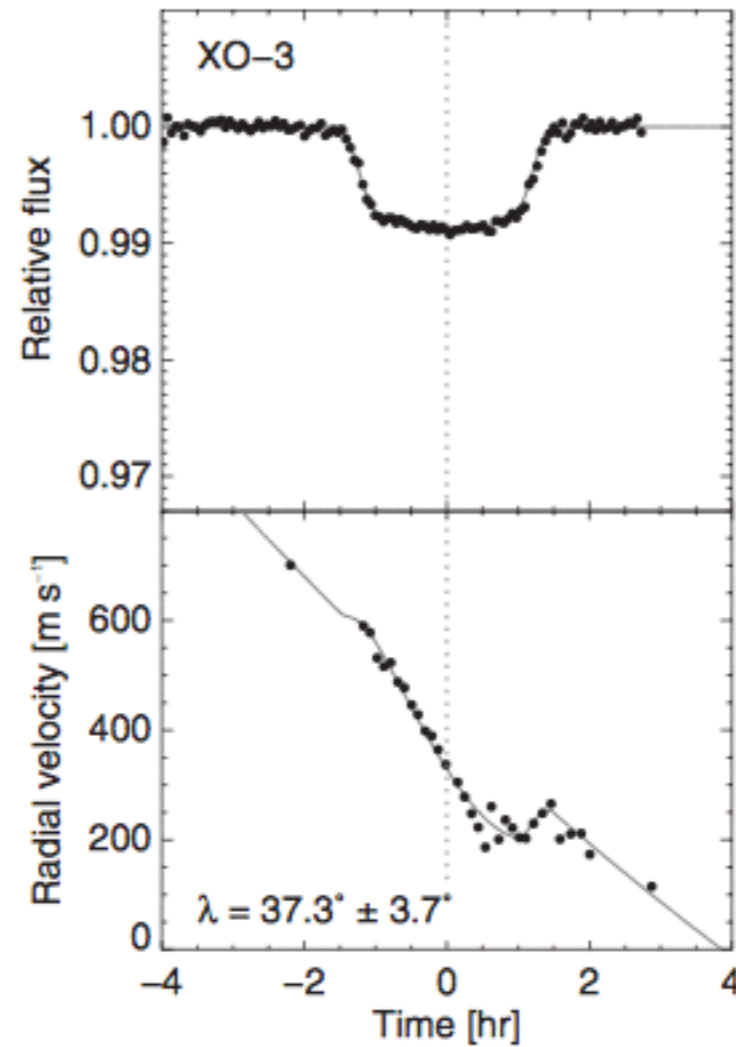
83 planets with measurements, 35 show substantial misalignment.
list maintained at: http://www.physics.mcmaster.ca/~rheller/

Importance of tidal interactions

WASP-8

HD 80606

Winn et al. 2010

Other ways to estimate obliquities:

- Measure Vsin(i) for many stars with transiting planets (Hirano et al. 2014; Morton & Winn, 2014)

- See Van Eylen et al. (2014), Chaplin et al. (2013) for combination of astroseismology and transits to determine obliquities.

- star-spot crossings (e.g. Desert et al. 2011).

Multiple transits across multiple star spots
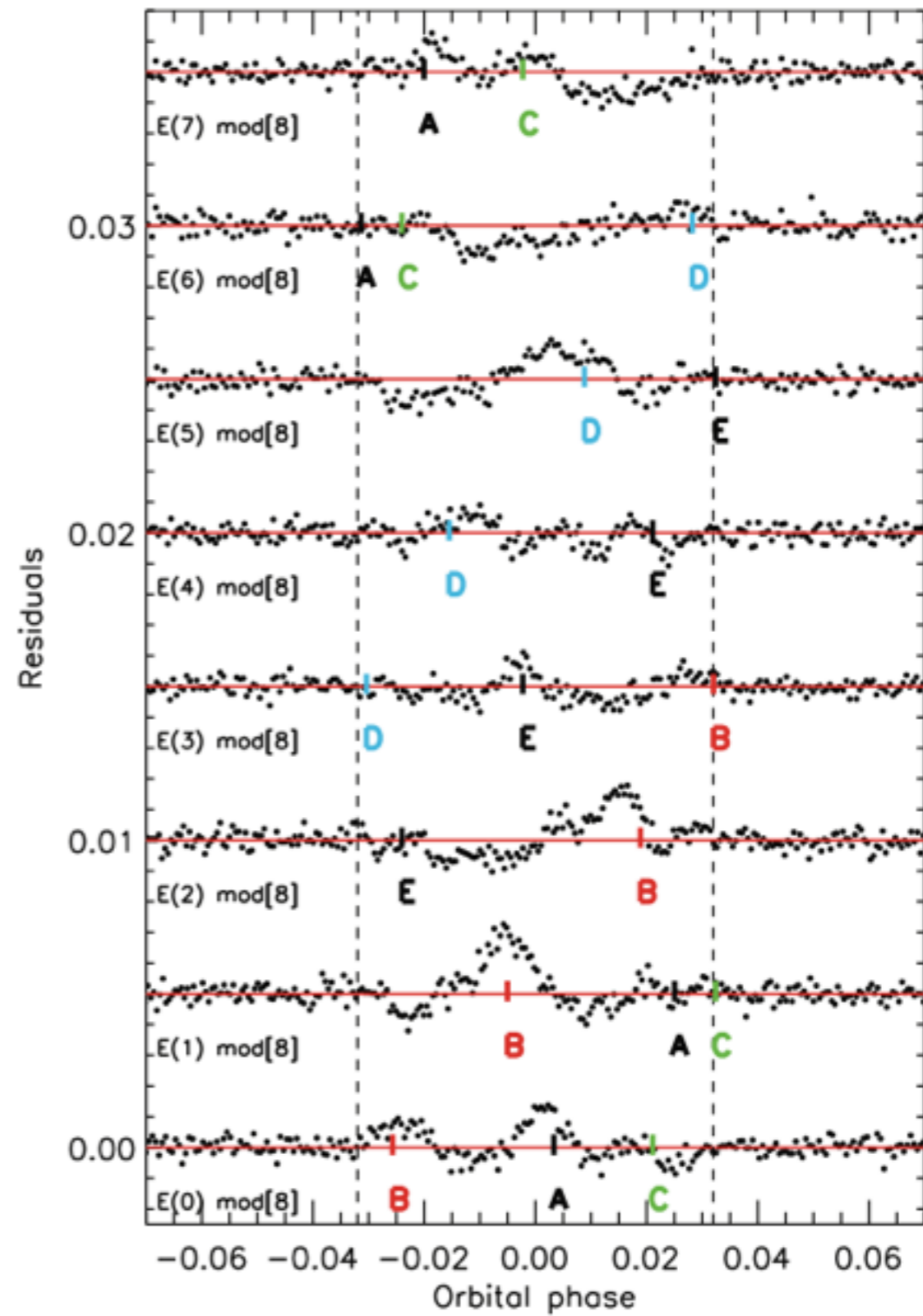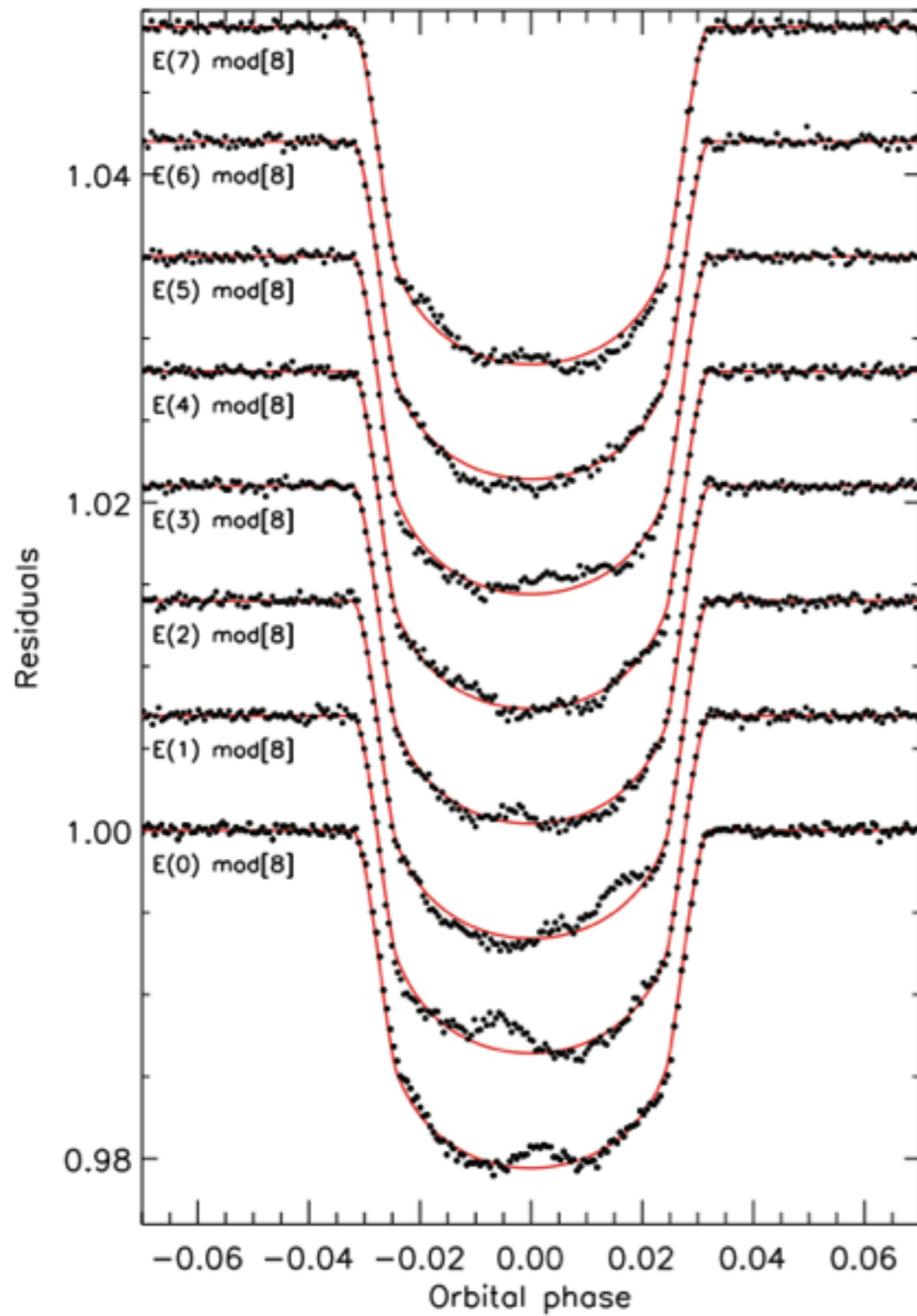
Obliquity < 15 degrees (Desert et al. 2011)

Next:

Micro-lensing

Direct Imaging